UNIVERSITY OF CALIFORNIA
RIVERSIDE

Characterizing the Inactivation Profile of BK Polyomavirus Through a Molecular Beacon Assay

A Dissertation submitted in partial satisfaction
of the requirements for the degree of

Doctor of Philosophy

in

Microbiology

by

Dane Charles Reano

August 2016

Dissertation Committee:

Dr. Marylynn V. Yates, Chairperson
Dr. Sharon Walker
Dr. A. L. N. Rao

The Dissertation of Dane Charles Reano is approved:

_____

_____

_____

Committee Chairperson

University of California, Riverside

ACKNOWLEDGEMENTS

I am grateful for financial support provided by an Integrative Graduate Education and Research Traineeship program from the National Science Foundation, Hatch Funds from the United States Department of Agriculture, and an Education Grant obtained from the Chino Basin Water Conservation District.

Portions of the dissertation includes reprinted material, with permission, from: Reano, D.C., Yates, M. V., 2016. Determining the Solar Inactivation Rate of BK Polyomavirus by Molecular Beacon. Environ. Sci. Technol. 50, 7090–7094.

Most importantly, I am thankful for the committee members and professors who have served as mentors, educators, and examples in support of my graduate and professional endeavors. To Drs. Gauvain, Mulchandani, Rao, Walker, and Yates, thank you for your continued guidance.

DEDICATION

This dissertation is dedicated to the educators who allowed me the freedom to surmount intellectual challenges through guidance and wisdom, and the family who constantly supported my efforts to do so. Thank you to my parents, Charles and Gail, who placed my education and success before their own; offering limitless support and opportunity. To Mariana, your love and intellect serve as my motivation in progressing towards success in all aspects that define me. To my sister Jennifer and nephew Bentley, you give me perspective and set the example that I will always strive towards. To Jean Mumbleau and Anna Peters, the educators that looked beyond my faults to see and develop my potential. And finally, to Dr. Yates, you have always believed in me, and provided me with the support that will forever shape my professional life. Thank you all.

ABSTRACT OF THE DISSERTATION

Characterizing the Inactivation Profile of BK Polyomavirus
Through a Molecular Beacon Assay

by

Dane Charles Reano

Doctor of Philosophy, Graduate Program in Microbiology
University of California, Riverside, August 2016
Dr. Marylynn V. Yates, Chairperson

Regulations set forth by the United States Environmental Protection Agency (EPA) have significantly elevated standards for water treatment by ultraviolet light irradiation (UV). These standards are justified by resistances exhibited by double stranded DNA (dsDNA) viruses from the *Adenoviridae* family to UV treatment at 253.7 nm (UV_{254}), but have not been validated by other waterborne microorganisms. Similarly structured microorganisms, like BK Polyomavirus (BKPyV), would allow for such assessments, but remain precluded by a lack of traditional infectious assays. Additionally, the rates of seroprevalence in human populations, as well as the modes of excretion, have generated interest in the utilization of polyomaviruses as alternative indicators of water quality.

Integrated assays, such as intracellularly delivered molecular beacons (MB), selectively target infectious virions, thereby surmounting limitations in current detection

methodologies. This research describes the development of integrated assays for BKPyV to characterize its disinfection profile following exposure to UV_{254}, chlorine, heat, and sunlight. The developed assays were also applied to Adenovirus 2 (Ad2) and Poliovirus 1 (PV1) following similar treatments. As expected, the genomic parallels between BKPyV and Ad2 resulted in similar resistance to UV_{254} inactivation, requiring 61.35 and 51.45 mJ/cm^2 to reduce viral titers by an order of magnitude, respectively. The obtained results support current regulations for UV treatment and assess the utility of BKPyV as an indicator organism of water quality.

TABLE OF CONTENTS

LIST OF FIGURES

LIST OF TABLES

ABBREVIATIONS

α, sample absorbance (at 254 nm)
A549, adenocarcinomic human alveolar basal epithelial cells
Ad2, Adenovirus 2
BGMK, buffalo green monkey kidney cells
BHQ-1, Black Hole Quencher® 1
BKPyV, BK Polyomavirus
BSA, bovine serum albumin fraction V
c, correction factor (qPCR)
CF, correction factor (sunlight)
CPE, cytopathic effect
C_t, threshold cycle
CT, contact time
CPP, cell penetrating peptide
DF, divergence factor
DMEM, Dulbecco's Modified Eagle Medium
DPD, N,N-diethyl-p-phenylenediamine
DPI, days post infection
dsDNA, double stranded DNA
EPA, United States Environmental Protection Agency
E, efficiency of qPCR
E_0, bulb output
E'_{avg}, average germicidal fluence rate
ET-qPCR, enzyme treated quantitative polymerase chain reaction
F, fluorophore
FBS, fetal bovine serum
FIO, fecal indicator organism
FRET, Förster/Fluorescent Resonance Energy Transfer
GC, genomic copy
H′, average germicidal fluence
HBS, HEPES buffered saline
$h\nu_{ex}$, light capable of exciting fluorophore
k_{obs}, inactivation rate
l, water path length
L, distance from bulb to sample
LT2, Long Term 2 Enhanced Surface Water Treatment Rule
MB, molecular beacon

MEM, Minimum Essential Medium
N, titer after treatment
N_0, initial titer
NT, nucleotide
NTC, non-template control
PA, plaque assay
PBS, phosphate buffered saline
PF, petri factor
PFU, plaque forming unit
PV1, Poliovirus 1
Q, quenching moiety
Qdot 525, quantum-dot excited at 525 nm
R^2, coefficient of determination
REM, renal epithelial media
RF, reflection factor
RPTEC, renal proximal epithelial tubule cells
ssRNA, single stranded-RNA
T_a, annealing temperature
Tat, Trans-activator of transcription
TBS, tris buffered saline
TE, tris-EDTA
TTBS, tris buffered saline with Tween® 20
UV, ultraviolet light (100-400 nm)
UV_{254}, ultraviolet light (253.7 nm)
UVB, ultraviolet light (280-320 nm)
WF, water factor

CHAPTER ONE: INTRODUCTION

A BRIEF HISTORY OF WATER TREATMENT, CURRENT CHALLENGES, AND LIMITATIONS TO TREATMENT BY ULTRAVIOLET LIGHT

The inactivation of waterborne pathogens through the addition of chlorine has saved millions of lives worldwide and is credited with halving rates of mortality within the United States (Cutler and Miller, 2005; McGuire, 2013). Although this practice began over a century ago, chlorine remains the most widely utilized disinfectant of water due to low cost, facile application, and broad effectiveness. However, the emergence of recalcitrant contaminants has supported investigations into alternative forms of water treatment, including UV (Freese and Nozaic, 2004).

In 1993, the contamination of Milwaukee's drinking water by *Cryptosporidium* resulted in an estimated 400,000 incidents of gastrointestinal illness. Interestingly, the water supply met all microbiological standards and exhibited inconclusive signs of contamination. Here, routine chlorination failed to deliver clean water due to resistances exhibited by *Cryptosporidium* parasites (Mac Kenzie et al., 1994). Similarly, many pharmaceuticals and personal care products remain recalcitrant to chlorine (Huber et al., 2005). Chlorination can also select for antibiotic resistant microorganisms in wastewater treatment plants (Huang et al., 2011). Finally, concerns regarding the formation of disinfection by-products, such as chloroform and other trihalomethanes, remain (Freese and Nozaic, 2004). Although no ideal form of water treatment exists, UV remains a viable alternative to assuage these concerns.

The first application of UV to treat water also occurred over a century ago, but was overshadowed by the effectiveness of chlorine. Unlike chlorine, traditional UV inactivates microorganisms primarily through inducing genomic damage. The application of an electrical current to liquid mercury suspended in an inert gas generates photons from a subset of the UV light spectra (100 – 400 nm) at 253.7 nm (UV_{254}). Energy from UV_{254} photons are primarily absorbed into pyrimidine bases of nucleic acids to generate cyclobutane pyrimidine dimers, and occasionally pyrimidine-pyrimidone 6-4 photoproducts (Fig. 1.1). The formation of these photoproducts sterically inhibits genome replication and transcription, thereby leaving a viable organism unable to propagate (Schuch and Menck, 2010). The universal presence of a genome makes water treatment by UV_{254} an effective means of inactivating chlorine resistant microorganisms, like *Cryptosporidium* (Hijnen et al., 2006). Similarly, UV_{254} does not select for antibiotic resistant genes and yields few, if any, disinfection by-products (Huang et al., 2013; Reckhow et al., 2010). However, resistances exhibited by adenoviruses to UV_{254} have significantly elevated standards for all UV water treatment standards in the USA (United States Environmental Protection Agency, 2005).

Adenoviruses are unenveloped dsDNA viruses of over 50 species spread over six subgroups (A-F). Adenoviruses 40 and 41, from subgroup F, are second only to rotaviruses as etiological agents of gastrointestinal illnesses and require over 186 mJ/cm^2 to achieve 99.99% (four-log) reduction in viral titers (Bounty et al., 2012). Comparatively, rotaviruses are double-stranded RNA viruses that also lack an envelope, yet require less than 40 mJ/cm^2 to achieve four-log inactivation similar to most other microorganisms

(Johnson et al., 2010). This resistance served as the impetus for elevating all UV treatment standards from 40 to 186 mJ/cm^2, as stated in the Long Term 2 Enhanced Surface Water Treatment Rule (LT2) (United States Environmental Protection Agency, 2005). Interestingly, adenoviruses may not actually be resistant to UV_{254}, but rather, induced genomic damage is repaired by host cells during subsequent infection (Eischeid et al., 2011). Adenoviruses are not only susceptible to other forms of UV treatment which target viral proteins, but also lose resistance to UV_{254} when assayed in genome repair deficient cells (Rainbow, 1980). Infectious assays for other unenveloped viruses possessing a dsDNA genome do not exist, therefore LT2 regulations, and the costs associated with meeting these standards, remain.

Indicator Organisms to Assess Water Quality

Ensuring water meets acceptable levels of microbiological quality presents two unique challenges for treatment plant operators. Firstly, not all microorganisms are removed during water treatment processes. Although some microorganisms remain, the risk to consumers is minimal; which explains the acceptance of the EPA to allow up to 500 colony forming units of heterotrophic plate count microorganisms per mL of drinking water (United States Environmental Protection Agency, 2011). Secondly, microbiological contaminants are inactivated or destroyed during water treatment processes, but are not removed. The inactivation of microorganisms abrogates a risk of infection to consumers, but does not preclude these remains from detection by alternative microbiological assays, such as PCR. Therefore, assessments of water quality must evaluate the viability of specific microbial contaminants (Yates, 2007).

Waterborne pathogens primarily follow the fecal-oral route of exposure and are integral in water quality assessments. The fecal-oral cycle begins with the ingestion of water containing pathogenic microorganisms and continues if contaminants establish an infection by replicating within the host gastrointestinal tract. After varied incubation times, hosts may periodically or acutely excrete pathogens through defecation at levels of up to 10E12 infectious units per gram of fecal material (Franks et al., 1998). This cycle is repeated if fecal material containing pathogens encounters water, food, or other fomites that are exposed to a new host. However, the vast number of pathogenic microorganisms that follow the fecal-oral cycle precludes their assessment in every water sample.

Therefore, water samples are tested for the presence of natural inhabitants of mammalian (preferably human) digestive tracts, termed fecal indicator organisms (FIO). Water samples containing FIO, like *E. coli*, are indicative of fecal contamination; hence, the risk of exposing consumers to other contaminants, including pathogens, increases (Girones et al., 2010).

Although effective, poor correlations between FIO and pathogens, particularly between bacterial FIO and viruses, can occur (Dorevitch et al., 2015; Ferguson et al., 2012; Payment and Locas, 2011). Furthermore, an ability to assess infectivity often relegates water quality assays to traditional culture methods, such as bacterial plate counts and viral plaque assays. Finally, water quality assessments must be rapid to generate relevant data for treatment plant operators and managers (Yates, 2007). This is of particular importance when restricting public access to recreational waters following sewage contamination (Nevers and Whitman, 2005). Due to these requirements, water quality assessments remain largely unchanged over time, with some methods utilizing techniques developed over a century ago, and the search for an ideal indicator of water quality continues.

POLYOMAVIRUSES AS ALTERNATIVE FECAL INDICATOR ORGANISMS

Originally identified in mice, members of the *Polyomaviridae* family received scientific attention when detected as frequent, but overlooked, contaminants of poliovirus vaccines produced by the Salk method (Knipe and Howley, 2013). Similarly, prevalence has generated interest in adopting polyomaviruses as FIO but remains complicated by an inability to easily quantify viral titers (Albinana-Gimenez et al., 2009; Girones et al., 2010; Hewitt et al., 2013). Polyomaviruses possess a circular dsDNA genome containing around 5000 nucleotides (NT) and are found in a variety of primate hosts. During replication, polyomaviruses utilize alternative splicing to produce three proteins, VP1, VP2, and VP3, for the formation of an unenveloped icosahedral capsid of 42.5 nm; however, only VP1 is necessary (Knipe and Howley, 2013; Nakanishi et al., 2006). Additionally, all polyomaviruses possess a large T antigen, which has multiple functions during viral replication including shifting cells into synthesis phase and blocking host tumor suppression genes. The function of the large T antigen is also likely responsible for the oncogenicity potential of polyomaviruses (Ahsan, 2006).

Until 2000, polyomaviruses were members of the *Papovaviridae* family ("Pa" – papillomavirus, "Po" – polyomavirus, "Va" – vacuolating virus) due to their ability to form tumors similar to other papovaviruses. Indeed, the name polyomavirus is representative of the various forms of cancer that can result from infection ("poly" – many, "oma" – cancer). Normally, permissive cells die after infection and do not develop into tumors; however, infected non-permissive cells, or viral mutants unable to complete the viral life cycle, can

retain functional large T antigens. The ability of this viral protein to block host tumor suppression genes, like p53, coupled with an inability to destroy host cells by polyomavirus replication can result in the formation of unregulated cell growth. It is for this reason that oncogenicity remains more resistant to inactivation than abrogating viral infectiousness, and why polyomaviruses are often characterized by latent, nonproductive, infections (Knipe and Howley, 2013).

Polyomaviruses establish a subacute latent infection in childhood that lasts throughout the lifetime of the host. Transmission likely occurs early in life from parent to child due to periodic excretion in the feces and urine of hosts. This is evidenced by a study of second and third generation Japanese-Americans, found to excrete strains common to Japan rather than strains circulating in the Americas (Kato et al., 1997). Furthermore, polyomaviruses retain a near ubiquitous seroprevalence in humans, with BKPyV antigens detected in 81 – 97 % of populations. Polyomaviruses are also universally present in sewage waters throughout the world and have exhibited correlations to the occurrence of waterborne pathogens (Antonsson et al., 2010; Payment and Locas, 2011; Vanchiere et al., 2009). Although these qualities may seem enticing benefits towards adoption as an FIO, infectious assays for BKPyV require significant time due to the ability of the virus to establish a latent, and characteristically nonproductive, infection (Girones et al., 2010). Therefore, a rapid detection scheme, capable of assessing viral infectivity, is necessary.

Integrated Methods to Assay Viral Infectivity

Integrated methods selectively target infectious virions while offering reduced assay times relative to traditional quantification methods. In traditional (non-integrated) plaque (PA), or tissue culture infective dose assays, cultured cell lines are exposed to a specific virus and incubated until the formation of visible cytopathic effects (CPE) in host cells. The formation of CPE indicates viral replication, and allows for the quantification of viral titers (Knipe and Howley, 2013). Alternatively, integrated methods, like immunofluorescence assays (IFA), enzyme treated quantitative polymerase chain reaction (ET-qPCR), and MB, do not require complete replication, or replication at all, to assay the presence and infectivity of viruses (Kovac et al., 2012; Moriyama and Sorokin, 2008; Sivaraman et al., 2013).

Like PA, IFA requires the infection of susceptible cells by a virus, but allows results to be obtained before the completion of viral replication. Results from IFA are obtained after the translation of specific viral proteins from host ribosomes instead of incubating infected cells until visualizing CPE. By targeting the formation of viral proteins within infected cells, IFA can reduce viral detection times to within a few days post infection (DPI) (Li et al., 2012). This is particularly important for viruses with relatively long incubation times or those that do not produce significant CPE during infection, such as BKPyV. However, IFA remains entirely dependent on the quality of the antibodies used, which can exhibit low specificity or low binding potential, and cannot be produced by most laboratories. Additionally, host cells must be treated to avoid nonspecific binding of the

secondary antibody, resulting in significant sample interaction and assay times before obtaining quantifiable results (Santos et al., 2012; Wölfel et al., 2006).

Integrated molecular methods, like integrated cell culture PCR and ET-qPCR, have been used to detect infectious viruses with or without exposure to cells. However, translating the presence of an amplifiable sequence to estimating viral titers has been difficult due to the variable amount of viral genomes produced during replication (Hatt and Löffler, 2012; Knight et al., 2016; Olsen et al., 2012). In integrated cell culture PCR, evidence of viral replication is determined in a manner similar to IFA by amplifying viral genomic material produced during early stages of infection. Chemically screened PCR assays, like ET-qPCR, avoid cell culture by removing noninfectious virions before amplification. For example, the addition of DNA intercalating agents, like propidium monoazide, binds to exposed DNA to block PCR amplification via steric interactions. Undamaged, infective, virions likely contain a complete capsid that protects contained genetic material from intercalation, thereby allowing for PCR amplification after genomic extraction. Similarly, ET-qPCR utilizes nucleases to degrade exposed genetic material before PCR. However, damage to viral components does not always abrogate infectivity, leaving questions as to the accuracy of chemically screened PCR assays in assessing viral titers (Diez-Valcarce et al., 2011; Pecson et al., 2009).

MOLECULAR BEACONS

Molecular beacons remain an emerging integrated method for quantifying viruses as they require initial stages of viral replication without the need for amplification. Generally, a MB includes a partially self-complimentary oligo able to form a stem-loop secondary structure and a reporter fluorophore/quencher pair. The loop portion of the oligo is specific to a target sequence while the opposite 5′ and 3′ ends are bound to a paired reporter fluorophore and quencher, respectively. The absence of a target sequence thermodynamically favors the formation of the closed stem-loop secondary structure, thereby bringing the reporter and quencher into close proximity. While closed, light capable of exciting the fluorophore, $h\nu_{ex}$, is transferred to the quencher via contact Förster/Fluorescent Resonance Energy Transfer (FRET) and released as heat. When a target sequence is present, the loop portion binds to form a hybrid molecule that relaxes the MB secondary structure; thus, the distance between the reporter and quencher increases, FRET is reduced, and fluorescence occurs (Figure 1.2; Tyagi and Kramer, 1996).

Attaching a cell penetrating peptide (CPP) to a MB specific to a sequence of viral mRNA creates an assay capable of detecting early stages of viral replication rapidly. Like IFA, a MB can detect an early stage of viral replication; specifically, the production of mRNA (Santangelo et al., 2006). Also similar, the MB is delivered by permeabilizing cells, but the relatively smaller size of the MB also allows for intracellular delivery by CPP (Santangelo, 2010; Yeh et al., 2008b). The first CPP to be discovered, Trans-activator of transcription (Tat), was believed to directly translocate the plasma membrane, but is now

believed to cross the cell membrane via endocytosis (Herce and Garcia, 2007; Silhol et al., 2002). Afterwards, cysteine residues of Tat form a pore in the cytosed vesicle to release the CPP and any attached compounds (Saalik et al., 2004). Alternatively, amino acids rich in guanidine groups ($HNC(NH_2)_2$), like arginine, may directly translocate the cytoplasm through an affinity towards plasma membrane phosphate groups (Lo and Wang, 2008).

Once intracellular, the MB can target complementary single stranded oligos, such as viral mRNA. Although the genomic structures of viruses are varied, the production of mRNA is an early and universal step in replication. In the presence of specific mRNA from viral replication, the MB will bind, FRET is relaxed and fluorescence occurs. Additionally, MB have been shown to be capable of differentiating between targets possessing one NT difference; thereby avoiding issues of specificity exhibited by antibodies used for IFA (Dunams et al., 2012). Furthermore, the MB is designed from readily available sequence data, making it more accessible to labs than antibody production (Yeh et al., 2008a).

Objectives and Approach

The genomic structure and near-ubiquitous seroprevalence make BKPyV a potentially important organism in assessing water quality and informing treatment policy; however, the ability of BKPyV to affect either is precluded by the lack of a rapid infectious assay. To this end, we applied the rationale of integrated methods to develop MB and ET-qPCR assays capable of detecting BKPyV, which were compared to standard quantification assays (IFA). These methods were used to characterize the disinfection profile of BKPyV following exposure to UV_{254}, chlorine, heat, and artificial sunlight. Furthermore, these detection and inactivation methods were applied to Ad2 and PV1. In lieu of IFA, Ad2 and PV1 were detected via traditional PA; nor were these viruses exposed to artificial sunlight. Obtaining this information assesses LT2 standards as well as the utility of BKPyV as an FIO (Reano and Yates, 2016).

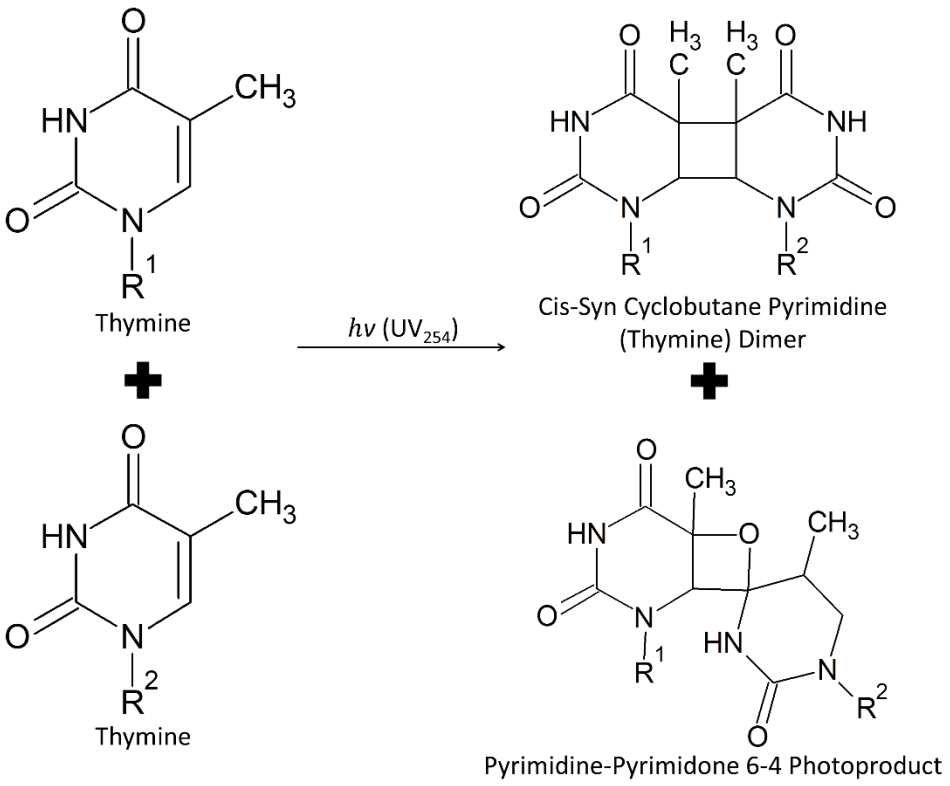

Figure 1.1. Photoproducts of pyrimidine bases (thymine) following exposure to UV_{254}. R^n, ribose sugar.

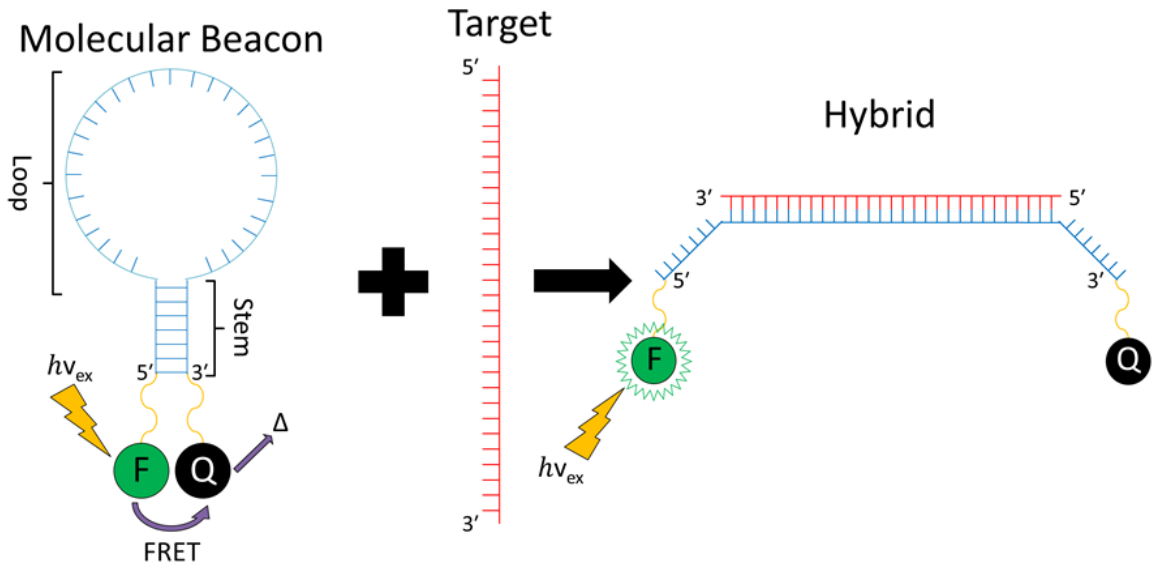

Figure 1.2. Molecular beacon structure and hybridization. Δ, heat; F, fluorophore; Q, quencher.

REFERENCES

Ahsan, N., 2006. Polyomaviruses and Human Diseases. Springer Science + Business Media, New York.

Albinana-Gimenez, N., Miagostovich, M.P., Calgua, B., Huguet, J.M., Matia, L., Girones, R., 2009. Analysis of adenoviruses and polyomaviruses quantified by qPCR as indicators of water quality in source and drinking-water treatment plants. Water Res. 43, 2011–2019. doi:10.1016/j.watres.2009.01.025

Antonsson, A., Green, A.C., Mallitt, K., O' Rourke, P.K., Pawlita, M., Waterboer, T., Neale, R.E., 2010. Prevalence and stability of antibodies to the BK and JC polyomaviruses: a long-term longitudinal study of Australians. J. Gen. Virol. 91, 1849–1853. doi:10.1099/vir.0.020115-0

Bounty, S., Rodriguez, R.A., Linden, K.G., 2012. Inactivation of adenovirus using low-dose UV/H2O2 advanced oxidation. Water Res. 46, 6273–6278. doi:10.1016/j.watres.2012.08.036

Cutler, D., Miller, G., 2005. The Role of Public Health Improvements in Health Advances: the Twentieth-Century United States. Demography 42, 1–22.

Diez-Valcarce, M., Kovac, K., Raspor, P., Rodriguez-Lazaro, D., Hernández, M., 2011. Virus genome quantification does not predict norovirus infectivity after application of food inactivation processing technologies. Food Environ. Virol. 3, 141–146. doi:10.1007/s12560-011-9070-9

Dorevitch, S., Deflorio-Barker, S., Jones, R.M., Liu, L., 2015. Water quality as a predictor of gastrointestinal illness following incidental contact water recreation. Water Res. 83, 94–103. doi:10.1016/j.watres.2015.06.028

Dunams, D., Sarkar, P., Chen, W., Yates, M. V., 2012. Simultaneous detection of infectious human echoviruses and adenoviruses by an in situ nuclease-resistant molecular beacon-based assay. Appl. Environ. Microbiol. 78, 1584–1588. doi:10.1128/AEM.05937-11

Eischeid, A.C., Thurston, J.A., Linden, K.G., 2011. UV disinfection of adenovirus: present state of the research and future directions. Crit. Rev. Environ. Sci. Technol. 41, 1375–1396. doi:10.1080/10643381003608268

Ferguson, A.S., Layton, A.C., Mailloux, B.J., Culligan, P.J., Williams, D.E., Smartt, A.E., Sayler, G.S., Feighery, J., McKay, L.D., Knappett, P.S.K., Alexandrova, E., Arbit, T., Emch, M., Escamilla, V., Matin, K.M., Alam, M.J., Streat, P.K., Yunus, M., Geen, A. Van, 2012. Comparison of fecal indicators with pathogenic bacteria and rotavirus in groundwater. Sci. Total Environ. 431, 314–322. doi:10.1016/j.scitotenv.2012.05.060

Franks, A.H., Harmsen, H.J.M., Raangs, G.C., Jansen, G.J., Schut, F., Welling, G.W., 1998. Variations of bacterial populations in human feces measured by fluorescent in situ hybridization with group-specific 16S rRNA-targeted oligonucleotide probes. Appl. Environ. Microbiol. 64, 3336–3345.

Freese, S.D., Nozaic, D.J., 2004. Chlorine: Is it really so bad and what are the alternatives? Water SA 30, 566–572. doi:10.4314/wsa.v30i5.5161

Girones, R., Ferrús, M.A., Alonso, J.L., Rodriguez-Manzano, J., Calgua, B., Corrêa, A. de A., Hundesa, A., Carratala, A., Bofill-Mas, S., 2010. Molecular detection of pathogens in water - the pros and cons of molecular techniques. Water Res. 44, 4325–4339. doi:10.1016/j.watres.2010.06.030

Hatt, J.K., Löffler, F.E., 2012. Quantitative real-time PCR (qPCR) detection chemistries affect enumeration of the Dehalococcoides 16S rRNA gene in groundwater. J. Microbiol. Methods 88, 263–270. doi:10.1016/j.mimet.2011.12.005

Herce, H.D., Garcia, A.E., 2007. Molecular dynamics simulations suggest a mechanism for translocation of the HIV-1 TAT peptide across lipid membranes. Proc. Natl. Acad. Sci. U. S. A. 104, 20805–10. doi:10.1073/pnas.0706574105

Hewitt, J., Greening, G.E., Leonard, M., Lewis, G.D., 2013. Evaluation of human adenovirus and human polyomavirus as indicators of human sewage contamination in the aquatic environment. Water Res. 47, 6750–6761. doi:10.1016/j.watres.2013.09.001

Hijnen, W.A.M., Beerendonk, E.F., Medema, G.J., 2006. Inactivation credit of UV radiation for viruses, bacteria and protozoan (oo)cysts in water: a review. Water Res. 40, 3–22. doi:10.1016/j.watres.2005.10.030

Huang, J.-J., Hu, H.-Y., Tang, F., Li, Y., Lu, S.-Q., Lu, Y., 2011. Inactivation and reactivation of antibiotic-resistant bacteria by chlorination in secondary effluents of a municipal wastewater treatment plant. Water Res. 45, 2775–2781. doi:10.1016/j.watres.2011.02.026

Huang, J.-J., Hu, H.-Y., Wu, Y.-H., Wei, B., Lu, Y., 2013. Effect of chlorination and ultraviolet disinfection on tetA-mediated tetracycline resistance of Escherichia coli. Chemosphere 90, 2247–2253. doi:10.1016/j.chemosphere.2012.10.008

Huber, M.M., Korhonen, S., Ternes, T.A., Von Gunten, U., 2005. Oxidation of pharmaceuticals during water treatment with chlorine dioxide. Water Res. 39, 3607–3617. doi:10.1016/j.watres.2005.05.040

Johnson, K.M., Kumar, M.R.A., Ponmurugan, P., Gananamangai, B.M., 2010. Ultraviolet radiation and its germicidal effect in drinking water purification. Jounral Phytol. 2, 12–19.

Kato, A., Kitamura, T., Sugimoto, C., Ogawa, Y., Nakazato, K., Nagashima, K., Hall, W.W., Kawabe, K., Yogo, Y., 1997. Lack of evidence for the transmission of JC polyomavirus between human populations. Arch. Virol. 142, 875–882.

Knight, A., Haines, J., Stals, A., Li, D., Uyttendaele, M., Knight, A., Jaykus, L.-A., 2016. A systematic review of human norovirus survival reveals a greater persistence of human norovirus RT-qPCR signals compared to those of cultivable surrogate viruses. Int. J. Food Microbiol. 216, 40–49. doi:10.1016/j.ijfoodmicro.2015.08.015

Knipe, D.M., Howley, P.M., 2013. Fields Virology, 6th ed. Lippincott Williams & Wilkins, Philadelphia.

Kovac, K., Bouwknegt, M., Diez-Valcarce, M., Raspor, P., Hernández, M., Rodríguez-lázaro, D., 2012. Evaluation of high hydrostatic pressure effect on human adenovirus using molecular methods and cell culture. Int. J. Food Microbiol. 157, 368–374. doi:10.1016/j.ijfoodmicro.2012.06.006

Li, Y.J., Wu, H.H., Weng, C.H., Chen, Y.C., Hung, C.C., Yang, C.W., Wang, R.Y.L., Sakamoto, N., Tian, Y.C., 2012. Cyclophilin A and nuclear factor of activated T cells are essential in cyclosporine-mediated suppression of Polyomavirus BK replication. Am. J. Transplant. 12, 2348–2362. doi:10.1111/j.1600-6143.2012.04116.x

Lo, S.S., Wang, S., 2008. An endosomolytic Tat peptide produced by incorporation of histidine and cysteine residues as a nonviral vector for DNA transfection. Biomaterials 29, 2408–2414. doi:10.1016/j.biomaterials.2008.01.031

Mac Kenzie, W.R., Hoxie, N.J., Proctor, M.E., Gradus, M.S., Blair, K.A., Peterson, D.E., Kazmierczak, J.J., Addiss, D.G., Fox, K.R., Rose, J.B., Davis, J.P., 1994. A massive outbreak in Milwaukee of Cryptosporidium infection transmitted through the public water supply. N. Engl. J. Med. 331, 161–167.

McGuire, M.J., 2013. The Chlorine Revolution. American Water Works Association, Denver, CO.

Moriyama, T., Sorokin, A., 2008. Intracellular trafficking pathway of BK Virus in human renal proximal tubular epithelial cells. Virology 371, 336–349. doi:10.1016/j.virol.2007.09.030

Nakanishi, A., Nakamura, A., Liddington, R., Kasamatsu, H., 2006. Identification of amino acid residues within Simian Virus 40 capsid proteins Vp1 , Vp2 , and Vp3 that are required for their interaction and for viral infection. J. Virol. 80, 8891–8898. doi:10.1128/JVI.00781-06

Nevers, M.B., Whitman, R.L., 2005. Nowcast modeling of Escherichia coli concentrations at multiple urban beaches of southern Lake Michigan. Water Res. 39, 5250–5260. doi:10.1016/j.watres.2005.10.012

Olsen, M.T., Bérubé, M., Robbins, J., Palsbøll, P.J., 2012. Empirical evaluation of humpback whale telomere length estimates ; quality control and factors causing variability in the singleplex and multiplex qPCR methods. BMC Genet. 13. doi:10.1186/1471-2156-13-77

Payment, P., Locas, A., 2011. Pathogens in water: value and limits of correlation with microbial indicators. Ground Water 49, 4–11. doi:10.1111/j.1745-6584.2010.00710.x

Pecson, B.M., Martin, L.V., Kohn, T., 2009. Quantitative PCR for determining the infectivity of bacteriophage MS2 upon inactivation by heat , UV-B Radiation , and singlet oxygen: Advantages and limitations of an enzymatic treatment to reduce false-positive results. Appl. Environ. Microbiol. 75, 5544–5554. doi:10.1128/AEM.00425-09

Rainbow, A.J., 1980. Reduced capacity to repair irradiated adenovirus in fibroblasts from Xeroderma pigmentosum heterozygotes. Cancer Res. 40, 3945–3949.

Reano, D.C., Yates, M. V., 2016. Determining the Solar Inactivation Rate of BK Polyomavirus by Molecular Beacon. Environ. Sci. Technol. 50, 7090–7094. doi:10.1021/acs.est.6b01541

Reckhow, D.A., Linden, K.G., Kim, J., Shemer, H., Makdissy, G., 2010. Effect of UV treatment on DBP formation. J. Am. Water Work. Assoc. 102, 100–113.

Saalik, P., Elmquist, A., Hansen, M., Padari, K., Saar, K., Viht, K., Langel, U., Pooga, M., 2004. Protein cargo delivery properties of cell-penetrating peptides. A comparative study. Bioconjug. Chem. 15, 1246–1253.

Santangelo, P., Nitin, N., LaConte, L., Woolums, A., Bao, G., 2006. Live-cell characterization and analysis of a clinical isolate of Bovine Respiratory Syncytial Virus , using molecular beacons. J. Virol. 80, 682–688. doi:10.1128/JVI.80.2.682

Santangelo, P.J., 2010. Molecular beacons and related probes for intracellular RNA imaging. Wiley Interdiscip. Rev. Nanomedicine Nanobiotechnology 2, 11–19. doi:10.1002/wnan.052

Santos, F.C.P. dos, Do, E.M.M., Katz, G., Angerami, R.N., Colombo, S., Souza, E.R. de, Labruna, M.B., Silva, M.V. da, 2012. Brazilian spotted fever: Real-time PCR for diagnosis of fatal cases. Ticks Tick. Borne. Dis. 3, 311–313. doi:10.1016/j.ttbdis.2012.10.027

Schuch, A.P., Menck, C.F.M., 2010. The genotoxic effects of DNA lesions induced by artificial UV-radiation and sunlight. J. Photochem. Photobiol. B Biol. 99, 111–116. doi:10.1016/j.jphotobiol.2010.03.004

Silhol, M., Tyagi, M., Giacca, M., Lebleu, B., Vive, E., 2002. Different mechanisms for

cellular internalization of the HIV-1 Tat-derived cell penetrating peptide and recombinant proteins fused to Tat. Eur. J. Biochem. 269, 494–501.

Sivaraman, D., Yeh, H.-Y., Mulchandani, A., Yates, M. V., Chen, W., 2013. Use of flow cytometry for rapid, quantitative detection of poliovirus-infected Cells via TAT peptide-delivered molecular beacons. Appl. Environ. Microbiol. 79, 696–700. doi:10.1128/AEM.02429-12

Tyagi, S., Kramer, F.R., 1996. Molecular beacons: probes that fluoresce upon hybridization. Nat. Biotechnol. 14, 303–308.

United States Environmental Protection Agency, 2011. Standard Operation Procedure for Quality Assurance of Purified Water.

United States Environmental Protection Agency, 2005. Technologies and Costs Document for the Final Long Term 2 Enhanced Surface Water Treatment Rule and Final Stage 2 Disinfectants and Disinfection Byproducts Rule. doi:10.1017/CBO9781107415324.004

Vanchiere, J.A., Abudayyeh, S., Copeland, C.M., Lu, L.B., Graham, D.Y., Butel, J.S., 2009. Polyomavirus shedding in the stool of healthy adults. J. Clin. Microbiol. 47, 2388–2391. doi:10.1128/JCM.02472-08

Wölfel, R., Pfeffer, M., Essbauer, S., Nerkelun, S., Dobler, G., 2006. Evaluation of sampling technique and transport media for the diagnostics of adenoviral eye infections. Graefe's Arch. Clin. Exp. Ophthalmol. 244, 1497–1504. doi:10.1007/s00417-006-0283-9

Yates, M. V., 2007. Classical indicators in the 21st century — far and beyond the coliform. Water Environ. Res. 79, 279–286. doi:10.2175/106143006X123085

Yeh, H.-Y., Hwang, Y.-C., Yates, M. V., Mulchandani, A., Chen, W., 2008a. Detection of Hepatitis A Virus by using a combined cell culture-molecular beacon assay. Appl. Environ. Microbiol. 74, 2239 – 2243. doi:10.1128/AEM.00259-08

Yeh, H.-Y., Yates, M. V., Mulchandani, A., Chen, W., 2008b. Visualizing the dynamics of viral replication in living cells via Tat peptide delivery of nuclease-resistant molecular beacons. Proc. Natl. Acad. Sci. U. S. A. 105, 17522–17525. doi:10.1073/pnas.0807066105

CHAPTER TWO: BK POLYOMAVIRUS DETECTION BY MOLECULAR BEACON

ABSTRACT

The ubiquitous detection of polyomaviruses in sewage samples and high rates of seroprevalence in human populations make BKPyV an attractive alternative to current FIO. However, the lack of a rapid detection assay limits further investigations towards its ability to assess water quality. Here, a MB developed for BKPyV reduced detection times equivalent to assays of current FIO and accurately quantified viral titers relative to the current standard for polyomavirus quantification (IFA, $R^2 = 0.97$). Despite an inability to deliver MB by CPP, the developed assay allows for rapid quantification of infective BKPyV to enable characterization of its disinfection profile.

INTRODUCTION

The detection of native microbiological inhabitants of human (and some mammalian) gastrointestinal tracts allows for indirect, but rapid, assessments of water quality. The need for rapid results capable of assessing microbiological viability often relegates these FIO to bacterial species, which can exhibit low correlations to viral pathogens (National Research Council, 2004). BK Polyomavirus remains a prospective alternative to standard FIO, but lacks a rapid detection assay capable of quantifying infective viral titers due to characteristically long replication times. The current standard for polyomavirus detection utilizes fluorescent antibodies that detect viral proteins made during replication, but still requires significant time to obtain results (Calgua et al., 2011). Molecular beacons remain an alternative integrated method capable of rapidly quantifying viral titers and assessing infectivity, but have not yet been applied to BKPyV.

Molecular beacons are self-complementary oligos capable of forming a stem-loop secondary structure and contain paired fluorescent and quenching moieties. When the stem-loop is formed, light capable of exciting the fluorophore is absorbed by the quencher and released as heat through contact FRET. The presence of a target sequence complementary to the loop region of the MB abrogates the formation of the stem-loop secondary structure through hybridization. This thermodynamically-favored reaction increases the distance between the fluorophore and quencher, FRET is relaxed, and a fluorescent signal emerges (Tyagi and Kramer, 1996). Due to the specificity between loop and target sequences, MB have been employed to differentiate between single nucleotide

polymorphisms, allow for multiplex qPCR assays, and here, to evidence viral replication (Dunams et al., 2012; Mhlanga and Malmberg, 2001; Vet et al., 1999).

The production of mRNA remains a universal stage of all viral replication and ideal target for MB assays to evidence infectivity. To reach viral mRNA, MB must cross the plasma membranes of infected cells, traditionally achieved by fixation or CPP delivery (Burris et al., 2013; Yeh et al., 2008). Although multiple CPP exist, all cross the plasma membrane via endocytotic-mediated uptake or direct translocation. The first CPP to be discovered, Tat (YGRKKRRQRRR), was identified in human immunodeficiency viruses and follows the former; while newer synthetic peptides, like R9 (RRRRRRRRR) directly cross the plasma membrane (Wang et al., 2014). Endocytosis remains less preferable than direct translocation due to the necessity of Tat, and attached cargoes (i.e., MB), to escape the endocytosed vesicle before entering the cytosol (Herce and Garcia, 2007). However, the addition of imidazole groups ($(CH)_2NCH$) contained in histidine amino acid residues can cause endosome rupture due to swelling. The ability of cationic guanidium groups ($HNC(NH_2)_2$) contained in arginine residues to interact with negatively charged phospholipid heads avoids this issued by directly crossing the plasma membrane (Liu et al., 2011). Following cytosolic delivery, the MB can signal for the presence of viral mRNA; however, CPP must not deliver this cargo to cellular nuclei to avoid autofluorescence (Nitin et al., 2004).

Although MB possess enough target specificity to differentiate between single nucleotide polymorphisms; the density of nuclear genetic material can form nonspecific bonds with the MB that yield autofluorescence. Some CPP, like Tat, even contain nuclear

localization signals capable of delivering the MB to the nucleus (Saalik et al., 2004). Regardless, previous studies have successfully employed Tat-delivered MB via covalent bonding between these two moieties (Nitin et al., 2004; Sivaraman et al., 2013). Alternatively, the reductive intracellular conditions of the cytoplasm (e.g., reductase and glutathione) allows for the formation of a reversible bond between thiol groups added to the MB and CPP (Hällbrink et al., 2001). This study utilized multiple CPP, varying in their attachment to the MB, to detect viral mRNA produced intracellularly. However, further modifications were necessary to prevent intracellular degradation of the MB.

In addition to oxidative sensitivity, inherent cellular mechanisms capable of eliminating foreign genetic material can cause MB degradation, and hence autofluorescence (Su et al., 2011; Tsourkas et al., 2002). For example, lacking the appropriate methylation pattern can mark foreign oligos, like the MB, for degradation. Additionally, MB can be composed of either DNA or, less stable, RNA. Although RNA exhibits enhanced affinity to RNA targets, the 2′ hydroxyl (OH) of RNA serves as a facile site for degradation (Wang et al., 2009). Utilizing 2′-*O*-methyl ribonucleotides in lieu of RNA confers resistance to both nucleases and hydrolysis by replacing the 2′ hydroxyl with a methoxy group (OCH_3). Alternatively, phosphorothioate linkages that replace phosphodiester bonds between NT further enhance resistance to nucleases, but may exhibit affinity to some proteomic targets and delivery compounds (Chen et al., 2009; Karim et al., 1995; Neumann and Smith, 1967; Waki et al., 2011).

MATERIALS AND METHODS

Propagation of BKPyV:

Primary human renal proximal tubule epithelial cells (RPTEC, CC-2553, Lonza, Basel, Switzerland), grown in renal epithelial media (REM) with 10% fetal bovine serum (FBS), allowed for the propagation of BKPyV obtained from the American Type Culture Collection (VR-837, Manassas, VA, USA). The REM consisted of a proprietary blend of human epidermal growth factor, hydrocortisone, epinephrine, insulin, triiodothyronine, transferrin, gentamicin, and amphotericin purchased from Lonza (CC-3190). All utilized FBS was heat inactivated at 56 °C for one hour with gentle mixing for the first 5 minutes, then kept at 4 °C until same-day use. Media was changed every two to three days and washed with HEPES Buffered Saline (HBS). A 2 × formulation for HBS is as follows; 50 mM HEPES, 274 mM NaCl, 10 mM KCl, 1.48 mM Na_2HPO_4, and 11.1 mM dextrose. The 2 × solution was adjusted to a pH of 7.05 with 10 N NaOH, 0.22 µm filter sterilized, and kept at 4 °C. Finally, the 2 × HBS was diluted to 1 × with H_2O, adjusted to a pH of 7.3 with 2N NaOH, 0.22 µm filter sterilized again, and stored at 4 °C. Subculturing with trypsin-EDTA 0.05 % occurred when flasks exceeded 80 % confluency and cells were discarded after nine passages. Unless otherwise stated, all incubation steps occurred at 37 °C with 5 % CO_2 under humidified conditions.

Propagation of BKPyV occurred in 80 % confluent monolayers of RPTEC. Specifically, T-75 cm^2 flasks were infected with 3 mL of viral inoculum diluted in REM containing 5 % FBS and allowed to incubate for 1 hour. Viral inocula were kept in flasks

and supplemented with 10 mL of REM 5 % FBS before incubating for up to four weeks. Media, changed on a weekly basis, was kept for the final production of BKPyV stocks by concentrating through centrifugation at 960 × g in a JA-17 rotor (Beckman Coulter, Brea, CA, USA) for 15 minutes at 4 °C. The resulting pellet was resuspended in 10 % of the original volume and stored at -80 °C. Cells were harvested after exhibiting 80 % CPE (~ 24 DPI) by mechanical disruption and concentrated similarly. All collected supernatants were pooled and freeze-thawed three times at -80 °C and 37 °C. Next, the pooled contents were layered on 4 mL of reassociation buffer (150 mM NaCl, 20 mM Tris base, 0.1 % v/v Tween® 20, 1 mM anhydrous $CaCl_2$, and 20 % w/v sucrose) and centrifuged for 2 hours at 100,000 × g in a SW-41 rotor (Beckman Coulter) at 4 °C. The resulting pellet was dissolved in 1 mL of buffer A (1 M Tris-Cl, 5 M NaCl, 0.1 M anhydrous $CaCl_2$), aliquoted, and stored at -80 °C until use.

Immunofluorescence Assay:

A modified IFA described by Moriyama and Sorokin (2008) was used to quantify BKPyV titers. Specifically, RPTEC were split into Nunc® Lab-Tek 8-well Permanox® chamber slides (0.8 cm^2 per well, C7182-1, Sigma-Aldrich, St. Louis, MO, USA) at a concentration of 1E5 cells per well and incubated overnight to reach 80 % confluency. Next wells were infected with 150 µL of viral inoculum diluted in REM 2 % FBS and allowed to incubate for one hour with gentle rocking every 15 minutes. After infection, inoculum was replaced with 300 µL REM 2 % FBS and allowed to incubate for 72 hours.

After incubation, wells were washed with 350 µL of autoclaved Tris Buffered Saline (TBS, 150 mM NaCl, 20 mM Tris base, pH 7.5) and fixed with 150 µL ice-cold absolute methanol for 20 minutes at -20 °C. Cellular permeabilization to allow for antibody delivery was achieved through the addition of 300 µL TBS containing 0.1 % (v/v) Tween® 20 (TTBS) and 1% (w/v) bovine serum albumin fraction V (BSA) for five minutes. Permeabilized cells were then blocked from nonspecific antibody binding by incubating each well with 300 µL TTBS 3% BSA for 30 minutes.

Viral particles were detected through the addition of an antibody specific to the large T antigen of the closely related SV40 Polyomavirus. Specifically, 150 µL of the primary IgG mouse antibody PAb416 (EMD Millipore, Billerica, MA, USA) was diluted to 1 µg/mL in TTBS 1 % BSA and added to each well before incubation at room temperature for 1 hour. Wells were then washed with 350 µL of TTBS 1 % BSA for 5 minutes at room temperature to remove unbound antibodies before the addition of the secondary antibody. Next, 150 µL of fluorescein-conjugated anti-mouse IgG antibodies from goats (DP02, EMD Millipore) were diluted to 5 µg/mL in TTBS 1 % BSA and allowed to incubate in wells for 40 minutes at room temperature. Unbound secondary antibodies were removed by washing wells with 350 µL of TTBS 1 % BSA for 5 minutes at room temperature (Calgua et al., 2011; Moriyama et al., 2007).

Before fluorescent microscopy, wells were stained and mounted with VECTASHIELD® Mounting Media containing DAPI (1.5 µg/mL, H-1200, Vector Laboratories, Burlingame, CA, USA). Imaging occurred on an IX71 inverted fluorescent microscope utilizing a 100W Hg bulb burner (U-RFL-T, Olympus, Tokyo, Japan) and a

Retiga EXi Fast 1394 CCD camera (QImaging, Surrey, BC, Canada). All filters used in experiments were obtained from Chroma Technology Corporation (Bellows Falls, VT, USA); specifically, DAPI (31000v2; AT350/50x;400dclp;D460/50m) and fluorescein (49002; ET470/40x;T495lpxr;ET525/50m). Finally, all images were processed with Image-Pro version 6.3 (Media Cybernetics, Incorporated, Rockville, MD, USA).

Molecular Beacon Design and Synthesis:

Identifying a MB target required identifying conserved regions of BKPyV. To this end, 30 BKPyV sequences, deposited in GenBank, were aligned through Clustal Omega (Sayers et al., 2009; Sievers et al., 2011). Conserved regions were converted to reverse complementary sequences for MB design. Candidate MB that met appropriate thermodynamic criteria were validated against known BKPyV transcripts to ensure target presence during replication (Vet and Marras, 2005). Final sequences were synthesized by Gene Link (Hawthorne, NY, USA) utilizing 2′-*O*-methyl ribonucleotides to enhance intracellular stability. The use of a 4-Thio-Uridine provided a NT with a free thiol group for CPP attachment. Phosphorothioate bonds were used to polymerize this nucleotide to the MB as a methoxy version was unavailable commercially (Figure 2.1). A quantum dot with $h\nu_{525}$ (Qdot 525) and Black Hole Quencher® 1 (BHQ-1) were attached to the 5′ and 3′ ends to enable FRET, respectively (Figure 2.2). The synthesized MB was diluted to 5 µM in water under anoxic conditions to preserve a thiol for CPP attachment (Klein, 2015).

Cell Penetrating Peptide Design and Attachment to the MB:

Combinations of Tat and R9, utilizing reversible or covalent bonds, were tested for MB delivery. The CPP were synthesized by Thermo Fisher Scientific (Waltham, MA, USA) above 80 % purity and reconstituted in water under anoxic conditions. Residues utilized acetylated and amidated N and C termini, respectively, to enhance stability and peptide activity (Hershko et al., 1984; Kim and Seong, 2001). Finally, glycine residues were added near the reaction site to ensure free rotation of the CPP (Table 2.1; Yu et al., 1992). Reversible attachment of the MB to the CPP occurred via thiols contained in cysteine and a modified NT of the MB (Figure 2.3). Cysteine-containing CPP were reconstituted to 5 µM and reacted with MB in a 1:1 ratio for 2 hours in the dark at room temperature, then overnight at 4 °C. Conjugated products were purified via overnight dialysis in Slide-A-Lyzer™ 10000 MWCO dialysis units (66385, Thermo Fisher Scientific) against 300 mL TBS at 4 °C. Covalent bonding between the CPP and MB occurred by reacting the thiol group of the MB with a maleimide on the CPP (Figure 2.4). Polymerization followed similar reaction and purification steps to reversible attachment; however, the CPP was reconstituted to 7.5 µM for a 1.5:1 reaction ratio.

Molecular Beacon Assay:

Initial attempts at BKPyV detection utilized a MB delivered by CPP. Specifically, 80 % confluent cells were infected with BKPyV in manner similar to IFA, and allowed to incubate overnight. Cells were then washed with TBS, exposed to 100 µL MB diluted to 5 nM or 25 pM in REM 2 % FBS, and allowed to incubate for 15 or 30 minutes at 37 °C. Wells were then aspirated and cells were washed with 300 µL of REM 2 % FBS before

fluorescent microscopy (Qdot 525 filter; 32010; E460SPUVv2;475dcxru;D525/40m; Chroma Technology Corporation).

To avoid cytotoxic effect induced by CPP delivery, MB assays were repeated through fixation. Chamber slides of 90 % confluent RPTEC were infected with BKPyV and allowed to incubate overnight. Next, cells were fixed with a 4 % paraformaldehyde solution made in HBS for 10 minutes, and permeabilized with TTBS for 5 min at room temperature. Each well then received 150 µL of unconjugated (i.e., lacking CPP) MB, diluted to 5 nM in REM 2% FBS, and was allowed to incubate at 37 °C for 30 minutes before imaging via fluorescent microscopy. The specificity of the MB was tested separately by adding 100 µL of an oligo diluted to 10 µM in TBS possessing a near-complementary sequence to the MB loop region, differing by one NT.

RESULTS

Molecular Beacon Design:

Alignment of 30 BKPyV sequences revealed VP1 a conserved region for MB design. Production of capsid protein VP1 occurs early in the replication cycle and is conserved among all polyomaviruses. Furthermore, VP1 remains the only integral component of capsid formation, making it an ideal MB target. The MB sequence and modifications can be found in Table 2.2.

Molecular Beacon Assay:

Cells continually exhibited cytotoxic effects after exposure to a variety of CPP-bound MB, despite varied concentrations and exposure times. Therefore, fixation and permeabilization provided an alternative approach to MB delivery. Results obtained from MB after fixation indicated a strong correlation to quantification by IFA (R^2 = 0.97), and exhibited no fluorescence following exposure to near-complementary oligos. Representative images of both assays are displayed in Figures 2.5 and 2.6, respectively.

DISCUSSION

The MB accurately quantified titers of BKPyV following cellular fixation. Although CPP have been utilized to deliver MB capable of detecting intracellular oligos, CPP yielded extensive cytotoxic effects in host cells. Interestingly, the mechanism of action for CPP HR9 was elucidated, in part, by subcellular localization of quantum dots following CPP delivery into (immortalized) cultured cells (Liu et al., 2011). Regardless, cellular fixation and permeabilization allowed for accurate quantification of BKPyV titers by MB. Fixation required additional steps and time relative to CPP delivery, but the MB still improved detection times of BKPyV significantly.

The improved assay times of BKPyV allows for potential adoption as a FIO. Immunoassays remain the standard for detection of infectious polyomaviruses as traditional culture methods (e.g., PA) are precluded by the extended viral replication periods (Li et al., 2012). Although effective, incubation times required for IFA results limit their utility as indicators of water quality (Girones et al., 2010). Similar to current FIO quantification protocols, results from the developed MB assay require less than 24 hours. Additionally, a MB is designed from information deposited in readily available sequence databases, and is capable of differentiating between targets differing by one NT (Mhlanga and Malmberg, 2001; Vet and Marras, 2005). Furthermore, the MB assay required fewer processing steps than IFA. Although the MB provides a viable assay to quantify BKPyV, the appropriateness of this virus as an FIO requires knowledge of its disinfection profile.

Table 2.1. Amino acid sequences of CPP used for QD delivery.

Peptide Sequence
CGGHHHHHRRRRRRRRRHHHHH
CRRRRRRRRRHHHHH
CGGYGRKKRRQRRR
CGGRRRRRRRRR
Maleimide-RRRQRRKKRGY
Maleimide-GGRRRRRRRRRHHHHH

Table 2.2. Alignment of BKPyV sequences used to design MB. *, conserved nucleotide; *, MB loop sequence

Accession Number	Position Start	Sequence	Position End
ref|NC_001538.1|	1646	T A A T A A A A G G A G G A G T A G A A G T T C T A G A A G T T A A A A C T G G G G T A G A T G C T A T	1697
dbj|AB485709.1|	1561	T A A T A A A A G G A G G A G T A G A A G T T C T A G A A G T T A A A A C T G G G G T A G A T G C T A T	1612
dbj|AB298942.1|	1526	T A A T A A A A G G A G G A G T A G A A G T T C T A G A A G T T A A A A C T G G G G T A G A T G C T A T	1577
dbj|AB369095.1|	1526	T A A T A A A A G G A G G A G T A G A A G T T C T A G A A G T T A A A A C T G G G G T A G A T G C T A T	1577
dbj|AB365170.1|	1526	T A A T A A A A G G A G G A G T A G A A G T T C T A G A A G T T A A A A C T G G G G T A G A T G C T A T	1577
dbj|AB217921.1|	1526	T A A T A A A A G G A G G A G T A G A A G T T C T A G A A G T T A A A A C T G G G G T A G A T G C T A T	1577
dbj|AB464954.1|	1526	T A A T A A A A G G A G G A G T A G A A G T T C T A G A A G T T A A A A C T G G G G T A G A T G C T A T	1577
dbj|AB298946.1|	1526	T A A T A A A A G G A G G A G T A G A A G T T C T A G A A G T T A A A A C T G G G G T A G A T G C T A T	1577
dbj|AB298944.1|	1526	T A A T A A A A G G A G G A G T A G A A G T T C T A G A A G T T A A A A C T G G G G T A G A T G C T A T	1577
dbj|AB298940.1|	1526	T A A T A A A A G G A G G A G T A G A A G T T C T A G A A G T T A A A A C T G G G G T A G A T G C T A T	1577
dbj|AB485694.1|	1526	T A A T A A A A G G A G G A G T A G A A G T T C T A G A A G T T A A A A C T G G G G T A G A T G C T A T	1577
dbj|AB298941.1|	1526	T A A T A A A A G G A G G A G T A G A A G T T C T A G A A G T T A A A A C T G G G G T A G A T G C T A T	1577
dbj|AB263926.1|	1526	T A A T A A A A G G A G G A G T A G A A G T T C T A G A A G T T A A A A C T G G G G T A G A T G C T A T	1577
dbj|AB263912.1|	1526	T A A T A A A A G G A G G A G T A G A A G T T C T A G A A G T T A A A A C T G G G G T A G A T G C T A T	1577
gb|JF894228.1|	1665	T A A T A A A A G G A G G A G T A G A A G T T C T A G A A G T T A A A A C T G G G G T A G A T G C T A T	1716
dbj|AB369090.1|	1526	T A A T A A A A G G A G G A G T A G A A G T T C T A G A A G T T A A A A C T G G G G T A G A T G C T A T	1577
dbj|AB301090.1|	1526	T A A T A A A A G G A G G A G T A G A A G T T C T A G A A G T T A A A A C T G G G G T A G A T G C T A T	1577
gb|JN192431.1|	1634	T A A T A A A A G G A G G A G T A G A A G T T C T A G A A G T T A A A A C T G G G G T A G A T G C T A T	1685
gb|DQ989801.1|	1259	T A A T A A A A G G A G G A G T A G A A G T T C T A G A A G T T A A A A C T G G G C T A G A T G C T A T	1310
gb|DQ989795.1|	1259	T A A T A A A A G G A G G A G T A G A A G T T C T A G A A G T T A A A A C T G G G C T A G A T G C T A T	1310
dbj|AB263915.1|	1526	T A A T A A A A G G A G G A G T A G A A G T T C T A G A A G T T A A A A C T G G G C T A G A T G C T A T	1577
dbj|AB263925.1|	1517	T A A T A A A A G G A G G A G T A G A A G T T C T A G A A G T T A A A A C T G G G C T A G A T G C T A T	1568
dbj|AB260031.1|	1526	T A A T A A A A G G A G G A G T A G A A G T T C T A G A A G T T A A A A C T G G G C T A G A T G C T A T	1577
dbj|AB369087.1|	1526	T A A T A A A A G G A G G A G T A G A A G T T C T A G A A G T T A A A A C T G G G C T A G A T G C T A T	1577
emb|FR720314.1|	1526	T A A T A A A A G G A G G A G T A G A A G T T C T A G A A G T T A A A A C T G G G C T A G A T G C T A T	1577
gb|DQ989799.1|	1259	T A A T A A A A G G A G G A G T A G A A G T T C T A G A A G T T A A A A C T G G G C T A G A T G C T A T	1310
dbj|AB269840.1|	1527	T A A T A A A A G G A G G A G T A G A A G T T C T A G A A G T T A A A A C T G G G G T A G A T G C T A T	1578
dbj|AB263916.1|	1525	T A A T A A A A G G A G G A G T A G A A G T T C T A G A A G T T A A A A C T G G G G T A G A T G C T A T	1576
gb|EF376992.1|	1516	T A A T A A A A G G A G G A G T A G A A G T T C T A G A A G T T A A A A C T G G G G T A G A T G C T A T	1567
dbj|AB263920.1|	1516	T A A T A A A A G G A G G A G T A G A A G T T C T A G A A G T T A A A A C T G G G G T A G A T G C T A T	1567
		* * * * * * * * * * *	

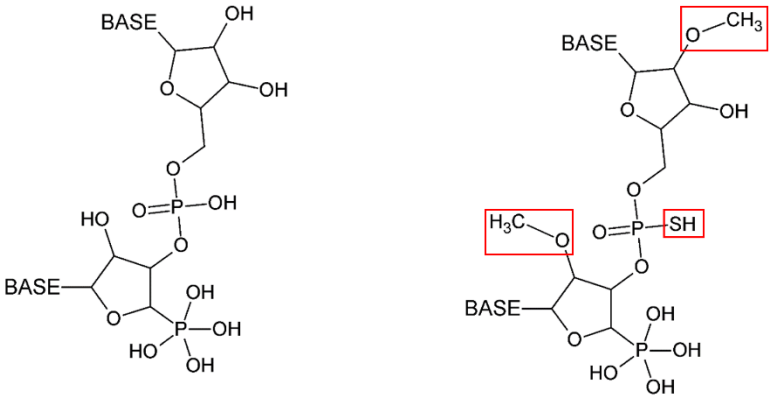

Figure 2.1. Natural (left) and modified (right) RNA NT used to enhance intracellular stability. Regions boxed in red demonstrate methoxy and phosphorothioate modifications.

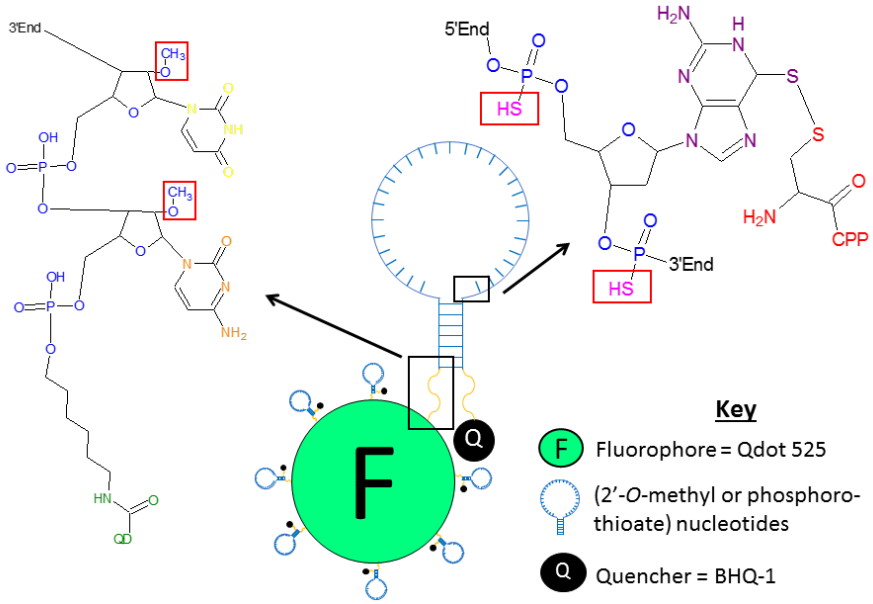

Figure 2.2. Design of Qdot 525-based MB. Arrows emphasize 2′-*O*-methyl, phosphorothioate, and 4-Thio-Uridine nucleotides.

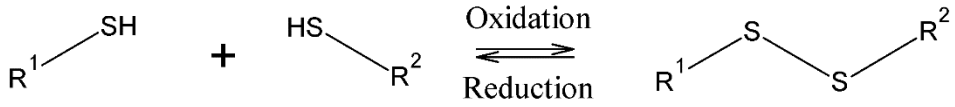

Figure 2.3. Oxidation/reduction reaction to form reversible bond between two thiol groups.

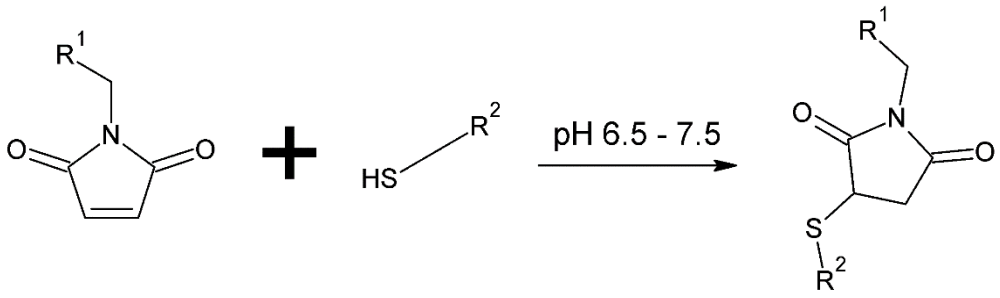

Figure 2.4. Reaction to form covalent bond between maleimide and thiol group.

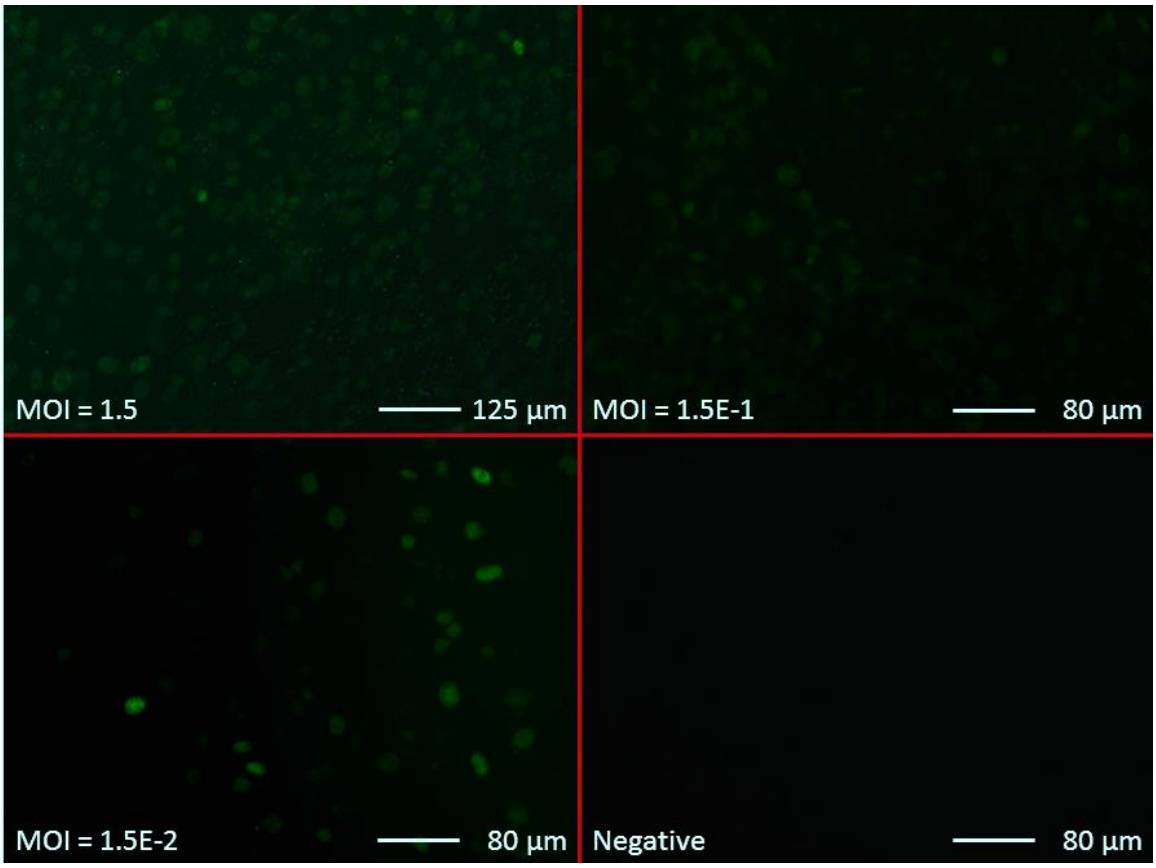

Figure 2.5. MB assay of RPTEC infected with BKPyV performed less than one DPI. Results span three orders of magnitude. Green fluorescence indicates active viral replication. MOI, multiplicity of infection.

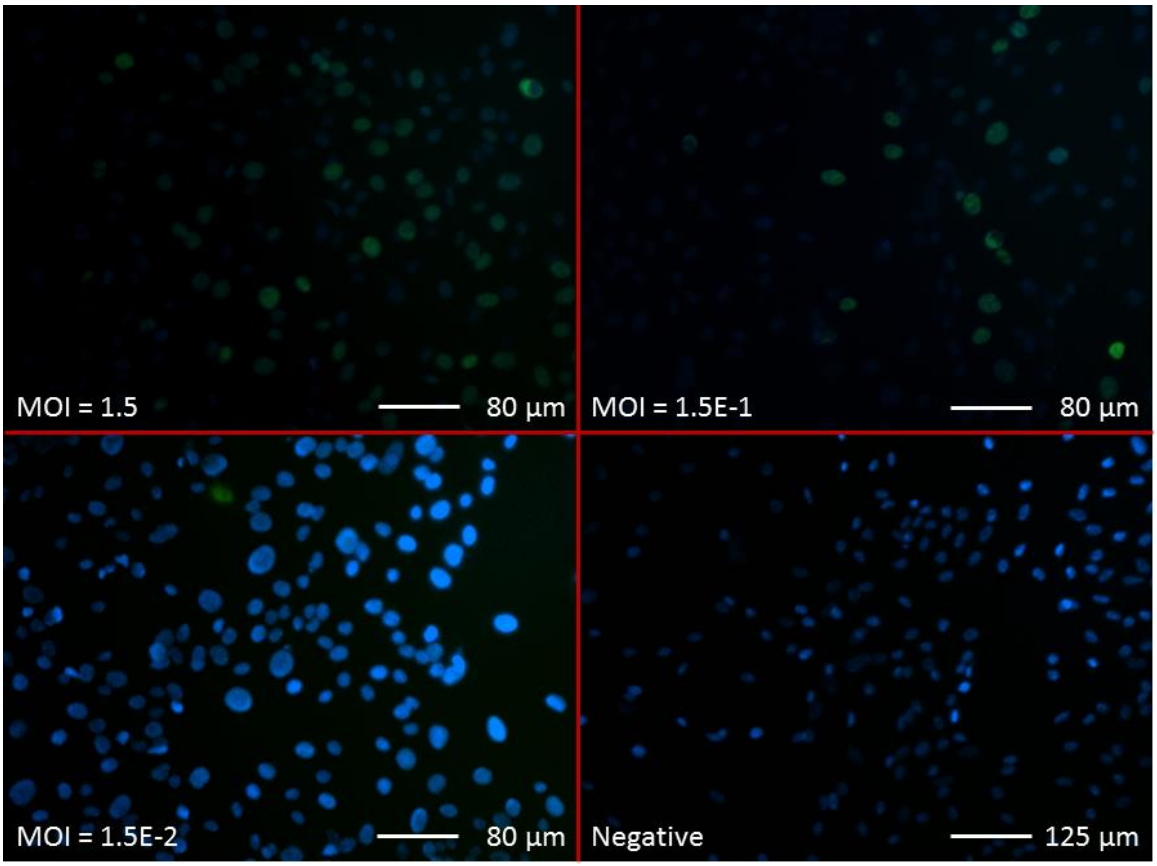

Figure 2.6. IFA of RPTEC performed less than three DPI. Cells are stained with DAPI (blue) and infected with BKPyV covering three orders of magnitude. Green fluorescence indicates active viral replication. MOI, multiplicity of infection.

REFERENCES

Burris, K.P., Wu, T.-C., Vasudev, M., Stroscio, M.A., Millwood, R.J., Stewart, C.N., 2013. Mega-Nano detection of foodborne pathogens and transgenes using molecular beacon and semiconductor quantum dot technologies. IEEE Trans. Nanobioscience 12, 233–238. doi:10.1109/TNB.2013.2263392

Calgua, B., Barardi, C.R.M., Bofill-Mas, S., Rodriguez-Manzano, J., Girones, R., 2011. Detection and quantitation of infectious human adenoviruses and JC polyomaviruses in water by immunofluorescence assay. J. Virol. Methods 171, 1–7. doi:10.1016/j.jviromet.2010.09.013

Chen, A.K., Behlke, M.A., Tsourkas, A., 2009. Sub-cellular trafficking and functionality of 2′-O-methyl and 2′-O-methyl-phosphorothioate molecular beacons. Nucleic Acids Res. 37. doi:10.1093/nar/gkp837

Dunams, D., Sarkar, P., Chen, W., Yates, M. V., 2012. Simultaneous detection of infectious human echoviruses and adenoviruses by an in situ nuclease-resistant molecular beacon-based assay. Appl. Environ. Microbiol. 78, 1584–1588. doi:10.1128/AEM.05937-11

Girones, R., Ferrús, M.A., Alonso, J.L., Rodriguez-Manzano, J., Calgua, B., Corrêa, A. de A., Hundesa, A., Carratala, A., Bofill-Mas, S., 2010. Molecular detection of pathogens in water - the pros and cons of molecular techniques. Water Res. 44, 4325–4339. doi:10.1016/j.watres.2010.06.030

Hällbrink, M., Florén, A., Elmquist, A., Pooga, M., Bartfai, T., Langel, Ü., 2001. Cargo delivery kinetics of cell-penetrating peptides. Biochim. Biophys. Acta - Biomembr. 1515, 101–109. doi:10.1016/S0005-2736(01)00398-4

Herce, H.D., Garcia, A.E., 2007. Molecular dynamics simulations suggest a mechanism for translocation of the HIV-1 TAT peptide across lipid membranes. Proc. Natl. Acad. Sci. U. S. A. 104, 20805–10. doi:10.1073/pnas.0706574105

Hershko, A., Heller, H., Eytan, E., Kaklij, G., Rose, I.A., 1984. Role of the α-amino group of protein in ubiquitin-mediated protein breakdown. Proc. Natl. Acad. Sci. U. S. A. 81, 7021–7025.

Karim, A.S., Johansson, C.S., Weltman, J.K., 1995. Maleimide-mediated protein conjugates of a nucleoside triphosphate gamma-S and an internucleotide phosphorothioate diester. Nucleic Acids Res. 23, 2037–2040.

Kim, K., Seong, B.L., 2001. Peptide amidation: production of peptide hormones in vivo and in vitro. Biotechnol. Bioprocess Eng. 6, 244–251.

Klein, D., 2015. Organic Chemistry, 2nd ed. John Wiley and Sons, Inc.

Li, Y.J., Wu, H.H., Weng, C.H., Chen, Y.C., Hung, C.C., Yang, C.W., Wang, R.Y.L., Sakamoto, N., Tian, Y.C., 2012. Cyclophilin A and nuclear factor of activated T cells are essential in cyclosporine-mediated suppression of Polyomavirus BK replication. Am. J. Transplant. 12, 2348–2362. doi:10.1111/j.1600-6143.2012.04116.x

Liu, B.R., Huang, Y., Winiarz, J.G., Chiang, H.-J., Lee, H.-J., 2011. Intracellular delivery of quantum dots mediated by a histidine- and arginine-rich HR9 cell-penetrating peptide through the direct membrane translocation mechanism. Biomaterials 32, 3520–3537. doi:10.1016/j.biomaterials.2011.01.041

Mhlanga, M.M., Malmberg, L., 2001. Using molecular beacons to detect single-nucleotide polymorphisms with real-time PCR. Methods 25, 463–71. doi:10.1006/meth.2001.1269

Moriyama, T., Marquez, J.P., Wakatsuki, T., Sorokin, A., 2007. Caveolar endocytosis is critical for BK virus infection of human renal proximal tubular epithelial cells. J. Virol. 81, 8552–8562. doi:10.1128/JVI.00924-07

Moriyama, T., Sorokin, A., 2008. Intracellular trafficking pathway of BK Virus in human renal proximal tubular epithelial cells. Virology 371, 336–349. doi:10.1016/j.virol.2007.09.030

National Research Council, 2004. Indicators for Waterborne Pathogens. The National Academies Press, Washington, DC.

Neumann, H., Smith, R.A., 1967. Cleavage of the disulfide bonds of cystine and oxidized glutathione phosphorothioate. Arch. Biochem. Biophys. 122, 354–361.

Nitin, N., Santangelo, P.J., Kim, G., Nie, S., Bao, G., 2004. Peptide-linked molecular beacons for efficient delivery and rapid mRNA detection in living cells. Nucleic Acids Res. 32. doi:10.1093/nar/gnh063

Saalik, P., Elmquist, A., Hansen, M., Padari, K., Saar, K., Viht, K., Langel, U., Pooga, M., 2004. Protein cargo delivery properties of cell-penetrating peptides. A comparative study. Bioconjug. Chem. 15, 1246–1253.

Sayers, E.W., Barrett, T., Benson, D.A., Bryant, S.H., Canese, K., Chetvernin, V., Church, D.M., DiCuccio, M., Edgar, R., Federhen, S., Feolo, M., Geer, L.Y., Helmberg, W., Kapustin, Y., Landsman, D., Lipman, D.J., Madden, T.L., Maglott, D.R., Miller, V., Mizrachi, I., Ostell, J., Pruitt, K.D., Schuler, G.D., Sequeira, E., Sherry, S.T., Shumway, M., Sirotkin, K., Souvorov, A., Starchenko, G., Tatusova, T.A., Wagner, L., Yaschenko, E., Ye, J., 2009. Database resources of the National Center for Biotechnology Information. Nucleic Acids Res. 37, D5–D15. doi:10.1093/nar/gkn741

Sievers, F., Wilm, A., Dineen, D., Gibson, T.J., Karplus, K., Li, W., Lopez, R., McWilliam, H., Remmert, M., Söding, J., Thompson, J.D., Higgins, D.G., 2011. Fast, scalable generation of high-quality protein multiple sequence alignments using Clustal Omega. Mol. Syst. Biol. 7. doi:10.1038/msb.2011.75

Sivaraman, D., Yeh, H.-Y., Mulchandani, A., Yates, M. V., Chen, W., 2013. Use of flow cytometry for rapid, quantitative detection of poliovirus-infected Cells via TAT peptide-delivered molecular beacons. Appl. Environ. Microbiol. 79, 696–700. doi:10.1128/AEM.02429-12

Su, X., Zhang, C., Zhao, M., 2011. Discrimination of the false-positive signals of molecular beacons by combination of heat inactivation and using single walled

carbon nanotubes. Biosens. Bioelectron. 26, 3596–3601. doi:10.1016/j.bios.2011.02.009

Tsourkas, A., Behlke, M.A., Bao, G., 2002. Hybridization of 2’-O-methyl and 2'-deoxy molecular beacons to RNA and DNA targets. Nucleic Acids Res. 30, 5168–5174. doi:10.1093/nar/gkg294

Tyagi, S., Kramer, F.R., 1996. Molecular beacons: probes that fluoresce upon hybridization. Nat. Biotechnol. 14, 303–308.

Vet, J.A.M., Majithia, A.R., Marras, S.A.E., Tyagi, S., Dube, S., Poiesz, B.J., Kramer, F.R., 1999. Multiplex detection of four pathogenic retroviruses using molecular beacons. Proc. Natl. Acad. Sci. U. S. A. 96, 6394–6399. doi:10.1073/pnas.96.11.6394

Vet, J.A.M., Marras, S.A.E., 2005. Design and optimization of molecular beacon real-time polymerase chain reaction assays. Methods Mol. Biol. 288, 273–290. doi:10.1007/s10126-007-9031-3

Waki, R., Yamayoshi, A., Kobori, A., Murakami, A., 2011. Development of a system to sensitively and specifically visualize c-fos mRNA in living cells using bispyrene-modified RNA probes. Chem. Commun. 47, 4204–4206. doi:10.1039/c0cc04639f

Walker, M.J., Montemagno, C., Bryant, J.C., Ghiorse, W.C., 1998. Method detection limit of PCR and immunofluorescence assay for Cryptosporidium parvum in soil. Appl. Environ. Microbiol. 64, 2281–2283.

Wang, F., Wang, Y., Zhang, X., Zhang, W., Guo, S., Jin, F., 2014. Recent progress of cell-penetrating peptides as new carriers for intracellular cargo delivery. J. Control. Release 174, 126–136. doi:10.1016/j.jconrel.2013.11.020

Wang, K., Tang, Z., Yang, C.J., Kim, Y., Fang, X., Li, W., Wu, Y., Medley, C.D., Cao, Z., Li, J., Colon, P., Lin, H., Tan, W., 2009. Molecular engineering of DNA: molecular beacons. Angew. Chemie - Int. Ed. 48, 856–870. doi:10.1002/anie.200800370

Yeh, H.-Y., Yates, M. V., Mulchandani, A., Chen, W., 2008. Visualizing the dynamics of viral replication in living cells via Tat peptide delivery of nuclease-resistant molecular beacons. Proc. Natl. Acad. Sci. U. S. A. 105, 17522–17525. doi:10.1073/pnas.0807066105

Yu, D., Armstrong, D.A., Rauk, A., 1992. Hydrogen bonding and internal rotation barriers of glycine and its zwitterions (hypothetical) in the gas phase. Can. J. Chem. 70, 1762–1772. doi:10.1139/v92-221

CHAPTER THREE: ESTABLISHING THE DISINFECTION PROFILES OF BK POLYOMAVIRUS, ADENOVIRUS 2, AND POLIOVIRUS 1 BY MOLECULAR BEACON

ABSTRACT

Regulations set forth by the EPA have significantly elevated standards for water treatment by UV. These standards are justified by resistance to UV_{254} inactivation demonstrated by dsDNA viruses from the *Adenoviridae* family, but have not been validated due to a lack of traditional infectious assays for similarly structured microorganisms. Integrated assays, such as ET-qPCR, IFA, and intracellularly delivered MB, selectively target infectious viral particles, thereby surmounting this limitation. These integrated techniques were developed and used to characterize the inactivation profiles of BKPyV, Ad2, and PV1 following exposure to UV_{254}, chlorine, and heat. As expected, BKPyV and Ad2 exhibited comparable resistances to UV_{254} (61.35 and 54.45 mJ/cm^2, respectively) to support LT2 standards, likely due to the structural and genomic parallels shared among these viruses. Additionally, MB exhibited similar inactivation rates (k_{obs}) when compared to current infectious assays (e.g. PA/IFA), which was often lost with ET-qPCR.

INTRODUCTION

Although UV_{254} does not directly destroy microorganisms, the universal presence of a genome yields UV_{254} with broad effectiveness in abrogating microbial replication. Photons from UV_{254} are absorbed into genomes to create dimers that block genomic replication and transcription, leaving a microorganism unable to reproduce (Cutler and Zimmerman, 2011). Most microorganisms remain susceptible to UV_{254} treatment; however, all members of the dsDNA *Adenoviridae* family require around four times the fluence (i.e., dose) to achieve similar levels of inactivation (Johnson et al., 2010). This resistance served as the impetus for elevating all standards of water treatment by UV light from 40 mJ/cm^2 to 186 mJ/cm^2 (Eischeid et al., 2011). Interestingly, this resistance is lost when propagating UV_{254}-treated adenoviruses in host cells that lack genome repair mechanisms. This annulled resistance suggests adenoviruses are not actually resistant to UV_{254} treatment, but rather, induced genetic damage is repaired during intracellular infection of host cells (Rainbow, 1980). Furthermore, this standard has not been validated due to a lack of infectious assays for similarly structured microorganisms, like BKPyV.

Traditional PA remain the standard for quantifying viral titers by relying on the formation of visible signs of CPE. The presence of CPE indicates active viral replication and can include cell rounding, the formation of inclusion bodies, and/or cell lysis. Although accurate, not all viruses produce clear signs of CPE; furthermore, cells (or at least controls) must remain alive until the formation of CPE, which can be problematic in viruses with extended replication cycles, such as BKPyV (Gonzalez-Hernandez et al., 2012).

Integrated assays, like IFA or ET-qPCR, selectively target infectious virions by detecting earlier stages of replication, or by eliminating potential false-positive signals (Lee and Jeong, 2004). An IFA detects the production of viral proteins by host cells during infection through the addition of antibodies. Although effective, antibodies can exhibit low target specificity and still require incubation times that exceed those for currently adopted FIO (Kim and Kim, 2013). Alternatively, an ET-qPCR assay requires the addition of a nuclease or intercalating agent before thermocycling. Viruses possessing damaged capsids (e.g., following treatment) are likely unable to establish infection and leave contained genomes susceptible to these chemical pretreatments. Due to a lack of cellular incubation, ET-qPCR assays can be performed within one day; however, this also precludes ET-qPCR from detecting infectious virions, relying instead on the ability of the chemical pretreatment to eliminate non-infectious (i.e., false-positive) signals (Prevost et al., 2016). The difference between detecting infectious and eliminating non-infectious virions is seen through low correlations between traditional infectious assays and ET-qPCR following inactivation methods that primarily targets proteins (Pecson et al., 2011).

Molecular Beacons remain an alternative integrated assay, but have not yet been employed to measure microbial inactivation. The MB assay utilizes the intracellular addition of a modified oligo to bind to a specific sequence of viral mRNA. The production of mRNA is a universal and early stage of viral replication, thereby surmounting both limitations of IFA and ET-qPCR (Dunams et al., 2012). Utilizing MB could be a near-universal alternative to traditional and integrated methods when quantifying viral titers, including after disinfection or treatment with antivirals. To test the effectiveness of MB,

the inactivation profiles of Ad2, BKPyV, and PV1 following treatment by UV_{254}, chlorination, and heat, were compared to traditional infectious assays. Multiple treatment methods were used to test the effectiveness of MB when quantifying infectious virions following varied mechanisms of inactivation (i.e., varied targets of inactivation; Araud et al., 2016; Beck et al., 2016; Wigginton et al., 2012).

MATERIALS AND METHODS

Viral Propagation:

The propagation of BKPyV followed guidelines outlined in Chapter Two with additional steps to disrupt viral aggregates. The formation of viral aggregates during replication can diminish the effectiveness of inactivation methods by shielding virions from exposure; therefore, all viruses were treated to ensure homogeneity (Calgua et al., 2014). Specifically, BKPyV aggregates were disrupted by diluting stocks in an equal volume of glycine-NaOH buffer (0.2M, pH 9.0) and vortex mixing for 15 minutes. Following homogenization, ultracentrifugation was repeated and the resulting pellet was dissolved in autoclaved phosphate buffered saline (PBS; 10 ×, 1 L, pH 7.3; 1.37 M NaCl, 27 mM KCl, 100 mM Na_2HPO_4, and 15 mM KH_2PO_4).

Adenocarcinomic human alveolar basal epithelial cells (A549, CCL-185, American Type Culture Collection) allowed for propagation of Ad2. Specifically, A549 were grown in 0.22 µm-filtered Dulbecco's Modified Eagle Medium (DMEM, 50-003-PB, Corning Inc., Corning, NY, USA) containing 1.85 g $NaHCO_3$, 50000 U of penicillin, 50 µg of streptomycin, and 50 mL FBS per 500 mL (pH 7.4). Cells were washed with PBS and subcultured with trypsin when reaching 80 % confluency. Stocks of Ad2 were prepared by infecting A549 with 2 mL of Ad2 (VR846, ATCC) diluted in PBS:DMEM (1:1). Adsorption was allowed by incubating T-75 cm^2 flasks for one hour with rocking every 15 minutes. Inocula were then removed and 15 mL of DMEM 2 % FBS was added to each flask and allowed to incubate until the formation of CPE (~ 3 DPI). Viral stocks were

harvested by first freeze-thawing flasks three times and adding contents to 50-mL centrifuge tubes. Next, an equal volume of chloroform was added to these tubes and mixed via vortex for two minutes to disrupt viral aggregates. Chloroform was removed by centrifuging tubes in a JA-17 rotor at 2200 × g for 15 minutes at 4 °C. Finally, supernatants were collected and filtered at 0.45-µm polyvinylidene fluoride membrane before aliquoting stocks to be stored at -80 °C.

Propagation of PV1 followed a similar method to Ad2 with minor modifications. Stocks of PV1 (VR-1562, American Type Culture Collection) were propagated in buffalo green monkey kidney cells (BGMK) grown in Minimum Essential Medium (MEM, 50-010-PC, Corning). A 500 mL formulation of MEM is as follows: 1.1 g $NaHCO_3$, 50 mL FBS, and pH 7.3 before filtering at 0.22-µm. Infection and harvesting of PV1 was similar to propagation of Ad2; however, stocks could be obtained after overnight incubation.

Ultraviolet Disinfection:

Samples were treated with UV_{254} generated from an 8 W germicidal bulb containing Hg under low pressure (G8T5/OF) which emits light almost exclusively at 253.7 nm. Light scattering was limited to one incident angle through the construction of a collimating light box (Figure 3.1). Utilizing this apparatus was necessary as radiometric measurements of UV_{254} can only be measured at one surface. Measurements (in W/cm^2) were obtained with an ILT1700 radiometer with a SED240/W light detector equipped with an NS254 filter (International Light Technologies, Peabody, MA, USA). Additional

discrepancies between bulb output and the amount of UV_{254} reaching samples must also be accounted for to obtain the average germicidal fluence rate (E'_{avg}, in mW/cm^2).

Firstly, light is reflected off the surface of the water and can be accounted for by calculating a reflection factor (RF):

$$RF = \left(\frac{N_2 - N_1}{N_2 + N_1}\right)^2$$

Where, N_1 and N_2 represent reflection constants of air and water, respectively.

Additionally, calculating the petri factor (PF) helps account for differences in fluence across surface of petri dish (i.e. relative to the position of the UV bulb). The PF is estimated by comparing radiometric readings taken at the center of the petri dish to measurements obtained in 0.5 cm intervals along the X and Y axes from the center of the petri dish. A PF is then calculated for each position and averaged. For example,

$$PF_{X_{1,0}} = \frac{X_{1,0}}{X_{0,0}}$$

Where, $X_{0,0}$ is the radiometric reading at the center of the petri dish and $X_{1,0}$ is the reading taken 1 cm to the right of center.

The Water Factor (WF) accounts for irradiance absorbed by water.

$$WF = \frac{1 - 10^{-\alpha l}}{\alpha l \times \ln(10)}$$

Where, l is the height of the water column (i.e. $\text{sample volume}/_{\pi r^2}$) and α represents the sample absorbance at 254 nm.

The amount of light that diverges across the sample path length can be estimated by the divergence factor (DF):

$$\mathrm{DF} = \frac{\mathrm{L}}{\mathrm{L} + l}$$

Where L represents the distance from the top of the sample to the UV lamp (in cm).

Combined, $E'_{avg} = RF \times PF \times WF \times DF \times E_0$ where E_0 is the average of radiometric readings taken before and after sample treatment.

Finally, the average germicidal fluence (i.e., dose, H′) is calculated by multiplying E'_{avg} by treatment time (in seconds), and is measured in mJ/cm^2 (Bolton and Linden, 2003).

Samples were treated by first diluting viral stocks in PBS by, at minimum, 1:100, to avoid significant absorbance of UV_{254}. Samples of 10 mL were added to 95 × 15 mm petri dishes and exposed to the collimating light box under gentle stirring with the lid removed. Leaving the bulb on for at least 30 minutes prior to treatment helped eliminate bulb fluctuation; therefore, samples were treated until reaching the desired fluence. After treatment, samples were kept in the dark at 4 °C until processing.

Thermal Inactivation:

Thermal treatment of samples served to inactivate viruses through protein denaturation (Schotte et al., 2014). Diluted samples were added to 1.5-mL centrifuge tubes

with septa (22-040-040/5, Fisher) until all air was removed and submerged in a water bath kept at 60 °C for desired treatment times. The titer of untreated samples was established by removing a control when reaching an internal temperature of 60 °C. Finally, samples were put on ice immediately after treatment and stored at 4 °C until analyses.

Chlorination:

In water, sodium hypochlorite (NaClO) decomposes to form hypochlorite (ClOH), and eventually hypochlorous acid (ClO^-) capable of oxidizing both genomic and proteomic targets. To this end, a 5 % NaClO solution was utilized to treat samples after standardizing the amount of free chlorine available to react with microorganisms through a colorimetric reaction (Deborde and von Gunten, 2008). Specifically, the amount of free chlorine present in the stock NaClO solution was measured every 30 days by the change in color of N,N-diethyl-p-phenylenediamine (DPD) to a pink Wurster dye via chlorine oxidation (Figure 3.1). Under gentle mixing, samples were treated with various doses of standardized NaClO for 10 minutes to achieve a desired contact time ($CT = \frac{\text{mg } Cl_2 * \text{min}}{\text{L}}$).

Free chlorine was also measured once after sample treatment to determine the minimum amount of sodium thiosulfate ($Na_2S_2O_3$) required to neutralize oxidation (see below). Values of free chlorine between 0.2 – 2.0 mg/L were measured on a DR/890 colorimeter utilizing Free Chlorine AccuVac Ampules (25020-25, Hach, Loveland, CO, USA), while values between 0.0 – 0.2 mg/L utilized a Chlorine Comparator (C-2511, CHEMetrics, Midland, VA, USA). To limit oxidation, free chlorine was quenched with 1.5 × the minimum amount of $Na_2S_2O_3$ for 10 minutes, which was determined by

measuring the amount of free chlorine present after treating samples. A stock neutralizing solution was prepared by dissolving 200 mg $Na_2S_2O_3$ in 1 L of H_2O and 0.22 µm-filter sterilizing before storage at 4 °C.

Viral Quantification by Plaque Assay:

Viruses Ad2 and PV1 were also selected due to their facile quantification by PA, while BKPyV was quantified by IFA (see Chapter II). Host A549 for Ad2 were split into 6-well plates (3516, Corning) at a rate of 4.8E5 cells per well and incubated overnight until reaching 80 % confluency. Next wells were aspirated before the addition of 250 mL of viral inocula, diluted in a 1:1 mixture of PBS and DMEM 2 % FBS, to each well. Plates were allowed to incubate for one hour, with rocking every 15 minutes, before aspiration and the addition of 2.5 mL of an agar overlay to each well. The agar overlay consisted of an autoclaved 1 % SeaKem ME agarose (50010, Lonza) mixed with equal parts of a 2 × DMEM 4 % FBS solution and kept at 60 °C before use. Wells were allowed to incubate between three to five days, or until the formation of visible plaques. After this period, the agar overlay was carefully removed to not disturb attached cells, washed with PBS, and simultaneously stained and fixed to enhance contrast and longevity, respectively. Each well received 1 mL of a stain/fixation solution consisting of 106 mM phenol, 9.8 mM crystal violet, and 12 % v/v ethanol. Wells were aspirated after five minutes and plaques were counted to quantify titers of Ad2.

Quantification of PV1 followed a similar PA to Ad2, with minor exceptions. Firstly, 12-well plates (3513, Corning) were seeded with 1.27E5 BGMK per well and

allowed to incubate overnight. Viral inocula were diluted in equal parts PBS and MEM 2 % FBS and 125 µL was added to each well. The agar overlay was similar to Ad2, but utilized a 2 × MEM 4 % FBS, and was removed up to two DPI, or until plaque visualization.

Viral quantification by ET-qPCR:

Design of primers and MB probes for qPCR reactions followed similar principals outlined in Chapter Two. Specifically, conserved regions were identified by aligning complete genomes deposited into GenBank through Clustal Omega. Primers were allowed to possess up to three mismatches, while MB required complete sequence conservation. Final products were subjected to BLAST searches excluding the target viral family (e.g., *Adenoviridae*) to ensure specificity. Finally, the lack of intracellular modifications allowed designed primers and MB to be synthesized by Eurofins-Operon (Louisville, KY, USA).

Before quantification, samples were treated with nucleases to remove free genetic material as well as genomes contained within damaged (presumably noninfectious) virions. For dsDNA viruses BKPyV and Ad2, DNA was removed via TURBO DNA-free kit (AM1907M, Invitrogen, Carlsbad, CA, USA). Specifically, 4 U of DNAse was added to 250 µL of treated samples and allowed to incubate at 37 °C for 25 minutes before adding 25 µL of DNAse inactivator contained within the kit. Samples were incubated for 5 minutes at room temperature with periodic mixing before centrifugation at 10000 × g for 1.5 minutes. The supernatant was collected and immediately processed for quantification.

Removal of RNA present in treated samples of PV1 followed a similar rationale utilizing nucleases before genome extraction. Ribonuclease A was obtained from Fisher

(EN0531) and diluted in an autoclaved Tris-Cl solution (65 mM Tris-Cl containing 50 % v/v glycerol, pH 7.4). Samples of 250 µL received 2 U of ribonuclease A and were incubated at 37 °C for 30 minutes. Ribonuclease A was inactivated with 3 U of SUPERase● In™ RNase Inhibitor (AM2694, Fisher) diluted in PBS (formulation above, with the following modifications; 2.7 mM KCl and 50 % v/v glycerol). After nuclease treatment, genomes of samples were extracted with a QIAamp MinElute Virus Spin Kit (57704 Qiagen, Hilden, Germany) and diluted in a Tris-EDTA (TE) solution. Unless specifically stated, all molecular work utilized TE buffer prepared by first making a 10 × solution with 100 mM Tris, 10 mM EDTA, and a pH of 8.0 before autoclaving. The 10 × solution was then diluted to 1 × and the pH was adjusted according to the sample genome (7.4 for RNA and 8.0 for DNA) before autoclaving and making aliquots.

The utilization of new primers and MB required each qPCR be optimized before obtaining k_{obs}. Initial qPCR followed a 'touchdown' protocol to ensure the formation of an amplicon. Specifically, genomic templates were diluted up to 1E-3, in triplicate, and cycled according to the following parameters: 1 cycle of 95 °C for 3 minutes; 45 cycles of 95 °C for 10 seconds, 50 °C for 15 seconds, 55 °C for 15 seconds, 60 °C for 15 seconds, and 72 °C for 15 seconds. A reverse transcription reaction was employed for PV1 before initial denaturation (see below) and fluorescent readings were always obtained at the first annealing step. Primers were kept at 400 mM and MB were always added at half the concentration of primers for all qPCR reactions (here 200 mM). A specific formulation for each 25 µL qPCR reaction is described below. Finally, products were visualized on a gel to confirm expected amplicon size.

After confirming each qPCR was capable of amplifying a specific target, primer concentration and annealing temperatures were optimized with an intercalating dye. Utilizing intercalating dyes, like SYBR® Green, allows a user to optimize qPCR parameters to maximize the production of amplicons while minimizing the formation of non-targets (e.g., primer-dimers). Extracted viral genomes were diluted 1E-1 and subjected to a qPCR consisting of varied primer concentrations versus a temperature gradient. The temperature gradient ranged ± 5 °C from the average of the theoretical annealing temperature (T_a) of both forward and reverse primers. The concentration of primers was tested at four different concentrations to allow each sample to be run in triplicate on a 96-well plate. Probes were not included in the reaction as an SsoAdvanced™ Universal SYBR® Green Supermix (172-5271, Bio-Rad, Irvine, CA, USA) served as the fluorescent moiety. Cycling consisted of 1 cycle of 95 °C for 3 minutes and 45 cycles of 95 °C for 10 seconds and varied gradient temperatures for 30 seconds. After cycling, melt-curves were established starting at 42 °C for 10 seconds and increased in 0.5 °C until reaching 95 °C.

The optimal primer concentration was established by identifying wells that produced a single amplicon of an expected size and did not amplify non-template controls (NTC) through investigating melt-curves. Within the set of optimal primer concentrations, the T_a possessing the earliest threshold cycle (C_t) was selected for further optimization by repeating the final reaction parameters with a temperature gradient of T_a ± 2.5 °C. Here, the template was diluted up to 1E-4 and the final T_a was selected by identifying wells with no NTC amplification and near perfect doubling each reaction cycle. Perfect doubling can

be identified by finding the efficiency ($E = 10^{-1/\text{slope}} - 1$) of a qPCR closest to 100 %, where slope is calculated from plotting C_t versus the dilution factor.

Optimization of qPCR was repeated for each virus and results are as follows: reagents for a 25 µL BKPyV qPCR consisted of 12.5 µL 2 × SsoAdvanced Probes Supermix (172-5281, Bio-Rad), 0.5 µL of 10 µM forward and reverse primers (final concentration 200 nM of each), 0.25 µL of 10 µM MB (final concentration 100 nM), 2.25 µL H_2O, and 9 µL of template. While cycling consisted of 1 cycle of 95 °C for 3 minutes and 45 cycles of 95 °C for 10 seconds then 53.3 °C for 30 seconds. All qPCR were performed in triplicate and diluted up to 10E-1 for treated (i.e., inactivated) samples. Cycling for Ad2 followed a similar protocol, but the T_a was optimized to 53.7 °C. Finally, PV1 varied somewhat from BKPyV and Ad2 due to the necessity of a reverse transcription step prior to cycling. Reaction ingredients for PV1 consisted of 12.5 µL 2 × SensiFAST™ Probe No-ROX One-Step Kit (BIO-76001, Bioline, Taunton, MA, USA), 1 µL of 10 µM forward and reverse primers (final concentration 400 nM of each), 0.5 µL of 10 µM MB (final concentration 200 nM), 0.25 µL reverse transcriptase, 0.5 µL RNase inhibitor, 0.25 µL DEPC-treated H_2O, and 9 µL of template. Finally, cycling consisted of 1 cycle of 45 °C for 10 minutes to allow for reverse transcription, 1 cycle of 95 °C for 2 minutes, and 45 cycles of 95 °C for 10 seconds then 56 °C for 30 seconds.

To quantify genomic copies (GC) of treated samples, C_t values of unknowns were compared to C_t values of standardized amplicons from transformed *E. coli* included with each reaction. After optimizing qPCR parameters, a regular PCR was performed on

genomes extracted from viral stocks, diluted to 1E-2, and H_2O replaced the use of MB. The PCR product was purified with a MinElute® PCR Purification Kit (28004, Qiagen) and reacted with dATP to provide a facile nucleotide for ligation. Specifically, 5 µL of purified PCR product was added to 2 µL of reaction buffer, 2 µL of 1 mM dATP (N04405, New England Biolabs, Ipswich, MA, USA), and 1 µL (5 U) of GoTaq polymerase (M3001, Promega, Madison, WI, USA). Vessels were incubated at 70 °C for 20 minutes before ligating into a pGEM-T vector system (A3610, Promega) utilizing a blue/white screen of competent JM109 *E. coli* and an ampicillin selective marker. Four white colonies were selected and propagated to be tested for successful transformation. After growth according to kit instructions, plasmids containing potential standards were extracted with a QIAprep® Spin Miniprep Kit (27104, Qiagen). After extraction, plasmids were diluted up to 1E-4 and qPCR was repeated according to the optimized conditions. The standards that performed best were selected, quantified via Nanodrop, diluted, aliquoted, and stored at –80 °C.

Quantification of Viruses by MB:

Additional MB were developed for Ad2 and PV1 following guidelines listed in Chapter Two. However, the MB for PV1 was designed to target negative-sense single-stranded RNA (-ssRNA) to ensure active viral replication of this +ssRNA virus. The MB for Ad2 and PV1 utilized traditional fluorophores and cellular fixation.

Calculating Inactivation:

In general, inactivation is measured by comparing titers before and after treatment (N and N_0, respectively). Due to the large number of microorganisms present during water treatment processes, it is more feasible to measure inactivation by orders of magnitude through logarithmic transformation. Specifically, log inactivation is equivalent to $\log\left(\frac{N}{N_0}\right)$; for example, 99 % removal of a specific microorganism is equivalent to reducing titers by two orders of magnitude, or two-log. The k_{obs} is equivalent to the slope of the regression line when plotting log inactivation versus treatment dose, and the inverse of k_{obs} is equal to the treatment dose required to reduce titers by one-log (Kamolsiripichaiporn et al., 2007).

Due to the inability of ET-qPCR to measure infectious virions, results may underestimate inactivation rates by quantifying GC from noninfectious virions. Comparing log inactivation values from qPCR data to traditional infectious assays at the same dose can improve this estimation through a correction factor, c (Calgua et al., 2014; Pecson et al., 2011). Specifically,

$$c = \frac{\log\left(\frac{N_{\mathrm{PA}}}{N_{0,\mathrm{PA}}}\right)}{\log\left(\frac{N_{\mathrm{qPCR}}}{N_{0,\mathrm{qPCR}}}\right)}$$

Where N_{PA} and $N_{0,PA}$ are treated and initial titers of viruses, respectively, as determined by PA, while N_{qPCR} and $N_{0,qPCR}$ are titers established at the same dose by ET-qPCR.

After determining c, the log inactivation for a traditional infectious assay (like PA) can be estimated from qPCR data by utilizing the following equation:

$$\log\left[\left(\frac{N_{\mathrm{qPCR}}}{N_{0,\mathrm{qPCR}}}\right)^{c}\right]$$

Finally, all statistical analyses, including determinations of k_{obs}, simple linear regressions, and analyses of covariance were generated in SAS Enterprise Guide version 5.1 (SAS Institute, Cary, NC).

RESULTS

Detection of Viruses by ET-qPCR and MB:

Quantification of viral titers by designed ET-qPCR and MB assays were compared to traditional infectious assays to ensure accuracy. Alignment of BKPyV sequences allowed for the design of primers and MB probes to amplify a 126-NT region encoding agnoprotein to capsid protein VP2 (Table 3.1). Tables 3.2 and 3.3. display similar designs obtained for Ad2 and PV1, encoding 139- and 147- NT amplicons of the penton gene and internal ribosomal entry site, respectively. Created standards demonstrate the efficacy of each created qPCR; specifically, BKPyV – E = 100.92 % (R^2 = 1.00), Ad2 – E = 103.91 % (R^2 = 1.00), and PV1 – E = 99.66 % (R^2 = 1.00). Finally, quantification of viral titers by qPCR exhibited good correlation to titers established by traditional infectious assays (BKPyV R^2 = 0.86, Ad2 R^2 = 0.97, and PV1 R^2 = 0.92).

Similar to results described in Chapter Two, MB were successfully designed for Ad2 and PV1 and exhibited good correlation to titers established by traditional PA. Alignment of 10 complete Ad2 genomes allowed a MB to be designed to target mRNA encoding for the penton portions of the viral capsid via reverse complementarity (Table 3.4). Conserved regions of PV1 encoding for RNA-dependent RNA polymerase were also identified through sequence alignments (Table 3.5). Design of all oligos utilized in qPCR and MB assays are summarized in Table 3.6. Both MB successfully detected viral replication (Figures 3.3 and 3.4) and exhibited strong correlations to titers established by PA (Figure 3.5).

Viral Inactivation:

Inactivation of BKPyV by UV_{254} exhibited agreement among all detection methods indicating 61.35 mJ/cm^2 as the average dose required for one-log inactivation (Figure 3.6). Figures 3.7 and 3.8 demonstrate inactivation of BKPyV obtained by chlorination and heat. Results from ET-qPCR assays indicated enhanced viral resistance to chlorination; however, the average CT obtained from IFA and MB assays was 1.58 $\frac{\text{mg Cl}_2 * \text{min}}{\text{L}}$. Furthermore, ET-qPCR results indicated no susceptibility to thermal inactivation, while the average between the other detection methods indicated titers of BKPyV are reduced by one order of magnitude every 42 minutes at 60 °C. A summary of BKPyV inactivation following treatment methods and correlations between detection methods are listed in Tables 3.7 and 3.8, respectively.

As confirmed by empirical evidence, Ad2 exhibited enhanced resistance to UV_{254} treatment; however, ET-qPCR results failed to reflect inactivation rates for other treatment methods relative to PA and MB (Eischeid et al., 2011; Prevost et al., 2016). The average fluence required for one-log inactivation of Ad2 among all detection methods was 51.45 mJ/cm^2 (Figure 3.9). Somewhat opposite to BKPyV, ET-qPCR results did not show significant inactivation of Ad2 after exposure to chlorine and less inactivation to heat relative to other detection methods (Figures 3.10 and 3.11, respectively). The average CT obtained by PA and MB was 0.57 $\frac{\text{mg Cl}_2 * \text{min}}{\text{L}}$, while Ad2 required slightly more than one hour at 60 °C to achieve one-log inactivation. A summary of inactivation results and correlations between detection methods is found in Tables 3.9 and 3.10, respectively.

Finally, PV1 exhibited relative sensitivity to all inactivation methods, but agreement between methods existed only for UV_{254} inactivation. The +ssRNA virus PV1 remained sensitive to inactivation by UV_{254}, requiring 11.1 mJ/cm^2 when averaging the inverse of k_{obs} values obtained between all three detection methods (Figure 3.12 and Table 3.11). The average CT value for PV1 was 0.76 $\frac{mg\ Cl_2 * min}{L}$, with ET-qPCR exhibiting slightly enhanced resistance relative to PA and MB; however, correlations between methods remained above 0.92 (Figure 3.13 and Table 3.12). Thermal inactivation required around 7.2 minutes when determined by PA and MB, while ET-qPCR exhibited 9.6 minutes per log-inactivation (Figure 3.14). This 33% increase is reflected in weak correlations between cell-free and infectious assays failing to rise above 0.36 and analysis of covariance neared significance (P = 0.13).

DISCUSSION

Resistance of BKPyV to UV_{254} Treatment:

Relative to Ad2, BKPyV exhibited slightly enhanced resistance to UV_{254} treatment. Generally, reducing viral titers by one order of magnitude requires less than 10 mJ/cm^2, while achieving similar inactivation in bacterial species requires around 3 mJ/cm^2 (Hijnen et al., 2006). Adenoviruses emerged as a notable exception, requiring over 40 mJ/cm^2 per log-inactivation, which may be explained by repair of genomic damage by host cells during intracellular infection (Rainbow, 1980). This effect has remained difficult to validate in other microorganisms due to a lack of infectious assays for similarly structured viruses. Here, BKPyV, Ad2, and PV1 required around 61.35, 54.45, 11.10 mJ/cm^2 per log-inactivation, thereby supporting host repair theories; however, further investigations regarding the nature of dsDNA viral resistance to UV_{254} cannot be made in this study.

Limitations of Assessing Viral Infectivity by ET-qPCR:

Characterizations of viral inactivation profiles by ET-qPCR remained strong when damage primarily targeted genomic regions; however, viruses exhibit non-traditional targets of inactivation (Wigginton et al., 2012). All utilized detection assays successfully characterized viral inactivation profiles following UV_{254} treatment, with $R^2 = 0.92$ being the lowest correlation between all methods. Due to UV_{254} damage being primarily genomic, it is unsurprising that ET-qPCR also characterized viral inactivation accurately (Cutler and Zimmerman, 2011). However, the use of other inactivation methods often abrogated these correlations, lowering R^2 values to as low as 0.02. Inactivation detected

by ET-qPCR even failed to detect fluctuations in genomic copy number in instances of expected genomic damage. For example, the nature of adenoviral inactivation by chlorination has yet to be determined, but would be expected to include, at least partial, oxidation of genomic targets, which was not seen in ET-qPCR data obtained in this study. A study from Gall et al. found chlorine-inactivated Ad2 could still attach to host cells but were unable to synthesize progeny DNA, nor transcribe certain genes, suggesting at least partial genomic damage. Also, like our data, very little damage was seen in genomic targets detected by qPCR (E1A and hexon genes) (Gall et al., 2015). Interestingly, inactivation of PV1 by chlorination, which is driven by genomic damage, exhibited strong correlations to other detection methods without the need to transform data with *c* (Jin et al., 2010).

However, the requirement to transform data further limits the utility of ET-qPCR in measuring viral inactivation. Without *c*, ET-qPCR overestimated PV1 inactivation by UV_{254} possessing a *c* value below 1 ($c = 0.57$) to elevate log inactivation for UV_{254} from 5.48 mJ/cm^2 to 9.98 mJ/cm^2. Although PV1 inactivation by UV_{254} is still driven by genomic damage, irradiation also enhances PV1 capsid permeability thus resulting in enhanced sensitivity to nuclease treatment (De Sena and Jarvis, 1981; Simonet and Gantzer, 2006). Furthermore, obtaining *c* requires inactivation data be obtained by traditional infectious assays before being applied to qPCR data, thus limiting the application of qPCR detection of viral inactivation to viruses which lack these traditional assays (Pecson et al., 2011).

Differences between the presence of a genomic target and an infectious virion help explain limitations in quantifying titers by pretreated-qPCR assays. Assays like ET-qPCR

assume all amplifiable targets are from infectious virions, which is not true, particularly for viruses with high particle-to-plaque forming unit (PFU) ratios (Knight et al., 2016). For example, polioviruses require, at minimum, five copies of each of four different VP proteins to form a capsid; however, RNA encoding for all enteroviruses are translated as a single polyprotein that is cleaved to form all necessary proteomic components. In other words, many proteins produced during PV1 replication will not be included in mature virions, and helps explain why enteroviruses have high particle-to-PFU ratios between 30-1000 which can complicate qPCR data (Knipe and Howley, 2013).

Alternatively, ET-qPCR assumes non-amplifiable targets will fully inactivate a virus. However, the formation of a non-amplifiable target, such as a genomic lesion induced by UV, does not ensure the microorganism is not infectious. Furthermore, genomic damage induced by UV is not uniform (Bounty et al., 2012). This is of particular importance for bacteria that can engage in photoreactivation, or dsDNA viruses which may be able to utilize host machinery to repair genomic damage (Hu et al., 2012; Rainbow, 1980). These estimations can be improved by utilizing qPCR targets covering larger percentages of the entire genome of an organism, but this would require multiple qPCR assays, thus limiting their utility in quantifying viral inactivation (Pecson et al., 2011).

Permuting qPCR with infectious assays selectively targets infectious virions, but also limits utility in assessments of water quality. Finding an underestimation or lack of correlation between qPCR and infectious assays remains well documented (Diez-Valcarce et al., 2011; Knight et al., 2016; Pecson et al., 2009). As seen in this study, the accuracy of ET-qPCR can also depend on the inactivation method used. However, utilizing cell

culture in conjunction with qPCR can improve results. In integrated cell culture qPCR, viruses are exposed to cells before amplification, thereby allowing early stages of viral replication to occur. Applying integrated cell culture to studying viral inactivation accurately reflected infectious viral titers of Ad2 and rotavirus following UV_{254} treatment (Li et al., 2009; Ryu et al., 2015). However, these methods required 48 hours of incubation before performing qPCR, which is similar to results obtained by PA, and remains more labor intensive than either IFA or MB.

Utility of MB in Assessing Viral Inactivation:

Accurate and rapid characterizations of viral inactivation profiles were obtained through the application of MB. Correlations between MB and traditional infectious assays (PA/IFA) remained above $R^2 > 0.87$ and analyses of covariance indicated no significant difference between k_{obs} ($P = 0.90$). Additionally, results obtained by MB were obtained for all viruses within 24 hours, thereby improving upon detection times for all traditional infectious assays. The MB employed in this study remained limited to detecting the production of an individual mRNA oligo; however, MB can also be developed to target specific genes of interest. Furthermore, the reliance on more readily-available genomic data allows a more universal approach of designing MB for studies of viral replication, including inactivation and the development of novel antivirals or vaccines.

Table 3.1. Alignment of BKPyV sequences used to design qPCR primers and probe. *, conserved nucleotide; *, utilized conserved nucleotide

Accession Number	Position Start	Sequence			Position End
ref|NC_001538.1|	649	G G G A C C T A G T T G C C A G T G T A T	G C T G G G G A G G C T G C T G C T G C T	C C C T T G C T A C T G T A G A G G G C A	774
dbj|AB485709.1|	564	G G G A C C T A G T T G C C A G T G T A T	G C T G G G G A G G C T G C T G C T G C T	C C C T T G C T A C T G T A G A G G G C A	689
dbj|AB298942.1|	529	G G G A C C T A G T T G C C A G T G T A T	G C T G G G G A G G C T G C T G C T G C T	C C C T T G C T A C T G T A G A G G G C A	654
dbj|AB369095.1|	529	G G G A C C T A G T T G C C A G T G T A T	G C T G G G G A G G C T G C T G C T G C T	C C C T T G C T A C T G T A G A G G G C A	654
dbj|AB365170.1|	529	G G G A C C T A G T T G C C A G T G T A T	G C T G G G G A G G C T G C T G C T G C T	C C C T T G C T A C T G T A G A G G G C A	654
dbj|AB217921.1|	529	G G G A C C T A G T T G C C A G T G T A T	G C T G G G G A G G C T G C T G C T G C T	C C C T T G C T A C T G T A G A G G G C A	654
dbj|AB464954.1|	529	G G G A C C T A G T T G C C A G T G T A T	G C T G G G G A G G C T G C T G C T G C T	C C C T T G C T A C T G T A G A G G G C A	654
dbj|AB298946.1|	529	G G G A C C T A G T T G C C A G T G T A T	G C T G G G G A G G C T G C T G C T G C T	C C C T T G C T A C T G T A G A G G G C A	654
dbj|AB298944.1|	529	G G G A C C T A G T T G C C A G T G T A T	G C T G G G G A G G C T G C T G C T G C T	C C C T T G C T A C T G T A G A G G G C A	654
dbj|AB298940.1|	529	G G G A C C T A G T T G C C A G T G T A T	G C T G G G G A G G C T G C T G C T G C T	C C C T T G C T A C T G T A G A G G G C A	654
dbj|AB485694.1|	529	G G G A C C T A G T T G C C A G T G T A T	G C T G G G G A G G C T G C T G C T G C T	C C C T T G C T A C T G T A G A G G G C A	654
dbj|AB298941.1|	529	G G G A C C T A G T T G C C A G T G T A T	G C T G G G G A G G C T G C T G C T G C T	C C C T T G C T A C T G T A G A G G G C A	654
dbj|AB263926.1|	529	G G G A C C T A G T T G C C A G T G T A T	G C T G G G G A G G C T G C T G C T G C T	C C C T T G C T A C T G T A G A G G G C A	654
dbj|AB263912.1|	529	G G G A C C T A G T T G C C A G T G T A T	G C T G G G G A G G C T G C T G C T G C T	C C C T T G C T A C T G T A G A G G G C A	654
gb|JF894228.1|	668	G G G A C C T A G T T G C C A G T G T A T	G C T G G G G A G G C T G C T G C T G C T	C C C T T G C T A C T G T A G A G G G C A	793
dbj|AB369090.1|	529	G G G A C C T A G T T G C C A G T G T A T	G C T G G G G A G G C T G C T G C T G C T	C C C T T G C T A C T G T A G A G G G C A	654
dbj|AB301090.1|	529	G G G A C C T A G T T G C C A G T G T A T	G C T G G G G A G G C T G C T G C T G C T	C C C T T G C T A C T G T A G A G G G C A	654
gb|JN192431.1|	637	G G G A C C T A G T T G C C A G T G T A T	G C T G G G G A G G C T G C T G C T G C T	C C C T T G C T A C T G T A G A G G G C A	762
gb|DQ989801.1|	262	G G G A C C T A G T T G C C A G T G T A T	G C T G G G G A G G C T G C T G C T G C T	C C C T T G C T A C T G T A G A G G G C A	387
gb|DQ989795.1|	262	G G G A C C T A G T T G C C A G T G T A T	G C T G G G G A G G C T G C T G C T G C T	C C C T T G C T A C T G T A G A G G G C A	387
dbj|AB263915.1|	529	G G G A C C T A G T T G C C A G T G T A T	G C T G G G G A G G C T G C T G C T G C T	C C C T T G C T A C T G T A G A G G G C A	654
dbj|AB263925.1|	520	G G G A C C T A G T T G C C A G T G T A T	G C T G G G G A G G C T G C T G C T G C T	C C C T T G C T A C T G T A G A G G G C A	645
dbj|AB260031.1|	529	G G G A C C T A G T T G C C A G T G T A T	G C T G G G G A G G C T G C T G C T G C T	C C C T T G C T A C T G T A G A G G G C A	654
dbj|AB369087.1|	529	G G G A C C T A G T T G C C A G T G T A T	G C T G G G G A G G C T G C T G C T G C T	C C C T T G C T A C T G T A G A G G G C A	654
emb|FR720314.1|	529	G G G A C C T A G T T G C C A G T G T A T	G C T G G G G A G G C T G C T G C T G C T	C C C T T G C T A C T G T A G A G G G C A	654
gb|DQ989799.1|	262	G G G A C C T A G T T G C C A G T G T A T	G C T G G G G A G G C T G C T G C T G C T	C C C T T G C T A C T G T A G A G G G C A	387
dbj|AB269840.1|	530	G G G A C C T A G T T G C C A G T G T A T	G C T G G G G A G G C T G C T G C T G C T	C C C T T G C T A C T G T A G A G G G C A	655
dbj|AB263916.1|	528	G G G A C C T A G T T G C C A G T G T A T	G C T G G G G A G G C T G C T G C T G C C	C C C T T G C T A C T G T A G A G G G C A	653
gb|EF376992.1|	519	G G G A C C T A G T T G C C A G T G T A T	G C T G G G G A G G C T G C T G C T G C C	C C C T T G C T A C T G T A G A G G G C A	644
dbj|AB263920.1|	519	G G G A C C T A G T T G C C A G T G T A T	G C T G G G G A G G C T G C T G C T G C C	C C C T T G C T A C T G T A G A G G G C A	644
		* *	* * * * * * * * * * * * * * * * * * * *	* *	

Table 3.2. Alignment of Ad2 sequences used to design qPCR primers and probe. *, conserved nucleotide; *, utilized conserved nucleotide

Accession Number	Position Start	Sequence			Position End
ref|AC_000017.1|	15620	A T C G C T T T C C C G A G A A C C A G A	C A C C A C C G T C A G T G A A A A C G T T C C T	G G A G T C C A G C G A G T G A C C A T	15758
gb|AF534906.1|	15620	A T C G C T T T C C C G A G A A C C A G A	C A C C A C C G T C A G T G A A A A C G T T C C T	G G A G T C C A G C G A G T G A C C A T	15758
ref|AC_000008.1|	15601	A T C G C T T T C C C G A G A A C C A G A	C A C C A C C G T C A G T G A A A A C G T T C C T	G G A G T C C A G C G A G T G A C C A T	15739
gb|AY601635.1|	15601	A T C G C T T T C C C G A G A A C C A G A	C A C C A C C G T C A G T G A A A A C G T T C C T	G G A G T C C A G C G A G T G A C C A T	15739
ref|AC_000007.1|	15596	A T C G C T T T C C C G A G A A C C A G A	C A C C A C C G T C A G T G A A A A C G T T C C T	G G A G T C C A G C G A G T G A C C A T	15734
ref|NC_001405.1|	15596	A T C G C T T T C C C G A G A A C C A G A	C A C C A C C G T C A G T G A A A A C G T T C C T	G G A G T C C A G C G A G T G A C C A T	15734
gb|J01917.1|ADRCG	15596	A T C G C T T T C C C G A G A A C C A G A	C A C C A C C G T C A G T G A A A A C G T T C C T	G G A G T C C A G C G A G T G A C C A T	15734
ref|NC_001454.1|	14485	A T C G T T T T C C T G A G A A T C A G A	T A C C A C C G T C A G T G A A A A C G T T C C C	G G A G T T C A G C G C G T G A C C A T	14623
gb|L19443.1|	14485	A T C G T T T T C C T G A G A A T C A G A	T A C C A C C G T C A G T G A A A A C G T T C C C	G G A G T T C A G C G C G T G A C C A T	14623
gb|DQ315364.2|	14497	A T C G C T T T C C T G A G A A T C A G A	T A C C A C C G T C A G T G A A A A C G T T C C C	G G A G T C C A G C G C G T G A C C A T	14635
		* * * * * * * * * * * * * * * * * *	* *	* * * * * * * * * * . * * * * * * * *	

Table 3.3. Alignment of PV1 sequences used to design qPCR primers and probe. *, conserved nucleotide; *, utilized conserved nucleotide

Accession Number	Position Start			Position End
dbj|D00625.1|POL2CG1	410	GAACAAGGTGTGAAGAGCCT	GTCCTCCGGCCCCTGAATGCGGCT	CGGAACCGACTACTTTGGGTG	556
gb|M12197.1|POL2LAN	410	GAACAAGGTGTGAAGAGCCT	GTCCTCCGGCCCCTGAATGCGGCT	CGGAACCGACTACTTTGGGTG	556
emb|HF913427.1|	375	GAACAAGGTGTGAAGAGCCT	GTCCTCCGGCCCCTGAATGCGGCT	CGGAACCGACTACTTTGGGTG	521
gb|DQ890388.1|	406	GAACAAGGTGTGAAGAGCCT	GTCCTCCGGCCCCTGAATGCGGCT	CGGAACCGACTACTTTGGGTG	552
gb|AY948201.1|	407	GAACAAGGTGTGAAGAGCCT	GTCCTCCGGCCCCTGAATGCGGCT	CGGAACCGACTACTTTGGGTG	553
gb|DQ890385.1|	406	GAACAAGGTGTGAAGAGCCT	GTCCTCCGGCCCCTGAATGCGGCT	CGGAACCGACTACTTTGGGTG	552
gb|DQ890387.1|	406	GAACAAGGTGTGAAGAGCCT	GTCCTCCGGCCCCTGAATGCGGCT	CGGAACCGACTACTTTGGGTG	552
gb|AY184220.1|	406	GAACAAGGTGTGAAGAGCCT	GTCCTCCGGCCCCTGAATGCGGCT	CGGAACCGACTACTTTGGGTG	552
gb|AY177685.1|	406	GAACAAGGTGTGAAGAGCCT	GTCCTCCGGCCCCTGAATGCGGCT	CGGAACCGACTACTTTGGGTG	552
gb|FJ859189.1|	408	GAACAGGGTGTGAAGAGCCT	GTCCTCCGGCCCCTGAATGCGGCT	CGGAACCGACTACTTTGGGTG	554
gb|FJ859186.1|	408	GAACAGGGTGTGAAGAGCCT	GTCCTCCGGCCCCTGAATGCGGCT	CGGAACCGACTACTTTGGGTG	554
gb|FJ859184.1|	408	GAACAGGGTGTGAAGAGCCT	GTCCTCCGGCCCCTGAATGCGGCT	CGGAACCGACTACTTTGGGTG	554
gb|FJ859191.1|	408	GAACAGGGTGTGAAGAGCCT	GTCCTCCGGCCCCTGAATGCGGCT	CGGAACCGACTACTTTGGGTG	554
gb|FJ859185.1|	408	GAACAGGGTGTGAAGAGCCT	GTCCTCCGGCCCCTGAATGCGGCT	CGGAACCGACTACTTTGGGTG	554
gb|FJ859187.1|	408	GAACAGGGTGTGAAGAGCCT	GTCCTCCGGCCCCTGAATGCGGCT	CGGAACCGACTACTTTGGGTG	554
gb|FJ859192.1|	408	GAACAGGGTGTGAAGAGCCT	GTCCTCCGGCCCCTGAATGCGGCT	CGGAACCGACTACTTTGGGTG	554
gb|FJ859190.1|	408	GAACAGGGTGTGAAGAGCCT	GTCCTCCGGCCCCTGAATGCGGCT	CGGAACCGACTACTTTGGGTG	554
gb|FJ859188.1|	408	GAACAGGGTGTGAAGAGCCT	GTCCTCCGGCCCCTGAATGCGGCT	CGGAACCGACTACTTTGGGTG	554
gb|AY184221.1|	408	GAACAGGGTGTGAAGAGCCT	GTCCTCCGGCCCCTGAATGCGGCT	CGGAACCGACTACTTTGGGTG	554
gb|K01392.1|POL3L37	408	GAACAGGGTGTGAAGAGCCT	GTCCTCCGGCCCCTGAATGCGGCT	CGGAACCGACTACTTTGGGTG	554
gb|GU180608.1|	408	GAACAGGGTGTGAAGAGCCT	GTCCTCCGGCCCCTGAATGCGGCT	CGGAACCGACTACTTTGGGTG	554
gb|EU684056.1|	408	GAACAGGGTGTGAAGAGCCT	GTCCTCCGGCCCCTGAATGCGGCT	CGGAACCGACTACTTTGGGTG	554
gb|AF111984.2|	408	GAACAAGGTGTGAAGAGCCT	GTCCTCCGGCCCCTGAATGCGGCT	CGGAACCGACTACTTTGGGTG	554
gb|AF111983.3|	408	GAACAAGGTGTGAAGAGCCT	GTCCTCCGGCCCCTGAATGCGGCT	CGGAACCGACTACTTTGGGTG	554
gb|AY560657.1|	409	GAACAAGATGTGAAGAGCCC	ATCCTCCGGCCCCTGAATGCGGCT	CGGAACCGACTACTTTGGGTG	555
gb|AF462419.1|	405	GAACAAGGTGTGAAGAGCCT	ATCCTCCGGCCCCTGAATGCGGCT	CGGAACCGACTACTTTGGGTG	551
gb|AF462418.1|	405	GAACAAGGTGTGAAGAGCCT	ATCCTCCGGCCCCTGAATGCGGCT	CGGAACCGACTACTTTGGGTG	551
gb|AF538840.1|	405	GAACAAGGTGTGAAGAGCCT	ATCCTCCGGCCCCTGAATGCGGCT	CGGAACCGACTACTTTGGGTG	551
gb|AF538842.1|	405	GAACAAGGTGTGAAGAGCCT	ATCCTCCGGCCCCTGAATGCGGCT	CGGAACCGACTACTTTGGGTG	551
gb|AF538843.1|	405	GAACAAGGTGTGAAGAGCCT	ATCCTCCGGCCCCTGAATGCGGCT	CGGAACCGACTACTTTGGGTG	551
gb|EF682354.1|	379	GAACAAGGTGTGAAGAGCCT	ATCCTCCGGCCCCTGAATGCGGCT	CGGAACCGACTACTTTGGGTG	525
gb|EF682348.1|	379	GAACAAGGTGTGAAGAGCCT	ATCCTCCGGCCCCTGAATGCGGCT	CGGAACCGACTACTTTGGGTG	525
gb|EF682357.1|	405	GAACAAGGTGTGAAGAGCCT	ATCCTCCGGCCCCTGAATGCGGCT	CGGAACCGACTACTTTGGGTG	551
gb|EF682347.1|	379	GAACAAGGTGTGAAGAGCCT	ATCCTCCGGCCCCTGAATGCGGCT	CGGAACCGACTACTTTGGGTG	525
gb|FJ769385.1|	405	GAACAAGGTGTGAAGAGCCT	ATCCTCCGGCCCCTGAATGCGGCT	CGGAACCGACTACTTTGGGTG	551
gb|FJ769383.1|	405	GAACAAGGTGTGAAGAGCCT	ATCCTCCGGCCCCTGAATGCGGCT	CGGAACCGACTACTTTGGGTG	551
gb|FJ769380.1|	405	GAACAAGGTGTGAAGAGCCT	ATCCTCCGGCCCCTGAATGCGGCT	CGGAACCGACTACTTTGGGTG	551
emb|V01148.1|	403	GAACAAGGTGTGAAGAGCCT	ATCCTCCGGCCCCTGAATGCGGCT	CGGAACCGACTACTTTGGGTG	549
gb|EU794964.1|	357	GAACAAGGTGTGAAGAGCCT	ATCCTCCGGCCCCTGAATGCGGCT	CGGAACCGACTACTTTGGGTG	503
ref|NC_002058.3|	405	GAACAAGGTGTGAAGAGCCT	ATCCTCCGGCCCCTGAATGCGGCT	CGGAACCGACTACTTTGGGTG	551
emb|V01149.1|	405	GAACAAGGTGTGAAGAGCCT	ATCCTCCGGCCCCTGAATGCGGCT	CGGAACCGACTACTTTGGGTG	551
gb|EU794962.1|	357	GAACAAGGTGTGAAGAGCCT	ATCCTCCGGCCCCTGAATGCGGCT	CGGAACCGACTACTTTGGGTG	503
gb|EU794960.1|	357	GAACAAGGTGTGAAGAGCCT	ATCCTCCGGCCCCTGAATGCGGCT	CGGAACCGACTACTTTGGGTG	503
gb|EU794954.1|	357	GAACAAGGTGTGAAGAGCCT	ATCCTCCGGCCCCTGAATGCGGCT	CGGAACCGACTACTTTGGGTG	503
emb|V01150.1|	405	GAACAAGGTGTGAAGAGCCT	ATCCTCCGGCCCCTGAATGCGGCT	CGGAACCGACTACTTTGGGTG	551
gb|EU794961.1|	357	GAACAAGGTGTGAAGAGCCT	ATCCTCCGGCCCCTGAATGCGGCT	CGGAACCGACTACTTTGGGTG	503
gb|EU794956.1|	357	GAACAAGGTGTGAAGAGCCT	ATCCTCCGGCCCCTGAATGCGGCT	CGGAACCGACTACTTTGGGTG	503
gb|KF537633.1|	410	GAACAAGGTGTGAAGAGCCT	GTCCTCCGGCCCCTGAATGCGGCT	CGGAACCGACTACTTTGGGTG	556
gb|AY278553.1|	409	GAACAAGGTGTGAAGAGCCC	GTCCTCCGGCCCCTGAATGCGGCT	CGGAACCGACTACTTTGGGTG	555
		***** * **********	*********************	*********************	

Table 3.4. Alignment of Ad2 sequences used to design MB. *, conserved nucleotide; *, MB loop sequence

Accession Number	Position Start	Sequence	Position End
ref|AC_000017.1|	15699	C C A G C C C C C A C C A T C A C C A C C G T C A G T G A A A A C G T T C C T G C T C T C A C A G A T C	15750
gb|AF534906.1|	15699	C C A G C C C C C A C C A T C A C C A C C G T C A G T G A A A A C G T T C C T G C T C T C A C A G A T C	15750
ref|AC_000008.1|	15680	C C A G C C C C C A C C A T C A C C A C C G T C A G T G A A A A C G T T C C T G C T C T C A C A G A T C	15731
gb|AY601635.1|	15680	C C A G C C C C C A C C A T C A C C A C C G T C A G T G A A A A C G T T C C T G C T C T C A C A G A T C	15731
ref|AC_000007.1|	15675	C C A G C C C C C A C C A T C A C C A C C G T C A G T G A A A A C G T T C C T G C T C T C A C A G A T C	15726
ref|NC_001405.1|	15675	C C A G C C C C C A C C A T C A C C A C C G T C A G T G A A A A C G T T C C T G C T C T C A C A G A T C	15726
gb|J01917.1|ADRCG	15675	C C A G C C C C C A C C A T C A C C A C C G T C A G T G A A A A C G T T C C T G C T C T C A C A G A T C	15726
ref|NC_001454.1|	14564	C C C G C T C C G A C C A T T A C C A C C G T C A G T G A A A A C G T T C C C G C C C T C A C A G A T C	14615
gb|L19443.1|	14564	C C C G C T C C G A C C A T T A C C A C C G T C A G T G A A A A C G T T C C C G C C C T C A C A G A T C	14615
gb|DQ315364.2|	14576	C C C G C T C C G A C C A T T A C C A C C G T C A G T G A A A A C G T T C C C G C C C T C A C A G A T C	14627
		* * . * * * * * * * * * * * * * * * * * * * * * *	

73

Table 3.5. Alignment of PV1 sequences used to design MB. *, conserved nucleotide; *, MB loop sequence

Accession Number	Position Start	Sequence	Position End
dbj|D00625.1|POL2CG1	6983	C C C A T G A G G T T G A T G C T A G T C T C C T A G C C C A A T C A G G A A A A A G A C T A T G G A C T	7034
gb|M12197.1|POL2LAN	6989	C C C A T G A G G T T G A T G C T A G T C T C C T A G C C C A A T C A G G A A A A A G A C T A T G G A C T	7040
emb|HF913427.1|	6954	C C C A T G A G G T T G A C G C T A G T C T C C T A G C C C A A T C A G G A A A A A G A C T A T G G A C T	7005
gb|DQ890388.1|	6989	C C C A T G A G G T T G A C G C T A G T C T C C T A G C C C A A T C A G G A A A A A G A C T A T G G A C T	7040
gb|AY948201.1|	6990	C C C A T G A G G T T G A T G C T A G T C T C C T A G C C C A A T C A G G A A A A A G A C T A T G G A C T	7041
gb|DQ890385.1|	6989	C C C A T G A A G T G G A C G C T A G T C T C C T A G C C C A A T C A G G A A A A A G A C T A T G G A C T	7040
gb|DQ890387.1|	6989	C C C A T G A A G T T G A C G C T A G T C T C C T A G C C C A A T C A G G A A A A A G A C T A T G G A C T	7040
gb|AY184220.1|	6989	C C C A T G A G G T T G A T G C T A G T C T C C T A G C C C A A T C A G G A A A A A G A C T A T G G A C T	7040
gb|AY177685.1|	6989	C C C A T G A G G T T G A T G C T A G T C T C C T A G C C C A A T C A G G A A A A A G A C T A T G G A C T	7040
gb|FJ859189.1|	6981	C C C A T G A A G T T G A C G C T A G T C T C C T A G C C C A A T C A G G A A A A A G A C T A T G G A C T	7032
gb|FJ859186.1|	6981	C C C A T G A G G T T G A C G C T A G T C T C C T A G C C C A A T C A G G A A A A A G A C T A T G G A C T	7032
gb|FJ859184.1|	6981	C C C A T G A G G T T G A C G C T A G T C T C C T A G C C C A A T C A G G A A A A A G A C T A T G G A C T	7032
gb|FJ859191.1|	6981	C C C A T G A G G T T G A C G C T A G T C T C C T A G C C C A A T C A G G A A A A A G A C T A T G G A C T	7032
gb|FJ859185.1|	6981	C C C A T G A G G T T G A C G C T A G T C T C C T A G C C C A A T C A G G A A A A A G A C T A T G G A C T	7032
gb|FJ859187.1|	6981	C C C A T G A G G T T G A C G C T A G T C T C C T A G C C C A A T C A G G A A A A A G A C T A T G G A C T	7032
gb|FJ859192.1|	6981	C C C A T G A G G T T G A T G C T A G T C T C C T A G C C C A A T C A G G A A A A A G A C T A T G G A C T	7032
gb|FJ859190.1|	6981	C C C A T G A G G T T G A C G C T A G T C T C C T A G C C C A A T C A G G A A A A A G A C T A T G G A C T	7032
gb|FJ859188.1|	6981	C C C A T G A G G T T G A C G C T A G T C T C C T A G C C C A A T C A G G A A A A A G A C T A T G G A C T	7032
gb|AY184221.1|	6981	C C C A T G A G G T T G A C G C T A G T C T C C T A G C C C A A T C A G G A A A A A G A C T A T G G A C T	7032
gb|K01392.1|POL3L37	6981	C C C A T G A G G T T G A C G C T A G T C T C C T A G C C C A A T C A G G A A A A A G A C T A T G G A C T	7032
gb|GU180608.1|	6981	C C C A T G A A G T T G A C G C T A G T C T C C T A G C C C A A T C A G G A A A A A G A C T A T G G A C T	7032
gb|EU684056.1|	6981	C C C A T G A A G T T G A C G C T A G T C T C C T A G C C C A A T C A G G A A A A A G A C T A T G G A C T	7032
gb|AF111984.2|	6993	C C C A T G A G G T T G A C G C T A G T C T C C T A G C C C A A T C A G G A A A A A G A C T A T G G A C T	7044
gb|AF111983.3|	6994	C C C A C G A G G T T G A C G C T A G T C T C C T A G C C C A A T C A G G A A A A A G A C T A T G G A C T	7045
gb|AY560657.1|	6994	C C C A T G A G G T T G A C G C T A G T C T C C T A G C C C A A T C A G G A A A A A G A C T A T G G A C T	7045
gb|AF462419.1|	6990	C C C A T G A A G T T G A C G C T A G T C T C C T A G C C C A A T C A G G A A A A A G A C T A T G G A C T	7041
gb|AF462418.1|	6990	C C C A T G A A G T T G A C G C T A G T C T C C T A G C C C A A T C A G G A A A A A G A C T A T G G A C T	7041
gb|AF538840.1|	6960	C C C A T G A A G T T G A C G C T A G T C T C C T A G C C C A A T C A G G A A A A A G A C T A T G G A C T	7011
gb|AF538842.1|	6982	C C C A T G A A G T T G A C G C T A G T C T C C T A G C C C A A T C A G G A A A A A G A C T A T G G A C T	7033
gb|AF538843.1|	6982	C C C A T G A A G T T G A C G C T A G T C T C C T A G C C C A A T C A G G A A A A A G A C T A T G G A C T	7033
gb|EF682354.1|	6964	C C C A T G A A G T T G A C G C T A G T C T C C T A G C C C A A T C A G G A A A A A G A C T A T G G A C T	7015
gb|EF682348.1|	6964	C C C A T G A A G T T G A C G C T A G T C T C C T A G C C C A A T C A G G G A A A A G A C T A T G G A C T	7015
gb|EF682357.1|	6990	C C C A T G A A G T T G A C G C T A G T C T C C T A G C C C A A T C A G G G A A A A G A C T A T G G A C T	7041
gb|EF682347.1|	6964	C C C A T G A A G T T G A C G C T A G T C T C C T A G C C C A A T C A G G G A A A A G A C T A T G G A C T	7015
gb|FJ769385.1|	6990	C C C A T G A A G T T G A C G C T A G T C T C C T A G C C C A A T C A G G A A A A A G A C T A T G G A C T	7041
gb|FJ769383.1|	6990	C C C A T G A A G T T G A C G C T A G T C T C C T A G C C C A A T C A G G A A A A A G A C T A T G G A C T	7041
gb|FJ769380.1|	6990	C C C A T G A A G T T G A C G C T A G T C T C C T A G C C C A A T C A G G A A A A A G A C T A T G G A C T	7041
emb|V01148.1|	6982	C C C A T G A A G T T G A C G C T A G T C T C C T A G C C C A A T C A G G A A A A A G A C T A T G G A C T	7033
gb|EU794964.1|	6942	C C C A T G A G G T T G A C G C T A G T C T C C T A G C C C A A T C A G G A A A A A G A C T A T G G A C T	6993
ref|NC_002058.3|	6990	C C C A T G A A G T T G A C G C T A G T C T C C T A G C C C A A T C A G G A A A A A G A C T A T G G A C T	7041
emb|V01149.1|	6990	C C C A T G A A G T T G A C G C T A G T C T C C T A G C C C A A T C A G G A A A A A G A C T A T G G A C T	7041
gb|EU794962.1|	6942	C C C A T G A A G T T G A C G C T A G T C T C C T A G C C C A A T C A G G A A A A A G A C T A T G G A C T	6993
gb|EU794960.1|	6942	C C C A T G A A G T T G A C G C T A G T C T C C T A G C C C A A T C A G G A A A A A G A C T A T G G A C T	6993
gb|EU794954.1|	6942	C C C A T G A A G T T G A C G C T A G T C T C C T A G C C C A A T C A G G A A A A A G A C T A T G G A C T	6993
emb|V01150.1|	6990	C C C A T G A A G T T G A C G C T A G T C T C C T A G C C C A A T C A G G A A A A A G A C T A T G G A C T	7041
gb|EU794961.1|	6942	C C C A T G A A G T T G A C G C T A G T C T C C T A G C C C A A T C A G G A A A A A G A C T A T G G A C T	6993
gb|EU794956.1|	6942	C C C A T G A A G T T G A C G C T A G T C T C C T A G C C C A A T C A G G A A A A A G A C T A T G G A C T	6993
gb|KF537633.1|	6995	C C C A T G A G G T T G A C G C T A G T C T C C T A G C C C A A T C A G G A A A A A G A C T A T G G A C T	7046
gb|AY278553.1|	6986	C C C A T G A G G T T G A C G C T A G T C T C C T A G C C C A A T C A G G A A A A A G A C T A T G G A C T	7037
		* *	

Table 3.6. Summary of designed primers and probes used in ET-qPCR and MB assays. Sequences listed in 5′ to 3′ directions; underlined regions indicate stem regions; FAM, carboxyfluorescein; DABCYL, 4-((4-(dimethylamino)phenyl)azo)benzoic acid; *, nucleotide containing free thiol group for CPP attachment (not utilized).

Virus	Application	Sequence/Modifications
BKPyV	Forward|Reverse Primer	GGGACCTAGTTGCCAGTGTA|TGCCCTCTACAGTAGCAAGG
	qPCR MB	FAM-CTTCGCGGCAGCAGCAGCCTCCCCAGCGCGAAG-DABCYL
	Intracellular MB	Qdot525-CAGAUCUUUUAACUUCUAGAACUUCUU*GAUCUG-BHQ-1
Ad2	Forward|Reverse Primer	ATCGCTTTCCCGAGAACCAG|ATGGTCACTCGCTGGACTC
	qPCR MB	FAM-CGCGGTCCACCGTCAGTGAAAACGTTCCACCGCG-DABCYL
	Intracellular MB	FAM-CAGAUGGGAACGUUUUCACUGAG*CAUCUG-BHQ-1
PV1	Forward|Reverse Primer	GAACAAGGTGTGAAGAGCC|CACCCAAAGTAGTCGGTTCC
	qPCR MB	FAM-CCACGCTCCTCCGGCCCCTGAATGCGGCGTGG-DABCYL
	Intracellular MB	FAM-CAGAUGUAGUCUCCUAGCCCAAUCAG*CAUCUG-BHQ-1

Table 3.7. Summary of BKPyV inactivation profile.

Detection	Fluence for 1-log Inactivation	CT for 1-log inactivation	Hours at 60°C for 1-log inactivation
IFA	63.06	1.57	0.69
MB	58.95	1.59	0.72
qPCR (Untransformed)	NA	2.42	NA (-73.26)
qPCR (Transformed)	62.03	NA	NA
c	1.77	NA	NA

Table 3.8. Correlations of inactivation rates for BKPyV between detection methods.

Treatment	Detection	Parameter	IFA	MB	qPCR
UV	IFA	R^2	1.00	NA	NA
	MB	R^2	0.91	1.00	NA
	qPCR (Transformed)	R^2	0.97	0.94	1.00
ClO	IFA	R^2	1.00	NA	NA
	MB	R^2	0.87	1.00	NA
	qPCR (Untransformed)	R^2	0.80	0.63	1.00
Heat	IFA	R^2	1.00	NA	NA
	MB	R^2	0.90	1.00	NA
	qPCR (Untransformed)	R^2	0.07	0.15	1.00

Table 3.9. Summary of Ad2 inactivation profile.

Detection	Fluence for 1-log Inactivation	CT for 1-log inactivation	Hours at 60°C for 1-log inactivation
PA	49.70	0.57	1.07
MB	52.06	0.56	1.00
qPCR (Untransformed)	NA	NA (42.69)	2.66
qPCR (Transformed)	52.59	NA	NA
c	2.72	NA	NA

Table 3.10. Correlations of inactivation rates for Ad2 between detection methods.

Treatment	Detection	Parameter	PA	MB	qPCR
UV	PA	R^2	1.00	NA	NA
	MB	R^2	0.96	1.00	NA
	qPCR (Transformed)	R^2	0.99	0.97	1.00
ClO	PA	R^2	1.00	NA	NA
	MB	R^2	0.97	1.00	NA
	qPCR (Untransformed)	R^2	0.02	0.03	1.00
Heat	PA	R^2	1.00	NA	NA
	MB	R^2	0.98	1.00	NA
	qPCR (Untransformed)	R^2	0.92	0.89	1.00

Table 3.11. Summary of PV1 inactivation profile.

Detection	Fluence for 1-log Inactivation	CT for 1-log inactivation	Hours at 60°C for 1-log inactivation
PA	11.10	0.89	0.12
MB	12.23	0.79	0.12
qPCR (Untransformed)	NA	0.59	0.16
qPCR (Transformed)	9.98	NA	NA
c	0.57	NA	NA

Table 3.12. Correlations of inactivation rates for PV1 between detection methods.

Treatment	Detection	Parameter	PA	MB	qPCR
UV	PA	R^2	1.00	NA	NA
	MB	R^2	0.96	1.00	NA
	qPCR (Transformed)	R^2	0.96	0.92	1.00
ClO	PA	R^2	1.00	NA	NA
	MB	R^2	0.98	1.00	NA
	qPCR (Untransformed)	R^2	0.95	0.92	1.00
Heat	PA	R^2	1.00	NA	NA
	MB	R^2	0.97	1.00	NA
	qPCR (Untransformed)	R^2	0.29	0.36	1.00

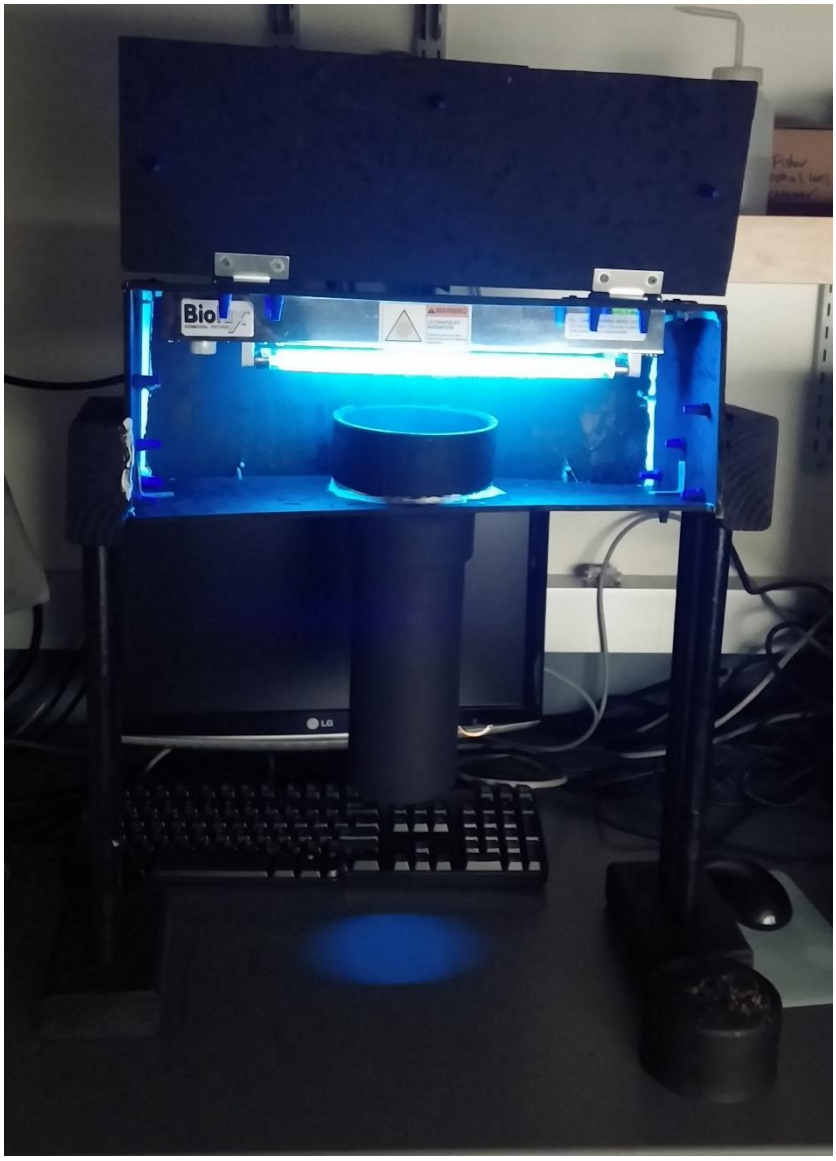

Figure 3.1. Collimating light box. Samples are placed below the collimating tube for treatment.

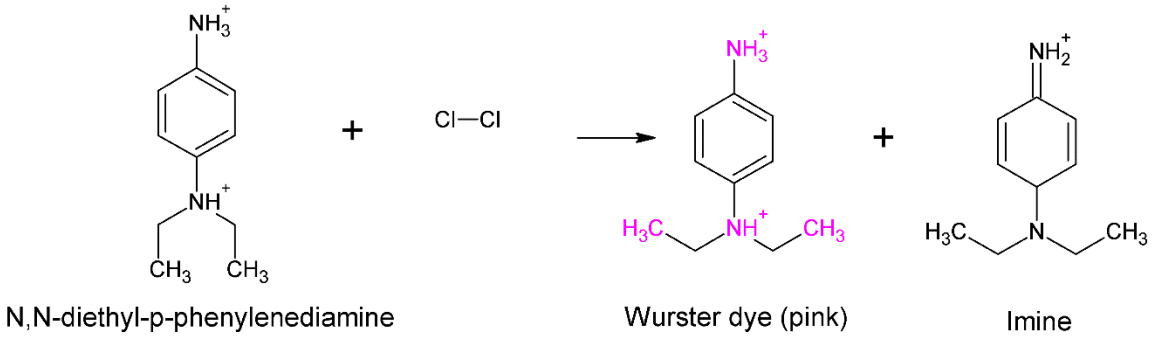

Figure 3.2. Colorimetric reaction of DPD via oxidation by chlorine.

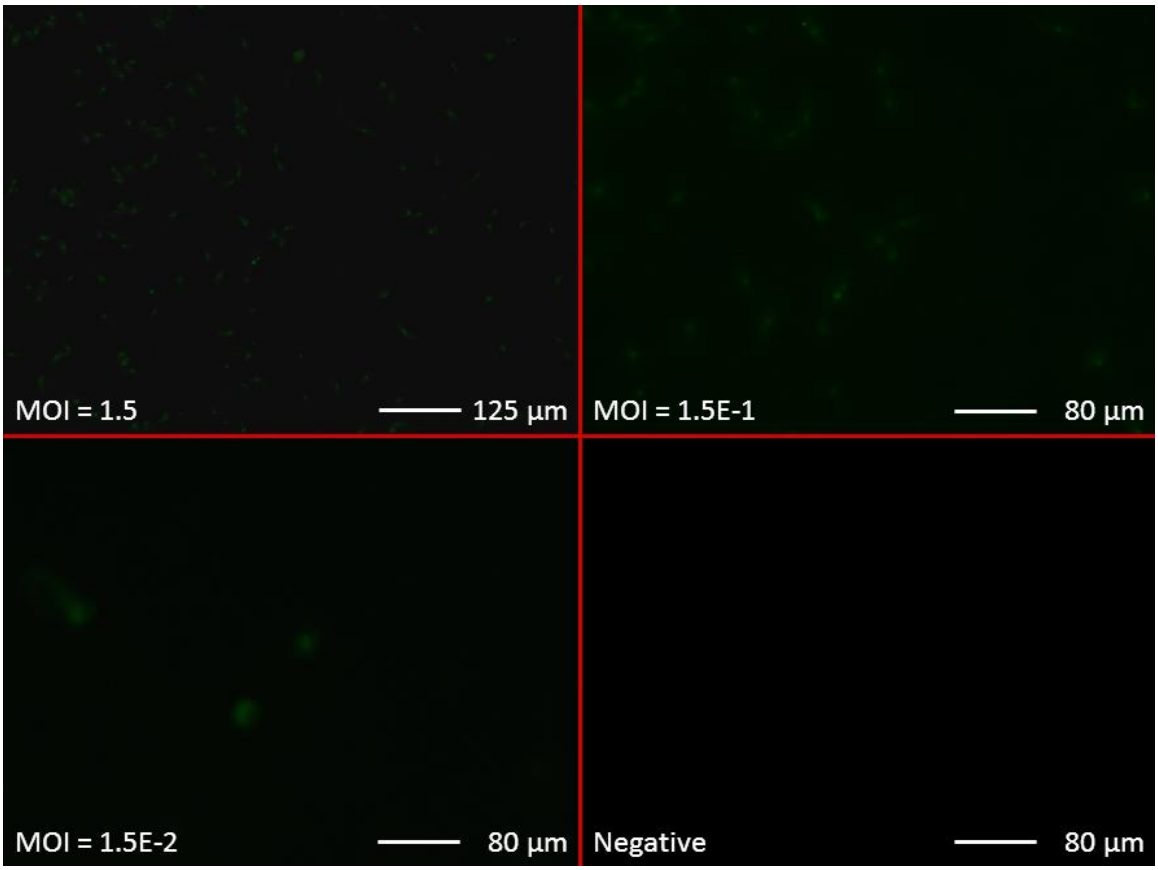

Figure 3.3. MB assay of A549 infected with Ad2 performed less than one DPI. Results span three orders of magnitude. Green fluorescence indicates active viral replication. MOI, multiplicity of infection.

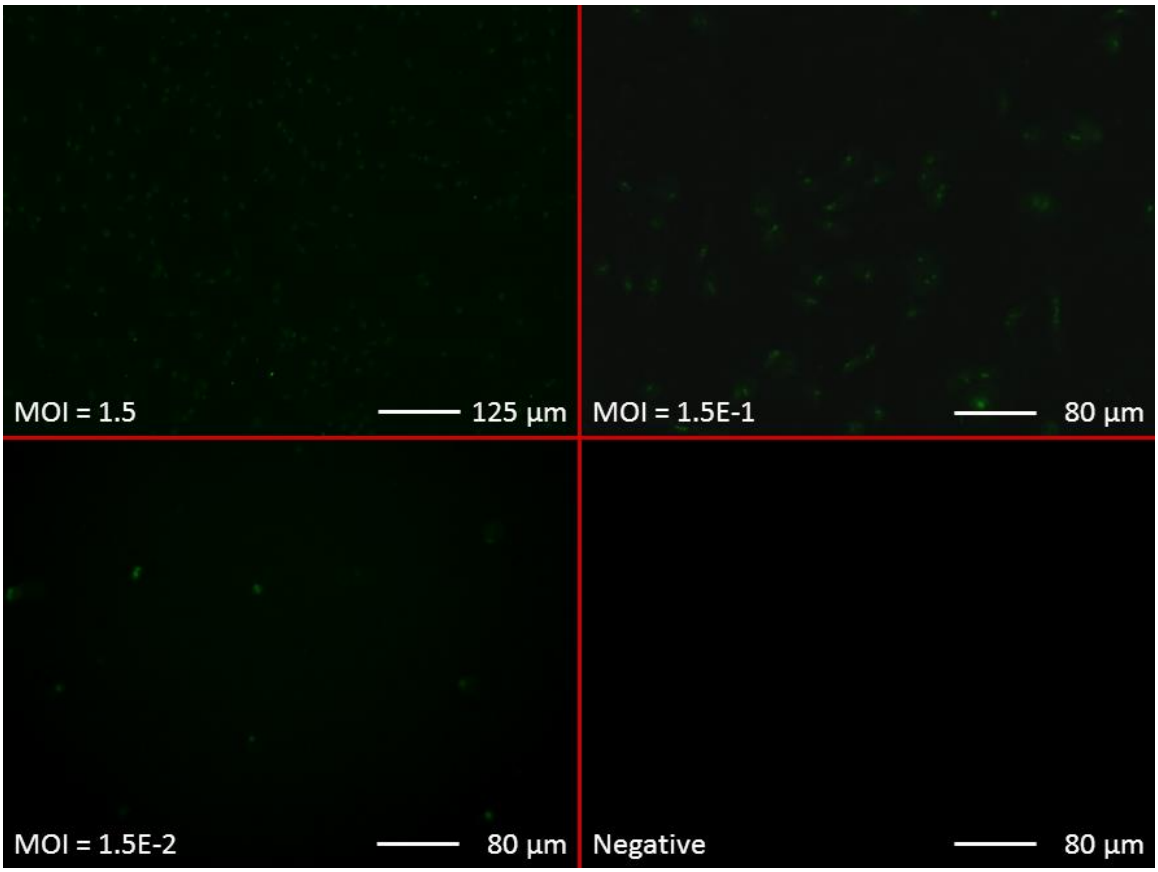

Figure 3.4. MB assay of BGMK infected with PV1 performed less than one DPI. Results span three orders of magnitude. Green fluorescence indicates active viral replication. MOI, multiplicity of infection.

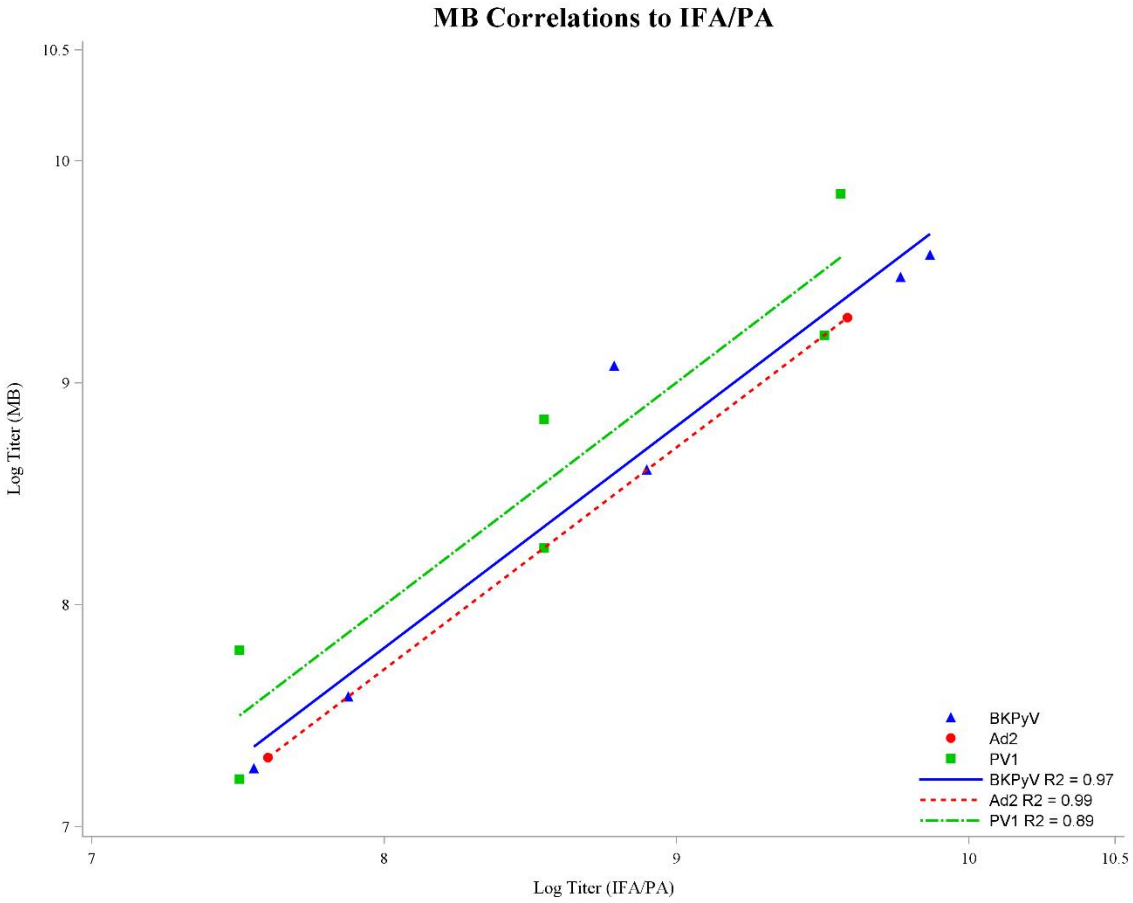

Figure 3.5. Correlations between viral titers established by MB versus traditional infectious assays.

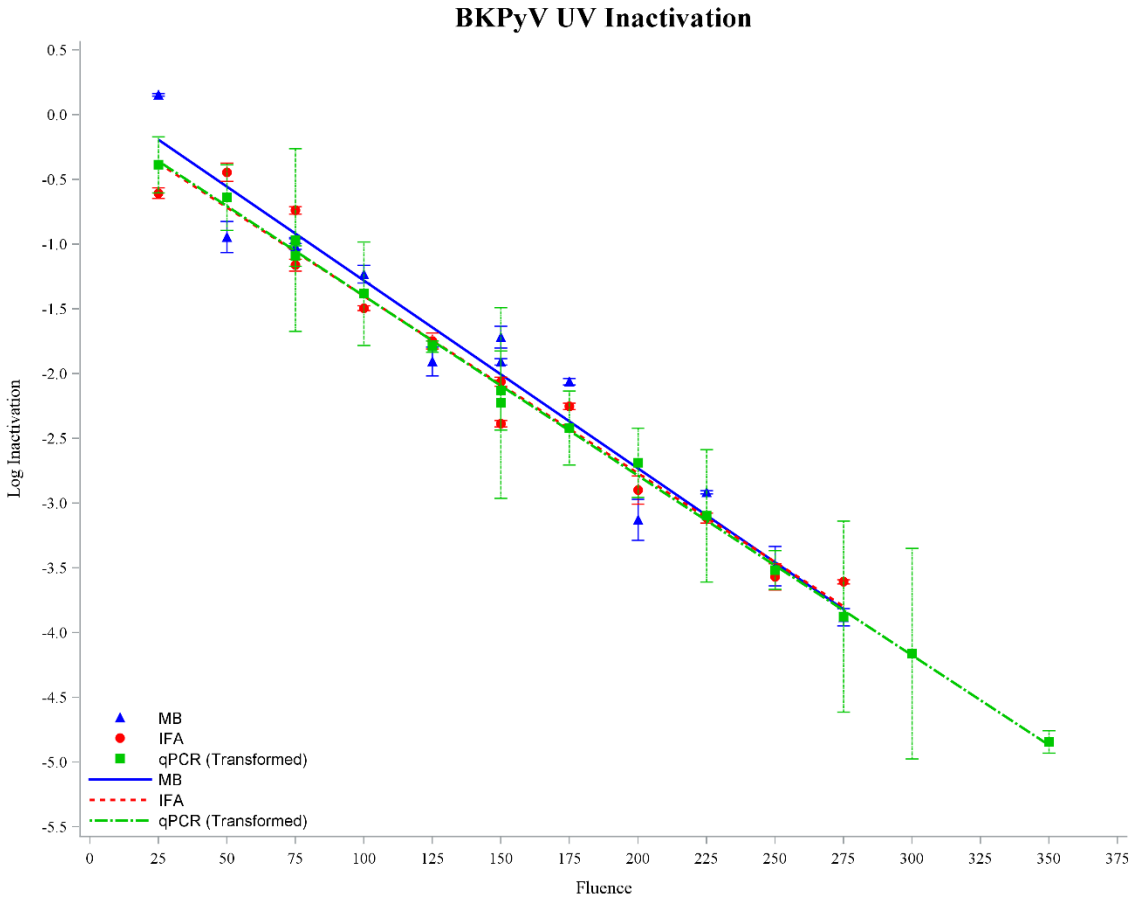

Figure 3.6. Inactivation of BKPyV by UV_{254} as detected by MB, IFA, and ET-qPCR.

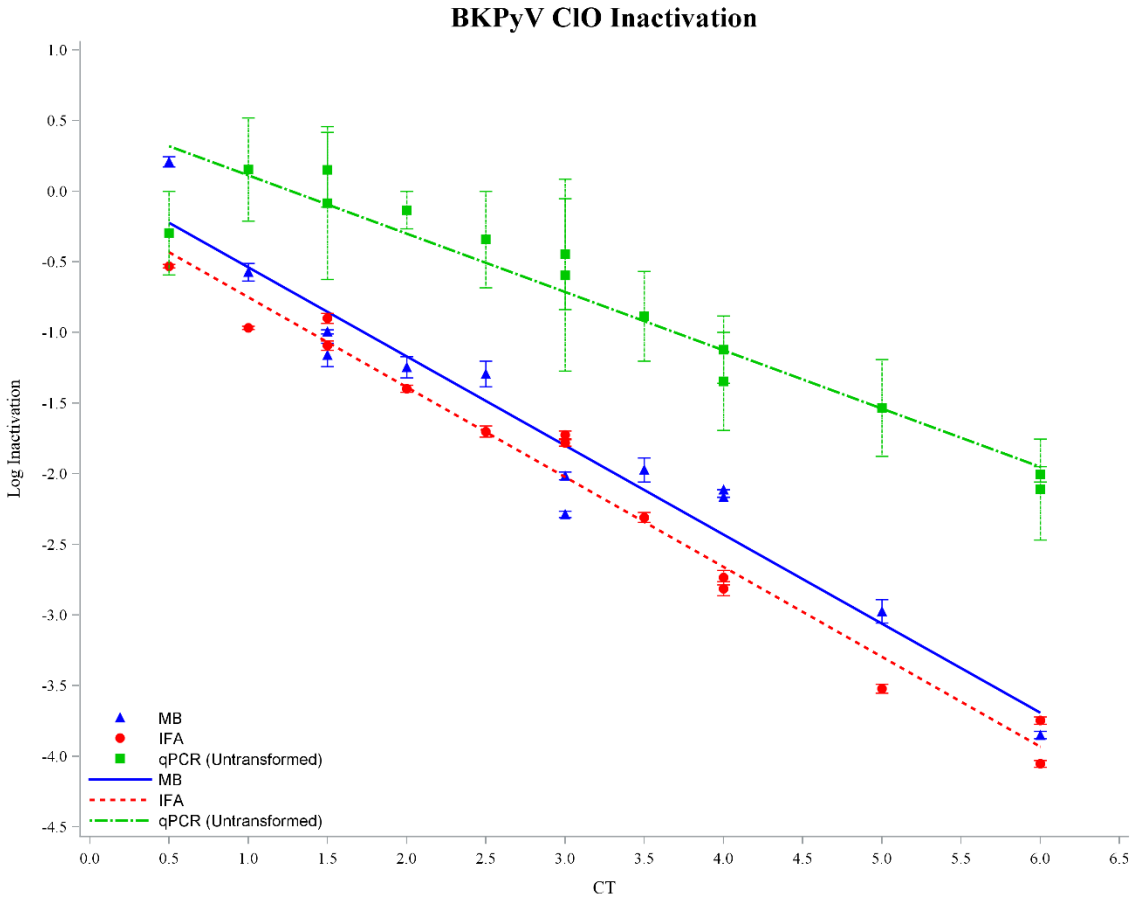

Figure 3.7. Inactivation of BKPyV by chlorination as detected by MB, IFA, and ET-qPCR.

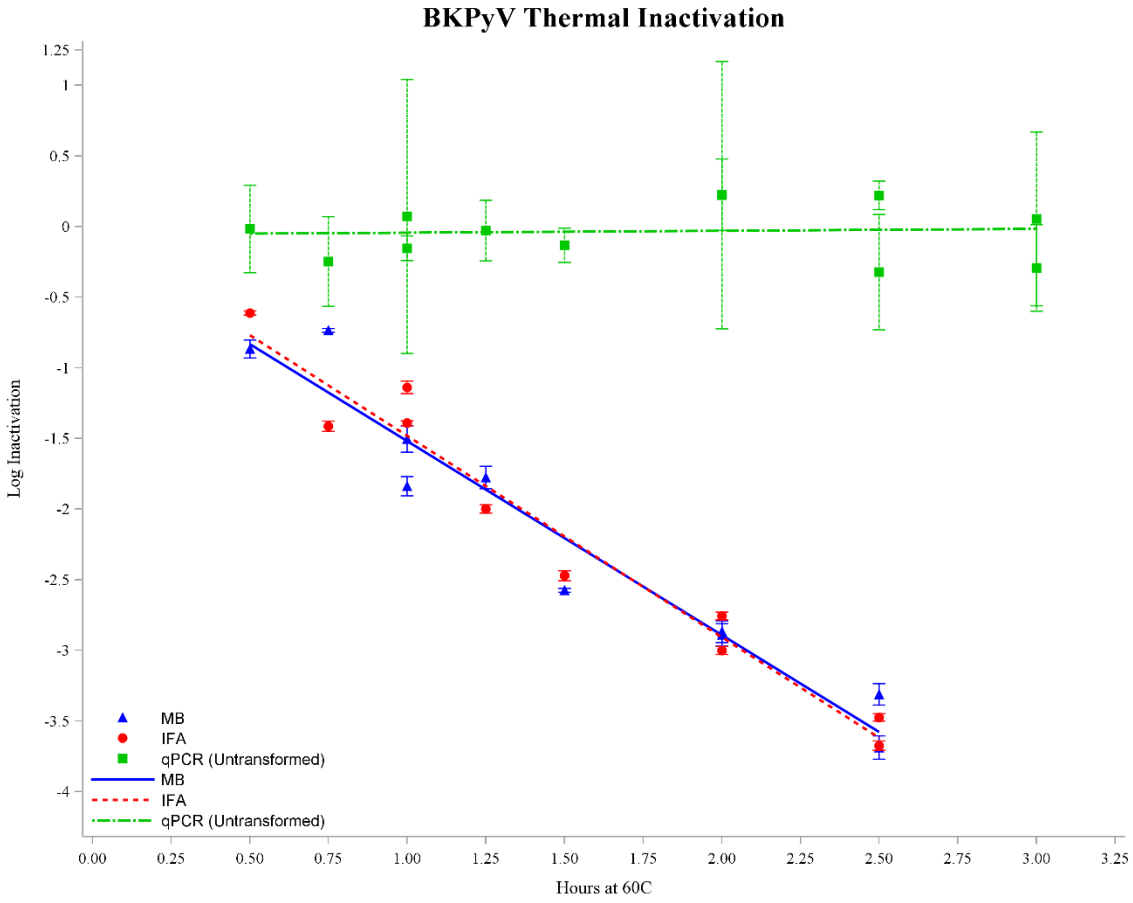

Figure 3.8. Inactivation of BKPyV at 60 °C as detected by MB, IFA, and ET-qPCR.

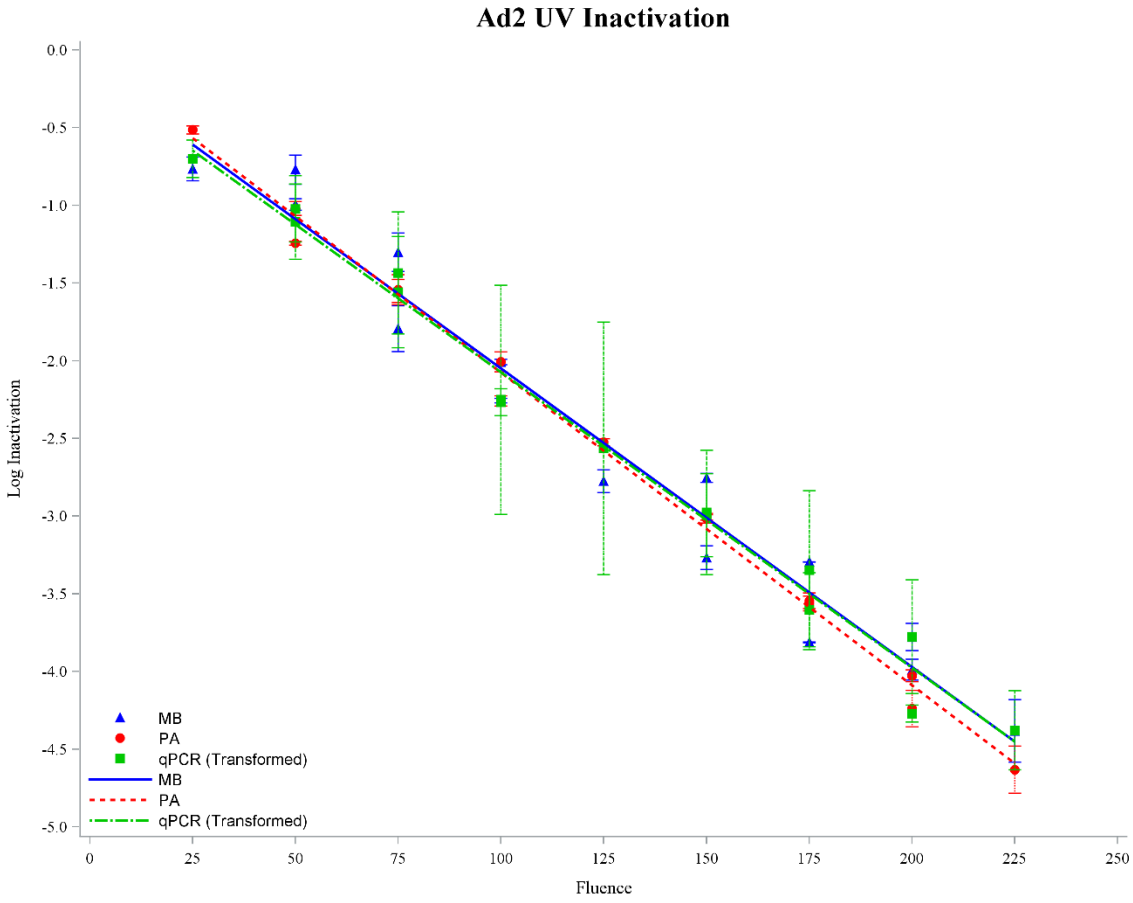

Figure 3.9. Inactivation of Ad2 by UV_{254} as detected by MB, PA, and ET-qPCR.

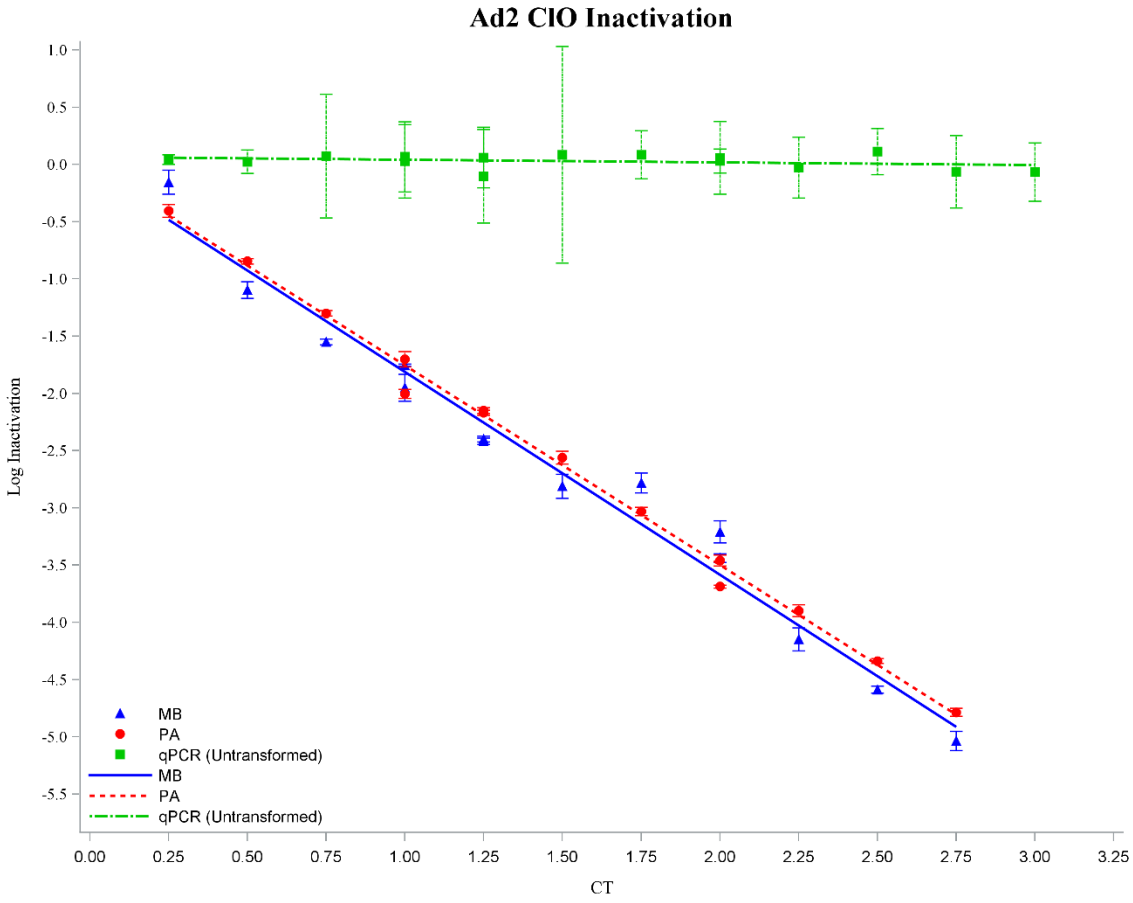

Figure 3.10. Inactivation of Ad2 by chlorination as detected by MB, PA, and ET-qPCR.

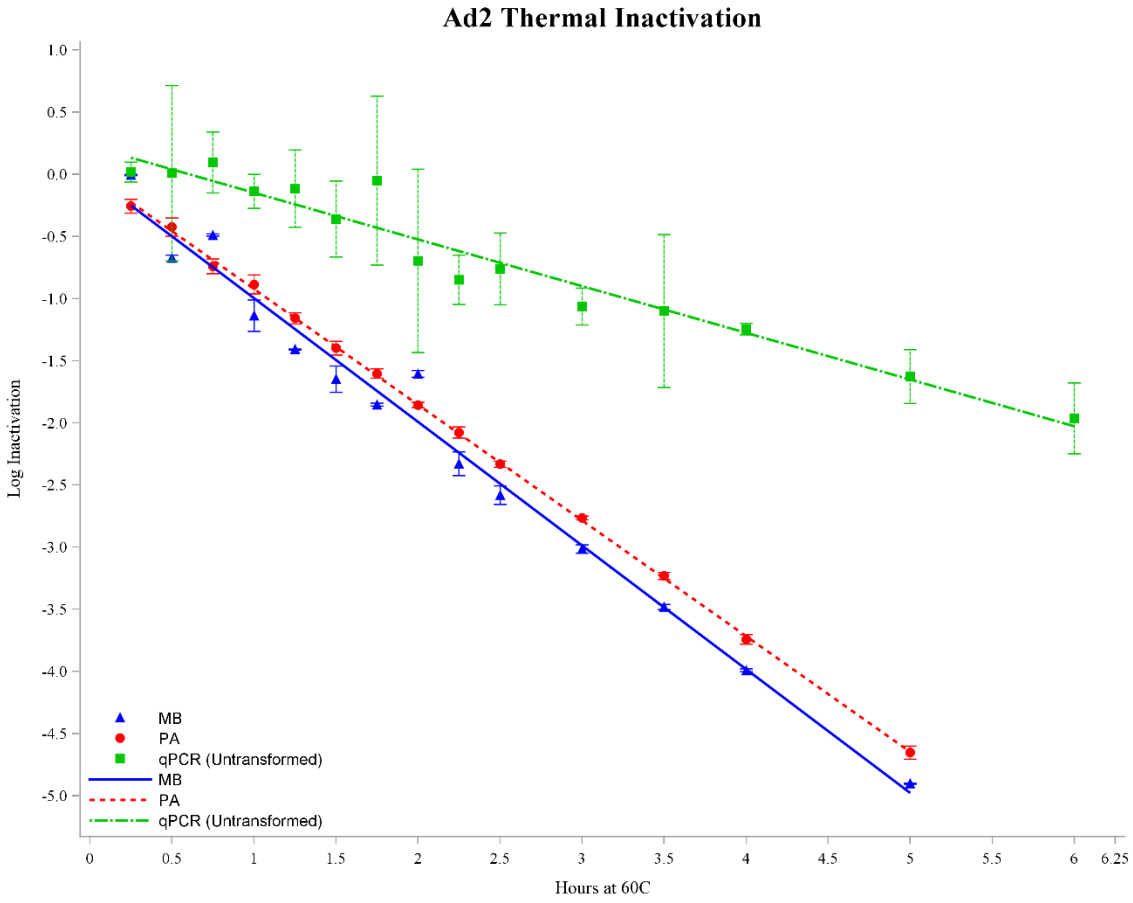

Figure 3.11. Inactivation of Ad2 by at 60 °C as detected by MB, PA, and ET-qPCR.

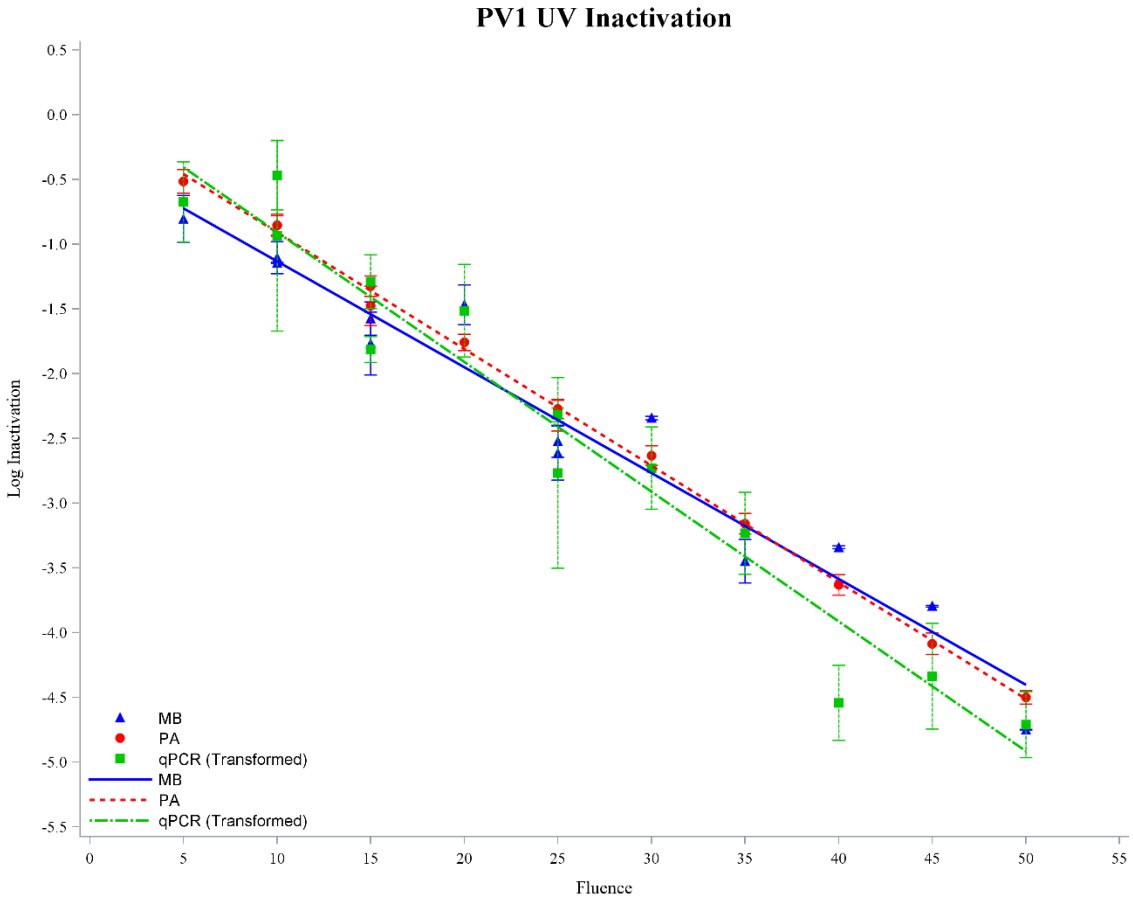

Figure 3.12. Inactivation of PV1 by UV_{254} as detected by MB, PA, and ET-qPCR.

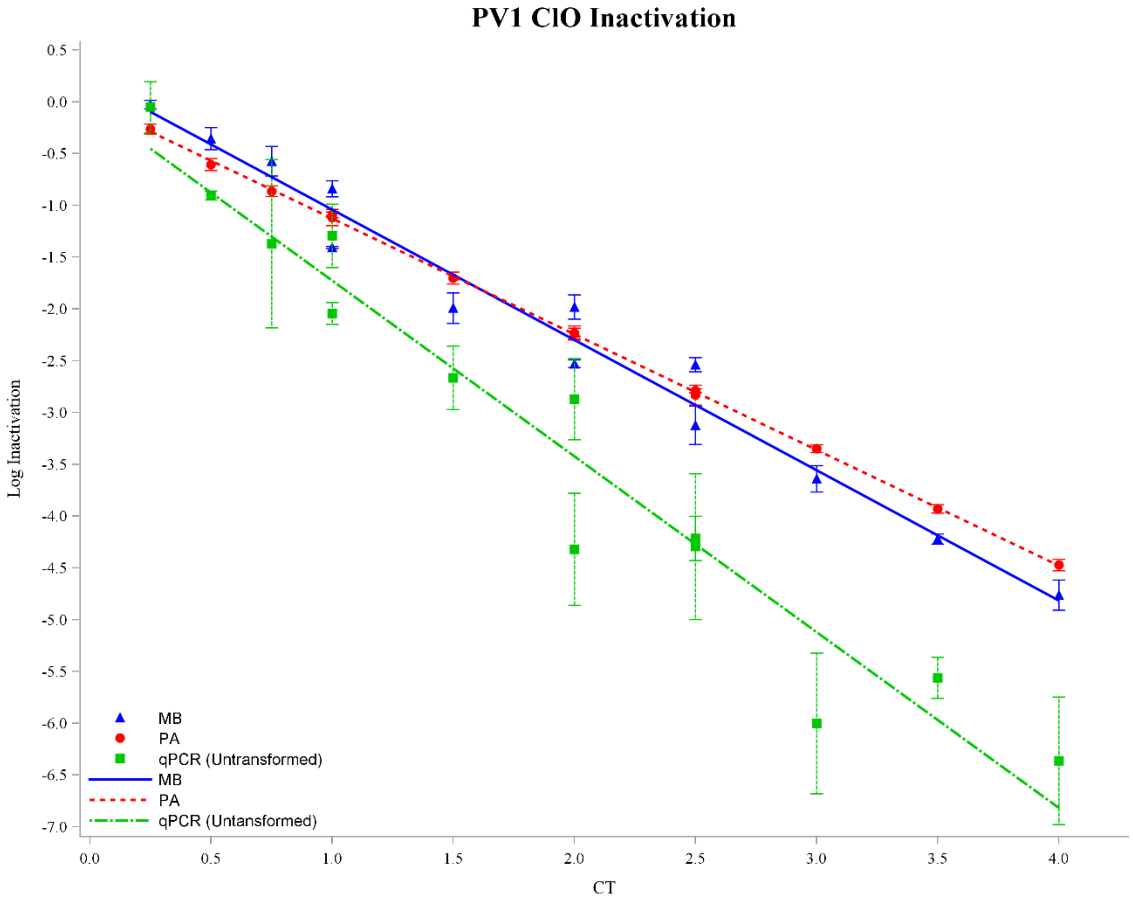

Figure 3.13. Inactivation of PV1 by chlorination as detected by MB, PA, and ET-qPCR.

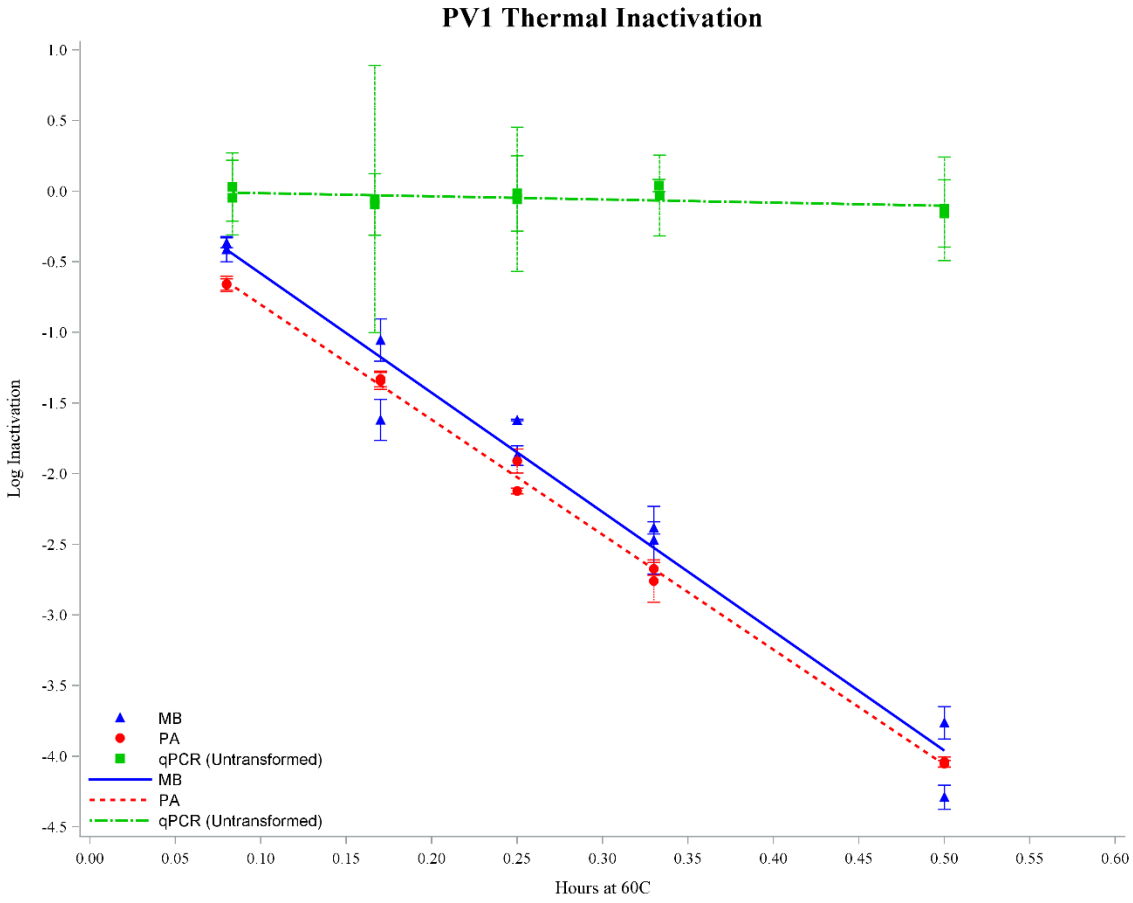

Figure 3.14. Inactivation of PV1 by at 60 °C as detected by MB, PA, and ET-qPCR.

REFERENCES

Araud, E., DiCaprio, E., Ma, Y., Lou, F., Gao, Y., Kingsley, D., Hughes, J.H., Li, J., 2016. Thermal inactivation of enteric viruses and bioaccumulation of enteric foodborne viruses in live oysters (Crassostrea virginica). Appl. Environ. Microbiol. Microbiol. 82, 2086–2099. doi:10.1128/AEM.03573-15

Beck, S.E., Rodriguez, R.A., Hawkins, M.A., Hargy, T.M., Larason, T.C., Linden, G., 2016. Comparison of UV-Induced Inactivation and RNA Damage in MS2 Phage across the Germicidal UV Spectrum 82, 1468–1474. doi:10.1128/AEM.02773-15.Editor

Bolton, J.R., Linden, K.G., 2003. Standardization of methods for fluence (UV dose) determination in bench-scale UV experiments. J. Environ. Eng. 129, 209–215.

Bounty, S., Rodriguez, R.A., Linden, K.G., 2012. Inactivation of adenovirus using low-dose UV/H2O2 advanced oxidation. Water Res. 46, 6273–6278. doi:10.1016/j.watres.2012.08.036

Calgua, B., Carratalà, A., Guerrero-Latorre, L., Corrêa, A. de A., Kohn, T., Sommer, R., Girones, R., 2014. UVC Inactivation of dsDNA and ssRNA Viruses in Water: UV Fluences and a qPCR-Based Approach to Evaluate Decay on Viral Infectivity. Food Environ. Virol. 6, 260–268. doi:10.1007/s12560-014-9157-1

Cutler, T.D., Zimmerman, J.J., 2011. Ultraviolet irradiation and the mechanisms underlying its inactivation of infectious agents. Anim. Heal. Res. Rev. 12, 15–23.

doi:10.1017/S1466252311000016

De Sena, J., Jarvis, D.L., 1981. Modification of the poliovirus capsid by ultraviolet light. Can. J. Microbiol. 27, 1185–1193.

Deborde, M., von Gunten, U., 2008. Reactions of chlorine with inorganic and organic compounds during water treatment-Kinetics and mechanisms: A critical review. Water Res. 42, 13–51. doi:10.1016/j.watres.2007.07.025

Diez-Valcarce, M., Kovac, K., Raspor, P., Rodriguez-Lazaro, D., Hernández, M., 2011. Virus genome quantification does not predict norovirus infectivity after application of food inactivation processing technologies. Food Environ. Virol. 3, 141–146. doi:10.1007/s12560-011-9070-9

Dunams, D., Sarkar, P., Chen, W., Yates, M. V., 2012. Simultaneous detection of infectious human echoviruses and adenoviruses by an in situ nuclease-resistant molecular beacon-based assay. Appl. Environ. Microbiol. 78, 1584–1588. doi:10.1128/AEM.05937-11

Eischeid, A.C., Thurston, J.A., Linden, K.G., 2011. UV disinfection of adenovirus: present state of the research and future directions. Crit. Rev. Environ. Sci. Technol. 41, 1375–1396. doi:10.1080/10643381003608268

Gall, A.M., Shisler, J.L., Mariñas, B.J., 2015. Analysis of the Viral Replication Cycle of Adenovirus Serotype 2 after Inactivation by Free Chlorine. Environ. Sci. Technol. 49, 4584–4590. doi:10.1021/acs.est.5b00301

Gonzalez-Hernandez, M.B., Cunha, J.B., Wobus, C.E., 2012. Plaque Assay for Murine Norovirus. J. Vis. Exp. doi:10.3791/4297

Hijnen, W.A.M., Beerendonk, E.F., Medema, G.J., 2006. Inactivation credit of UV radiation for viruses, bacteria and protozoan (oo)cysts in water: A review. Water Res. 40, 3–22. doi:10.1016/j.watres.2005.10.030

Hu, X., Geng, S., Wang, X., Hu, C., 2012. Inactivation and photorepair of enteric pathogenic microorganisms with ultraviolet irradiation. Environ. Eng. Sci. 29, 549–553. doi:10.1089/ees.2010.0379

Jin, M., Zhao, Z.-G., Wang, X.-W., Shen, Z.-Q., Xu, L., Yu, Y.-M., Qiu, Z.-G., Chen, Z.-L., Wang, J.-F., Huang, A.-H., Li, J.-W., 2010. The 40-80 nt region in the 5'-NCR of genome is a critical target for inactivating poliovirus by chlorine dioxide. J. Med. Virol. 30, 526–535. doi:10.1002/jmv

Johnson, K.M., Kumar, M.R.A., Ponmurugan, P., Gananamangai, B.M., 2010. Ultraviolet radiation and its germicidal effect in drinking water purification. Jounral Phytol. 2, 12–19.

Kamolsiripichaiporn, S., Subharat, S., Udon, R., Thongtha, P., Nuanualsuwan, S., 2007. Thermal inactivation of foot-and-mouth disease viruses in suspension. Appl. Environ. Microbiol. 73, 7177–7184. doi:10.1128/AEM.00629-07

Kim, M.S., Kim, T.S., 2013. R-phycoerythrin-conjugated antibodies are inappropriate for intracellular staining of murine plasma cells. Cytom. Part A 83A, 452–460.

doi:10.1002/cyto.a.22276

Knight, A., Haines, J., Stals, A., Li, D., Uyttendaele, M., Knight, A., Jaykus, L.-A., 2016. A systematic review of human norovirus survival reveals a greater persistence of human norovirus RT-qPCR signals compared to those of cultivable surrogate viruses. Int. J. Food Microbiol. 216, 40–49. doi:10.1016/j.ijfoodmicro.2015.08.015

Knipe, D.M., Howley, P.M., 2013. Fields Virology, 6th ed. Lippincott Williams & Wilkins, Philadelphia.

Lee, H.K., Jeong, Y.S., 2004. Comparison of total culturable virus assay and multiplex integrated cell culture-PCR for reliability of waterborne virus detection. Appl. Environ. Microbiol. 70, 3632–3636. doi:10.1128/AEM.70.6.3632-3636.2004

Li, D., Gu, A.Z., He, M., Shi, H.-C., Yang, W., 2009. UV inactivation and resistance of rotavirus evaluated by integrated cell culture and real-time RT-PCR assay. Water Res. 43, 3261–3269. doi:10.1016/j.watres.2009.03.044

Pecson, B.M., Ackermann, M., Kohn, T., 2011. Framework for using quantitative PCR as a nonculture based method To estimate virus infectivity. Environ. Sci. Technol. 45, 2257–2263.

Pecson, B.M., Martin, L.V., Kohn, T., 2009. Quantitative PCR for determining the infectivity of bacteriophage MS2 upon inactivation by heat , UV-B Radiation , and singlet oxygen: Advantages and limitations of an enzymatic treatment to reduce false-positive results. Appl. Environ. Microbiol. 75, 5544–5554.

doi:10.1128/AEM.00425-09

Prevost, B., Goulet, M., Lucas, F.S., Joyeux, M., Moulin, L., Wurtzer, S., 2016. Viral persistence in surface and drinking water : Suitability of PCR pre-treatment with intercalating dyes. Water Res. 91, 68–76. doi:10.1016/j.watres.2015.12.049

Rainbow, A.J., 1980. Reduced capacity to repair irradiated adenovirus in fibroblasts from Xeroderma pigmentosum heterozygotes. Cancer Res. 40, 3945–3949.

Ryu, H., Cashdollar, J.L., Fout, G.S., Schrantz, K. a., Hayes, S., 2015. Applicability of integrated cell culture quantitative PCR (ICC-qPCR) for the detection of infectious adenovirus type 2 in UV disinfection studies. J. Environ. Sci. Heal. Part A 50, 777–787. doi:10.1080/10934529.2015.1019795

Schotte, L., Strauss, M., Thys, B., Halewyck, H., Filman, D.J., Bostina, M., Hogle, J.M., Rombaut, B., 2014. Mechanism of action and capsid-stabilizing properties of VHHs with an in vitro antipolioviral activity. J. Virol. 88, 4403–13. doi:10.1128/JVI.03402-13

Simonet, J., Gantzer, C., 2006. Inactivation of Poliovirus 1 and F-specific RNA phages and degradation of their genomes by UV irradiation at 254 nanometers. Appl. Environ. Microbiol. 72, 7671–7677. doi:10.1128/AEM.01106-06

Wigginton, K.R., Pecson, B.M., Sigstam, T., Bosshard, F., Kohn, T., 2012. Virus inactivation mechanisms: impact of disinfectants on virus function and structural integrity. Environ. Sci. Technol. 46, 12069–12078. doi:10.1021/es3029473

CHAPTER FOUR: DETERMINING THE SOLAR INACTIVATION RATE OF BK POLYOMAVIRUS BY MOLECULAR BEACON

ABSTRACT

Microbiological water quality assessments, made through quantifying FIO, can exhibit poor correlations to pathogens. The development of a MB assay to detect BKPyV provides an alternative to current FIO but environmental survivability must also be established before adoption into FIO canon. Applying the developed MB allowed for characterization of the inactivation rate of BKPyV following exposure to a solar simulator (k_{obs} = 0.578 ± 0.024 h^{-1}). Furthermore, results exhibited a strong correlation to data obtained from a traditional IFA (k_{obs} = 0.568 ± 0.011 h^{-1}; R^2 = 0.93). However, the simulated decay of BKPyV raises concerns regarding its appropriateness as an FIO.

INTRODUCTION

As described, water quality assessments are made through quantification of FIO in lieu of analyzing samples for specific pathogenic microorganisms. Ideal FIO must, at minimum, exhibit correlation to pathogens, possess rapid detection assays, and exhibit enhanced resistance to water treatment processes and natural decay. Decaying more slowly in the environment relative to the pathogen of interest is of particular importance as it helps ensure the pathogen is absent when the FIO is not detected (National Research Council, 2004). Furthermore, this information can be used to establish the duration of beach closures following sewage contamination, as well as the distance between sewage outfalls and recreational shorelines (Nevers and Whitman, 2005; Yang et al., 2000).

Environmental decay can be affected by a variety of factors; however, the process is driven by sunlight. Ultraviolet waves from sunlight between 280-320 nm (UVB) can directly damage genomic and some proteomic targets of microorganisms (Davies-Colley et al., 1999; Silverman et al., 2013). Induced genomic damage is similar to, albeit less efficient than, UV_{254} inactivation (Romero et al., 2011). Wavelengths of UVB can also excite photosensitive compounds inherent to the microorganism to form reactive intermediates (e.g., reactive oxygen species) that cause inactivation. Alternatively photosensitive compounds external to the microorganism (i.e., exogenous), such as natural organic matter, can also absorb UVB and other wavelengths of sunlight to form similar reactive intermediates (Silverman et al., 2015).

To date, no study has characterized the survival of BKPyV in the environment. Attenuating a portion of solar inactivation may lead to long survivability of BKPyV in the environment. Furthermore, viruses have been shown to be more stable in environments relative to bacteria, which have served to inform standards of outfall distance and beach closure duration (Noble et al., 2003; Silverman et al., 2013; Yang et al., 2000). To this end, k_{obs} was established for BKPyV by both MB and IFA. Due to the variability in photosensitive compounds present in the external environment, k_{obs}, was limited to endogenous inactivation.

MATERIALS AND METHODS

Solar Inactivation:

Fluctuations in daily solar output as well as the hypothesized lengthy treatment times, required the use of a solar simulator. Sunlight was generated artificially with a Sol2A solar simulator equipped with a 1000 W ozone-free xenon lamp and 1.5 global air mass filter (94062A, Newport Corporation, Irvine, CA, USA). The Xe lamp coupled with an air mass filter accurately replicates the spectra of sunlight after passing through the atmosphere in accordance with the American Society for Testing and Materials standard E927-10 (ASTM International, 2014). Regardless, a comparison between natural and artificial sunlight was made by comparing spectral output of the solar simulator to readings of natural sunlight taken on a sunny day in Riverside, CA. These measurements were made with an ILT950 spectroradiometer (International Light Technologies) every 1.4 nm (the resolution of the spectroradiometer). Total irradiance of both sources of light were obtained with an ILT1700 radiometer equipped with a SED005/W light detector capable of measuring 250-675 nm thereby covering the ultraviolet and near entire visible spectra.

Treatment samples consisted of BKPyV, diluted in 200 or 100 mL (n = 12 and 10, respectively) of PBS. Samples were treated under the solar simulator with gentle stirring and 1 mL was periodically removed to quantify BKPyV titers by MB and IFA, in triplicate. A control was included for each set of experiments by placing a sample covered in aluminum foil under the solar simulator for half of the maximum treatment time.

Inactivation studies were repeated until reaching a minimum of three-log reduction in viral titers, and specific treatment times were repeated twice.

Measurements of Inactivation:

Inactivation was calculated as described in Chapter Three (Love et al., 2010). To account for light attenuation due to column depth and matrix absorbance, k_{obs}, required a correction factor (CF) (Grandbois et al., 2008). Additionally, due to a lack of photosensitive compounds present in treatment media, inactivation was expected to be driven by endogenous effects from the UVB spectra of sunlight (Romero et al., 2011). Therefore, the CF was limited to this same spectrum of light:

$$\mathrm{CF} = \frac{k_{\mathrm{obs,thin}}}{k_{\mathrm{obs,thick}}}$$

Where $k_{obs,thin}$ represents the sum of light absorbed at the surface of the sample

$$k_{\mathrm{obs,thin}} = 2.303 \sum_{\lambda=280}^{320} \alpha_\lambda I_{\lambda,0}$$

With α_λ and $I_{\lambda,0}$ equating to the sample absorbance and irradiance at the surface of the sample for a specific wavelength as measured by spectrophotometer and spectroradiometer, respectively

$k_{obs,thick}$ estimates the sum of irradiance, $\langle I_\lambda \rangle_z$, at a specific depth ($z$) and wavelength:

$$k_{\mathrm{obs,thick}} = 2.303 \sum_{\lambda=280}^{320} \alpha_\lambda \langle I_\lambda \rangle_z$$

$$\langle I_\lambda \rangle_z = I_{\lambda,0} \left(\frac{1 - 10^{-\alpha_\lambda z}}{2.303 \alpha_\lambda z} \right)$$

RESULTS

The solar simulator delivered 481.2 W/m^2 over 250-675 nm, with UVB accounting for 1.41 % of the total output. Natural sunlight exhibited 195.0 W/m^2 and accounted for 1.09 % of total solar output. Spectroradiometric measurements of the solar simulator and natural sunlight can be found in Figures 4.1 and 4.2. Following treatment by the solar simulator, samples quantified by MB indicated a k_{obs} of 0.578 ± 0.024 h^{-1} (R^2 = 0.92), while IFA resulted in k_{obs} of 0.568 ± 0.011 h^{-1} (R^2 = 0.97, Figure 4.3). Additionally, the correlation coefficient between inactivation rates obtained from both assays was strong (R^2 = 0.93) and analysis of covariance indicated no significant difference between rates of inactivation (P = 0.94).

DISCUSSION

Sunlight induces both proteomic and genomic damage, in a direct or indirect manner (Silverman et al., 2013). Viruses possessing a dsDNA genome can exhibit resistance to genomic damage due to subsequent repair from host cells during intracellular infection (Eischeid et al., 2011). Therefore, BKPyV was expected to possess some level of resistance to solar inactivation, thereby enhancing its utility as an FIO. Ensuring waters are of acceptable quality in the absence of FIO detection requires the FIO be more resistant to environmental conditions than the pathogen(s) of interest (National Research Council, 2004). However, relative to other pathogens and FIO, BKPyV did not exhibit resistance to treatment by a solar simulator.

Comparing k_{obs} to empirical values reveals BKPyV is, at best, slightly more resistant to solar inactivation. The traditional FIO, *E. coli*, exhibits relative sensitivity to endogenous solar inactivation with a k_{obs} of 3.97 h^{-1} (Nguyen et al., 2015). However, the viral FIO, MS2, possesses a ssRNA genome and a k_{obs} of 0.28 h^{-1}, making it one of the most recalcitrant microorganisms to solar inactivation (Silverman et al., 2015). Other studies have established the inactivation rate of similarly structured Ad2 (k_{obs} = 0.28 or 0.59 h^{-1}) without utilizing a CF (Love et al., 2010; Silverman et al., 2013). However, similarities in experimental setup, including the use of a 1000 W Xe bulb, allows for direct comparisons by removing the CF applied to the k_{obs} obtained for BKPyV. Doing so reduces k_{obs} to 0.53 h^{-1}, thereby revealing BKPyV is, at best, slightly more resistant to solar inactivation than the pathogen of interest. Combined with the ease of assaying for more resistant viruses, like MS2, complicates the adoption of BKPyV as an FIO.

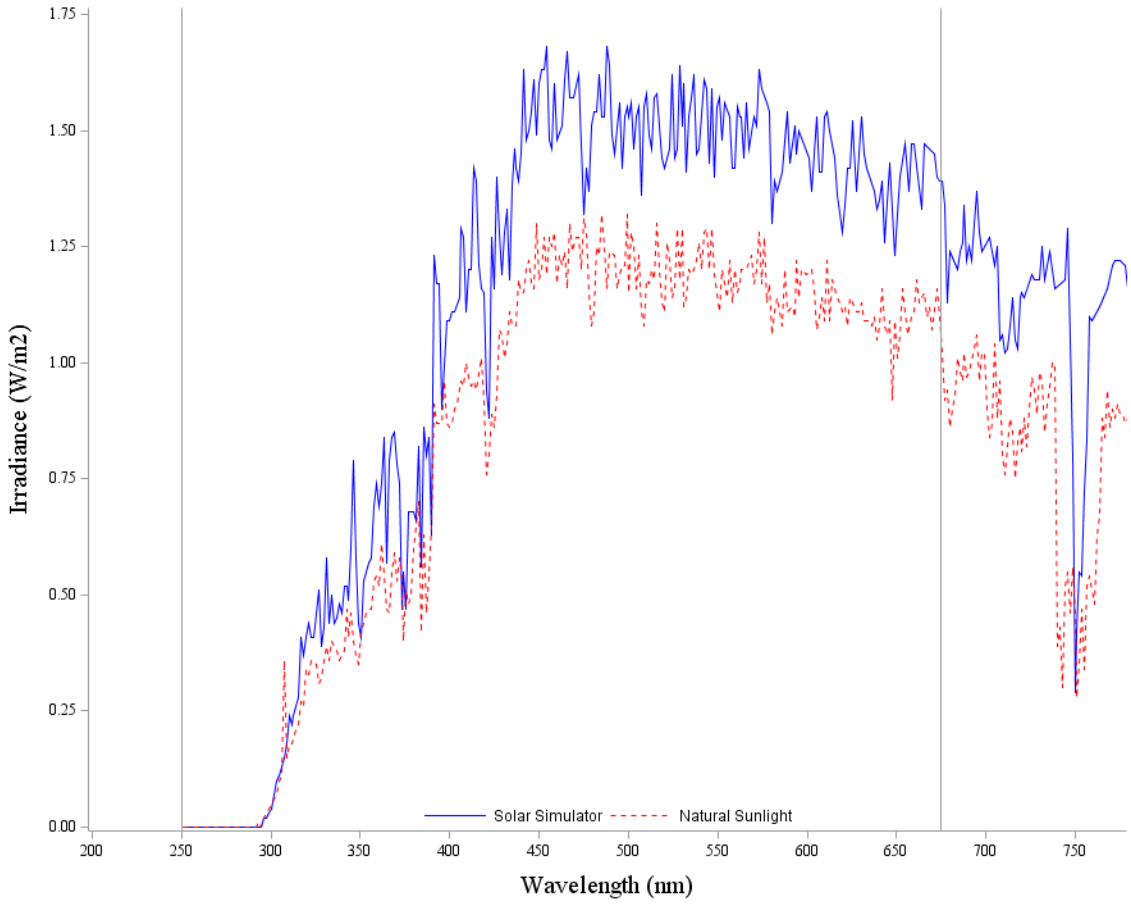

Figure 4.1. Comparing irradiance from natural and artificial sunlight. Reference lines are placed at 250 and 675 nm to indicate the range of the radiometer. Natural sunlight readings were obtained on May 11th, 2016 in Riverside, CA, USA.

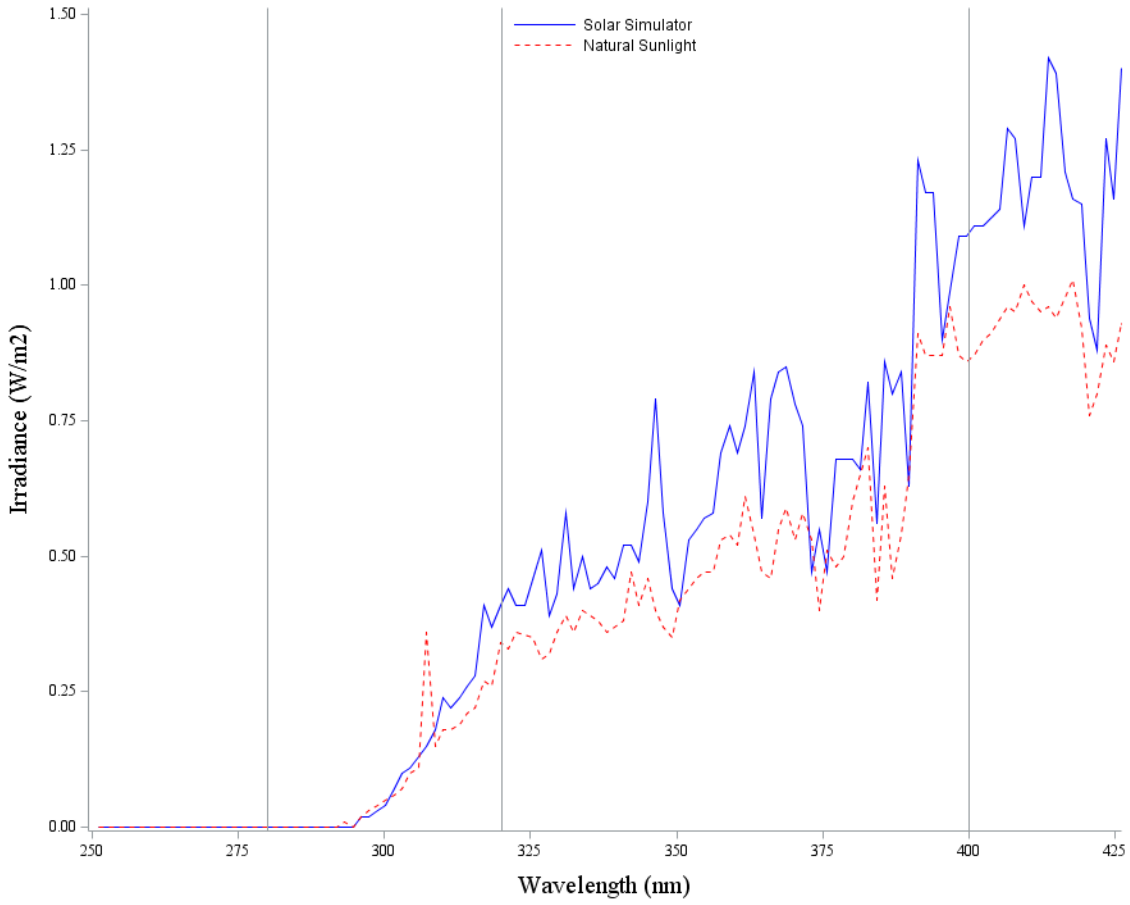

Figure 4.2. Subset of Figure 4.1, limited to UV spectra. Vertical reference lines indicate UVB and UVA (320-400 nm) spectra.

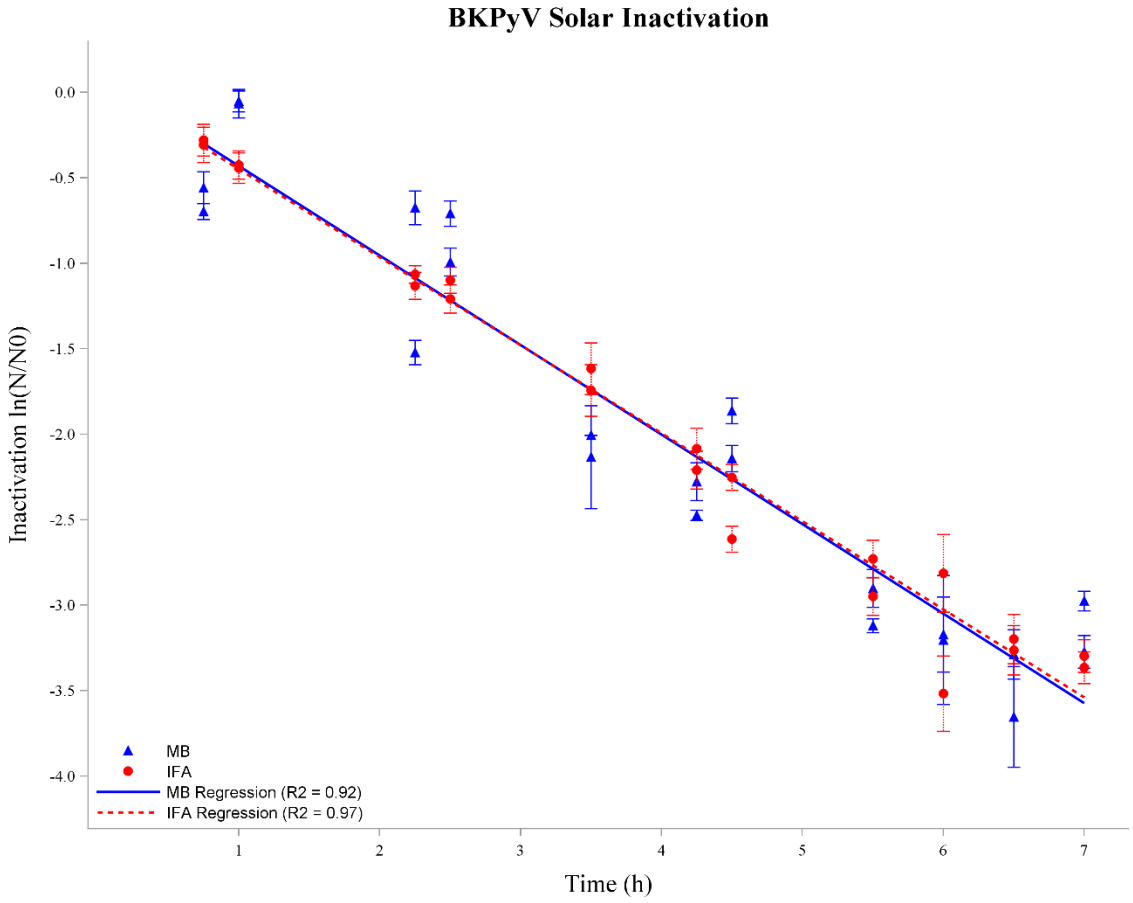

Figure 4.3. Solar inactivation as measured by IFA and MB.

REFERENCES

ASTM International, 2014. Annual Book of ASTM Standards, Volume 12. ed. ASTM International, West Conshohocken, PA.

Calgua, B., Carratalà, A., Guerrero-Latorre, L., Corrêa, A. de A., Kohn, T., Sommer, R., Girones, R., 2014. UVC Inactivation of dsDNA and ssRNA Viruses in Water: UV Fluences and a qPCR-Based Approach to Evaluate Decay on Viral Infectivity. Food Environ. Virol. 6, 260–268. doi:10.1007/s12560-014-9157-1

Davies-Colley, R.J., Donnison, A.M., Speed, D.J., Ross, C.M., Nagels, J.W., 1999. Inactivation of faecal indicator microorganisms in waste stabilisation ponds: Interactions of environmental factors with sunlight. Water Res. 33, 1220–1230. doi:10.1016/S0043-1354(98)00321-2

Eischeid, A.C., Thurston, J.A., Linden, K.G., 2011. UV disinfection of adenovirus: present state of the research and future directions. Crit. Rev. Environ. Sci. Technol. 41, 1375–1396. doi:10.1080/10643381003608268

Grandbois, M., Latch, D.E., McNeill, K., 2008. Microheterogeneous concentrations of singlet oxygen in natural organic matter isolate solutions. Environ. Sci. Technol. 42, 9184–9190. doi:10.1021/es8017094

Love, D.C., Silverman, A., Nelson, K.L., 2010. Human virus and bacteriophage inactivation in clear water by simulated sunlight compared to bacteriophage inactivation at a Southern California beach. Environ. Sci. Technol. 44, 6965–6970.

doi:10.1021/es1001924

National Research Council, 2004. Indicators for Waterborne Pathogens. The National Academies Press, Washington, DC.

Nevers, M.B., Whitman, R.L., 2005. Nowcast modeling of Escherichia coli concentrations at multiple urban beaches of southern Lake Michigan. Water Res. 39, 5250–5260. doi:10.1016/j.watres.2005.10.012

Nguyen, M.T., Jasper, J.T., Boehm, A.B., Nelson, K.L., 2015. Sunlight inactivation of fecal indicator bacteria in open-water unit process treatment wetlands: Modeling endogenous and exogenous inactivation rates. Water Res. 83, 282–292. doi:10.1016/j.watres.2015.06.043

Noble, R.T., Moore, D.F., Leecaster, M.K., McGee, C.D., Weisberg, S.B., 2003. Comparison of total coliform, fecal coliform, and enterococcus bacterial indicator response for ocean recreational water quality testing. Water Res. 37, 1637–1643. doi:10.1016/S0043-1354(02)00496-7

Romero, O.C., Straub, A.P., Kohn, T., Nguyen, T.H., 2011. Role of temperature and Suwannee River natural organic matter on inactivation kinetics of rotavirus and bacteriophage MS2 by solar irradiation. Environ. Sci. Technol. 45, 10385–10393.

Silverman, A.I., Nguyen, M.T., Schilling, I.E., Wenk, J., Nelson, K.L., 2015. Sunlight inactivation of viruses in open-water unit process treatment wetlands: modeling endogenous and exogenous inactivation rates. Environ. Sci. Technol. 49, 2757–

2766. doi:10.1021/es5049754

Silverman, A.I., Peterson, B.M., Boehm, A.B., McNeill, K., Nelson, K.L., 2013. Sunlight inactivation of human viruses and bacteriophages in coastal waters containing natural photosensitizers. Environ. Sci. Technol. 47, 1870–1878. doi:10.1021/es3036913

Yang, L., Chang, W.-S., Huang, M.-N. Lo, 2000. Natural disinfection of wastewater in marine outfall fields. Water Res. 34, 743–750.

CHAPTER FIVE: CONCLUSIONS

The application of MB successfully characterized the inactivation profile of BKPyV, thereby generating evidence in support of regulations for water treatment by UV. Specifically, BKPyV possessed enhanced resistance to UV_{254} similar to Ad2 (61.35 and 54.45 mJ/cm^2, respectively). Although the solar decay of Ad2 was not tested in this study, BKPyV exhibited enhanced sensitivity to sunlight as compared to empirical evidence (Love et al., 2010; Silverman et al., 2013). Interestingly, neither virus exhibits elevated resistance to sunlight thereby questioning the utility of BKPyV in serving as an FIO for pathogenic adenoviruses or for general water quality.

The agreement between all inactivation profiles established by MB and traditional infectious assays support the adoption of MB when quantifying infectious viral titers. Correlations between these assays ranged between $0.87 \leq R^2 \leq 0.98$ while exhibiting no significant differences in established k_{obs} ($0.90 \leq P \leq 0.99$). Obtaining k_{obs} by qPCR required damage remain limited to genomic targets and also required a correction factor (c) obtained from infectious assays, thereby limiting utility. Similar to the production of novel qPCR assays, MB rely on readily available genomic information for design. Furthermore, MB detection assays require incubation times similar to current FIO protocols while delivering superior quantification of viral titers, and thus, may serve as a near universal approach in the detection and quantification of viruses.

REFERENCES

Love, D.C., Silverman, A., Nelson, K.L., 2010. Human virus and bacteriophage inactivation in clear water by simulated sunlight compared to bacteriophage inactivation at a Southern California beach. Environ. Sci. Technol. 44, 6965–6970. doi:10.1021/es1001924

Silverman, A.I., Peterson, B.M., Boehm, A.B., McNeill, K., Nelson, K.L., 2013. Sunlight inactivation of human viruses and bacteriophages in coastal waters containing natural photosensitizers. Environ. Sci. Technol. 47, 1870–1878. doi:10.1021/es3036913